CAVELIER
ABOGADOS

SUPERINTENDENCIA DE INDUSTRIA Y COMERCIO
No. 13-187439- -00015-0000
Fecha: 2015-09-18 17:35:26 Dep: 2020 DIR NUEVASCR
Tra: 11 PATENTEIYII Eve: 378 FASENACIONALI
Act: 412 REPOSPRESRECU Folios: 79

Señor Superintendente
SUPERINTENDENCIA DE INDUSTRIA Y COM
E. S. D.

Referencia	:	Expediente No. **13.187.439**
Asunto	:	Solicitud de patente: "**MÉTODOS Y PRODUCTOS DE FARMACO PARA TRATAR ENFERMEDAD DE ALZHEIMER**"
Solicitante	:	ZINFANDEL PHARMACEUTICALS, INC. AND TAKEDA PHARMACEUTICAL COMPANY LIMITED
Fecha de solicitud	:	6 de Agosto de 2013

I. RECURSO VÍA GUBERNATIVA

Yo, Luz Clemencia DE PÁEZ, en mi condición de apoderada de la sociedad **ZINFANDEL PHARMACEUTICALS, INC. AND TAKEDA PHARMACEUTICAL COMPANY LIMITED** solicitante de la patente de la referencia, por el presente escrito atentamente manifiesto a usted que debidamente notificada de la Resolución No. **39046** del 30 de Julio del 2015, interpongo en su contra el recurso de **REPOSICIÓN**, para que sea revocada y en consecuencia se conceda el privilegio de patente de invención para "**MÉTODOS Y PRODUCTOS DE FARMACO PARA TRATAR ENFERMEDAD DE ALZHEIMER**" a favor de **ZINFANDEL PHARMACEUTICALS, INC. AND TAKEDA PHARMACEUTICAL COMPANY LIMITED**.

II. OPORTUNIDAD DE LA IMPUGNACIÓN

La Resolución No. **39046** del 30 de Julio del 2015, con fecha de publicación listado del 4 de Agosto del 2015, fecha de vencimiento del 4 de Septiembre del 2015, y fecha del término legal 18 de Septiembre del 2015.

III. LA DECISIÓN RECURRIDA

3.1 Mediante la Resolución objeto de la presente impugnación, el Superintendente de Industria y Comercio decidió:

3.1.1 Denegar la patente de invención a la creación titulada: "**MÉTODOS Y PRODUCTOS DE FARMACO PARA TRATAR ENFERMEDAD DE ALZHEIMER**"

3.2 En la parte motiva de la providencia, se mencionaron los siguientes fundamentos:

3.2.1 Mediante escrito radicado bajo el no. 13-187439-00009-0000 del 7 de Mayo de 2015, respondió oportunamente el requerimiento formulado y presentó nuevas reivindicaciones 1 a 70 que reemplazan las originalmente presentadas. Se aceptó el nuevo pliego reivindicatorio presentado, como quiera que se ajusta a las prescripciones contenidas en el artículo 34 de la Decisión 486.

3.2.2 De acuerdo con el Artículo 14 de la Decisión 486, los usos no son susceptibles de protección, por consiguiente las reivindicaciones 1 a 15 y 21 a 53 no puede ser objeto de patente.

3.2.3 No se aceptan las reivindicaciones 1 a 15, 21 a 53, 16 a 20, 69 y 70 por cuanto están referidas a una composición empelada en el tratamiento o a un método que comprende la detección de un genotipo en un sujeto a partir de una muestra biológica el cual no divulga etapas in vitro.

3.2.4 Que las reivindicaciones 54 a 68 no cumplen con el requisito de nivel inventivo.

IV. OBJETO DEL RECURSO

De acuerdo con los argumentos que expongo a continuación, solicito atentamente a su Despacho lo siguiente:

1. Revocar la Resolución No. **39046** del 30 de Julio del 2015.

2. Conceder el privilegio de patente de invención para "**MÉTODOS Y PRODUCTOS DE FARMACO PARA TRATAR ENFERMEDAD DE ALZHEIMER**" a favor de

ZINFANDEL PHARMACEUTICALS, INC. AND TAKEDA PHARMACEUTICAL COMPANY LIMITED.

V. PRESENTACIÓN DE UNA SOLICITUD DIVISIONAL Y MODIFICACIÓN DE UNA SOLICITUD EN TRÁMITE

En virtud del Artículo 36 de la Decisión 486 mediante el cual se establece la posibilidad de dividir la solicitud en dos o más fraccionarias, se presenta en esta oportunidad una solicitud divisional, junto con un pliego reivindicatorio conformado por 50 reivindicaciones, donde en la solicitud original se encuentran las reivindicaciones relacionadas con un método in vitro para determinar el riesgo incrementado de desarrollar daño cognitivo del tipo Alzheimer y una composición que comprende pioglitazona de dosis baja o una sal farmacéuticamente aceptable de la misma y en la solicitud divisional las reivindicaciones de una composición que comprende pioglitazona de dosis baja para utilizarse en el tratamiento de daño cognitivo del tipo Alzheimer contenidas en el pliego reivindicatorio presentado junto con la respuesta a la acción oficial No. 15691, presentado el 7 de Mayo del 2015.

Teniendo en cuenta que se cumplen con los requerimientos exigidos por el artículo mencionado, se solicita atentamente dar trámite a esta solicitud divisional.

Por otra parte, de acuerdo con el artículo 34 de la Decisión 486 de la Comisión de la Comunidad Andina, donde se establece que la modificación de una solicitud es posible en cualquier momento del trámite mientras no implique una ampliación de la solicitud inicial, me permito presentar un nuevo pliego reivindicatorio conformado por 20 reivindicaciones.

Por lo tanto, los argumentos esgrimidos a continuación con respecto a la patentabilidad de la invención, en los términos del capítulo reivindicatorio modificado, resultan plenamente predicables del capítulo reivindicatorio sobre el cual la patente fue negada. En efecto, la no ampliación de la materia en el nuevo pliego es evidencia suficiente de que el presente recurso controvierte el análisis de patentabilidad efectuado por su Despacho, de tal manera que el presente recurso cumple con los requisitos de ley para su aceptación y trámite.

CAVELIER
ABOGADOS

VI. FUNDAMENTOS DEL RECURSO

Respetuosamente me permito disentir de lo expuesto por ese Despacho en la Resolución objeto del presente recurso, toda vez que la presente solicitud sí cumple con los requerimientos de novedad y nivel inventivo exigidos en la Decisión 486, como se demostrará a continuación:

6.1 La presente solicitud sí tiene nivel inventivo

A pesar de lo anterior y con el fin de demostrar que la presente solicitud cumple no sólo con el requerimiento de novedad sino también con el requerimiento de nivel inventivo, se pone de presente lo siguiente:

El artículo 18 de la Decisión 486 señala lo siguiente:

> ***"Artículo 18.-*** *Se considerará que una invención tiene nivel inventivo, si para una persona del oficio normalmente versada en la materia técnica correspondiente, esa invención no hubiese resultado obvia ni se hubiese derivado de manera evidente del estado de la técnica".*

Consecuentemente, una invención se considerará inventiva si la misma no hubiese resultado obvia a partir del arte previo, para una persona del oficio normalmente versada en la materia. Esto a su vez implica que el Examinador a cargo de esta evaluación debe colocarse en el momento exacto en el que el inventor buscaba resolver el problema técnico contemplado en la solicitud y para el cual poseía la literatura y el conocimiento disponibles en dicho momento.

Siguiendo entonces los lineamientos de la Jurisprudencia aplicable al análisis del nivel inventivo de una solicitud de patente, se considera que una anterioridad o una combinación de dos anterioridades puede afectar dicho requerimiento de patentabilidad, si una persona medianamente versada en la materia encuentra enseñanzas o sugerencias claras que, a partir de un conocimiento medio en dicho campo, le permitan llegar de manera obvia a la invención reivindicada. Adicionalmente se considera que una mejora sustancial, un efecto inesperado o una ventaja con respecto al arte previo es un indicio de nivel inventivo, por cuanto aporta un salto tecnológico en la regla técnica.

Respecto a lo anterior, el Tribunal de Justicia de la Comunidad Andina ha expuesto en la Interpretación Prejudicial del proceso 13-IP-2010:

> *"En este orden de ideas, se puede concluir que una invención goza de nivel inventivo cuando a los ojos de un experto medio en el asunto de que se trate, se necesita algo más que la simple aplicación de los conocimientos técnicos en la materia para llegar a ella, es decir, que de conformidad con el estado de la técnica el invento no es consecuencia clara y directa de dicho estado".*
> [señalado fuera del texto]

Por lo anterior, se entiende que para que una persona medianamente versada en la materia pudiera derivar de manera obvia una invención, requeriría simplemente aplicar sus conocimientos técnicos. En contraste, todo aquello que va más allá de la simple aplicación de los conocimientos técnicos y que no ha sido revelado en el estado de la técnica, debe ser considerado inventivo.

A este respecto, respetuosamente manifestamos nuestro desacuerdo con el análisis llevado a cabo por el Examinador y con las conclusiones del mismo y solicitamos atentamente la reconsideración de las razones por las cuales se decidió negar la patente, con base en la siguiente información:

Con base a los documentos citados por el señor Examinador, ponemos de presente que una persona versada en la materia no habría tratado el deterioro cognitivo de tipo Alzheimer con una dosis más baja de pioglitazona que las que son ampliamente conocidas en el estado de la técnica para tratar la diabetes, por lo que se encontraría lejos de llegar al rango reivindicado en la presente solicitud que corresponde a 0.5-9 miligramos.

Así mismo, es conocido que los rangos normales utilizados en el tratamiento de la diabetes para dosis de pioglitazona corresponden a 15-45 miligramos. Sin embargo, para lograr concentraciones terapéuticas de drogas en el cerebro, se esperaría que se requiriera un dosis más grande que la de los tejidos periféricos. Lo anterior, teniendo en cuenta que el tratamiento de desórdenes del sistema nervioso central implica pasar a través de la barrera hematoencefálica, que es un obstáculo que no se encuentra presente en los tejidos periféricos.

De hecho, al seguir la administración de la pioglitazona, es posible observar que la concentración en el cerebro es menor que la concentración en los tejidos periféricos y en los órganos del cuerpo como un todo. Como se puede observar en Anexos, en la tabla 7 del documento de Maeshiba *et al.* Así que, por lo menos, teniendo en cuenta la baja permeabilidad de la barrera hematoencefálica, una persona versada en la materia hubiese optimizado el tratamiento del deterioro cognitivo de tipo Alzheimer con el incremento de la dosis de pioglitazona con respecto a la dosis ampliamente conocida que es utilizada en el tratamiento de la diabetes. De hecho, son múltiples los artículos científicos que enfatizan en la necesidad de tratar el desorden del Alzheimer con cantidades relativamente altas de pioglitazona, como es el caso de Landreth y Henika (Ver Anexos) por citar algunos, pero fue posible determinar que existen más de 20 artículos científicos que reportan los efectos de la pioglitazona en patologías relacionadas con el Alzheimer en modelos preclínicos. Claramente, ninguna de estas referencias reporta una administración menor que la dosis humana equivalente a 70 mg/día de pioglitazona.

Adicionalmente, para el momento en que se presentó la presente invención era conocimiento general que reducir la dosis de una droga resultaría en el incremento del efecto terapéutico. Tal y como indica Perelson y Deeks que mencionan que la noción de que la dosis de una droga y el efecto están relacionados es un principio básico de la farmacología y que generalmente se resume en una curva de respuesta a la dosis que se obtiene experimentalmente.

La pioglitazona demostró seguir una curva de respuesta a la dosis estándar para respuestas fisiológicas relacionadas con diabetes de tipo 2, como el que se describe en Perelson. Por su parte, en Miyazaki et al. En la figura 1, al menos las dosis en el rango de 7.5 a 45 mg de pioglitazona por día, existe un efecto dependiente de la dosis de la droga en el número de parámetros fisiológicos, y estos efectos son particularmente significativos en el rango de 15 a 45 mg. Adicionalmente, la etiqueta del producto indica que si no hace efecto se debe subir la dosis que se está consumiendo.

Así mismo señalamos que el valor EC_{50} determinado in vitro hubiese impactado las consideraciones de dosificación al informar la afinidad de ciertos compuestos a su receptor, y la afinidad relativa de diferentes drogas al mismo receptor bajo las mismas condiciones. Y teniendo en cuenta que los valores EC_{50} determinados in vitro no dependen típicamente del tejido objetivo, es evidente que **no hubiese existido ninguna motivación razonable para que una persona versada en la materia esperara que concentraciones más bajas de pioglitazona fueran suficientes para afectar la**

respuesta en el cerebro, teniendo en cuenta que las dosis probadas de pioglitazona en diabetes, no eran efectivas.

Con base en lo anterior, una persona versada en la materia no habría esperado que el tratamiento para el deterioro cognitivo de tipo Alzheimer pudiese ser tratado con una dosis de 0.5 a 9 mg de pioglitazona, teniendo en cuenta que existen artículos como el de Geldmacher que menciona que estudia el efecto de pioglitazona en la enfermedad del Alzheimer, donde quedaba demostrada que incluso con las dosis comerciales más altas de pioglitazona no había ningún efecto significativo en el tratamiento. Por consiguiente, el principio básico de la farmacología, que indica que cuando se incrementa la dosis se llega también al incremento del efecto, no había llevado a la persona versada en la materia a explorar dosis más bajas de pioglitazona como las que se reivindican en la presente solicitud.

Así, en los argumentos arriba presentados se pueden identificar claramente un indicio de presencia de nivel inventivo de acuerdo con el numeral 2.13.5.3.1 de la "GUÍA PARA EXAMEN DE SOLICITUDES DE PATENTE DE INVENCIÓN Y MODELO DE UTILIDAD" de su despacho:

- Efecto técnico sorprendente, ya que en las composiciones farmacéuticas que presentan dosis bajas de pioglitazona de la presente invención, se logra obtener un efecto no esperado en el tratamiento del Alzheimer.

En consecuencia, se le debe otorgar una compensación a mi representada que demuestra nuevos hechos (efectos sorprendentes e inesperados) a las enseñanzas descritas en el estado de la técnica y que contribuyen con el desarrollo de la tecnología.

Por lo tanto, un técnico con conocimientos medios en la materia no estaba en condiciones de plantearse el problema, tampoco de resolverlo en la forma en que se reivindica y tampoco de prever el resultado, por lo que la presente solicitud posee la altura inventiva para que se le conceda el privilegio solicitado.

8

6.2 Concesión de Solicitudes equivalentes

Aunque compartimos la opinión de su Despacho, en cuanto a que la concesión de una solicitud de patente en otros países, equivalente a la solicitud Colombiana, no obliga a su Despacho a otorgar el privilegio de patente para la misma invención, sí constituye un antecedente favorable para el estudio de patentabilidad que respetuosamente solicitamos tener en cuenta. Por lo tanto, informamos a su Despacho que la presente invención ha sido otorgada en la Oficina de Patentes de Estados Unidos, patente No. 9102666 y por la Oficina de Patentes de Nueva Zelanda.

A este respecto, deseamos poner de presente que si bien cada país es autónomo de conceder o negar una solicitud luego de la realización del estudio de fondo, es claro que el hecho de que la novedad y el nivel inventivo de una invención hayan sido reconocidos por varias oficinas a nivel mundial, es un indicio de la patentabilidad de la misma toda vez que (i) el estudio de novedad y nivel inventivo en todas las Oficinas de Patentes del mundo es realizado por personas con conocimientos técnicos en el área de interés que son consideradas personas idóneas para emitir conceptos sobre la patentabilidad de una invención y que (ii) los resultados de los exámenes de novedad o de patentabilidad efectuados respecto a solicitudes extranjeras pueden ser reconocidos como suficientes para acreditar el cumplimiento de las condiciones de patentabilidad de la invención, tal como se señala en el artículo 46 de la Decisión 486:

*"**Artículo 46.-** La oficina nacional competente podrá requerir el informe de expertos o de organismos científicos o tecnológicos que se consideren idóneos, para que emitan opinión sobre la patentabilidad de la invención. Asimismo, cuando lo estime conveniente, podrá requerir informes de otras oficinas de propiedad industrial.*
De ser necesario, a efectos del examen de patentabilidad y a requerimiento de la oficina nacional competente, el solicitante proporcionará, en un plazo que no excederá de 3 meses, uno o más de los siguientes documentos relativos a una o más de las solicitudes extranjeras referidas total o parcialmente a la misma invención que se examina:
a) copia de la solicitud extranjera;

b) copia de los resultados de exámenes de novedad o de patentabilidad efectuados respecto a esa solicitud extranjera;

(...)

La oficina nacional competente podrá ***reconocer los resultados de los exámenes referidos en el literal b) como suficientes para acreditar el cumplimiento de las condiciones de patentabilidad de la invención****" (Negrilla fuera del texto).*

Conclusión

El documento D1 no resulta anterioridad válida capaz de afectar el nivel inventivo de la invención de la presente solicitud. Por todo lo anterior, consideramos que la presente solicitud cumple a cabalidad con los requerimientos de patentabilidad exigidos por la legislación actual, por lo que atentamente solicitamos en consideración lo siguiente:

VII. PETICIÓN

Por todo lo anterior, solicito a ese Despacho lo siguiente:

7.1 Que al considerar las razones precedentes se revoque la decisión contenida en la Resolución No. **39046** del 30 de Julio del 2015, en cuanto resuelve negar el privilegio de patente de invención.

7.2. Que se acepte el nuevo pliego reivindicatorio presentado con este escrito, conformado por 20 reivindicaciones.

7.3. Que se otorgue el privilegio de patente de invención para "**MÉTODOS Y PRODUCTOS DE FARMACO PARA TRATAR ENFERMEDAD DE ALZHEIMER**" a favor de **ZINFANDEL PHARMACEUTICALS, INC. AND TAKEDA PHARMACEUTICAL COMPANY LIMITED**.

VIII. NOMBRE Y DIRECCIÓN

El nombre y la dirección del solicitante recurrente son los siguientes:

10

ZINFANDEL PHARMACEUTICALS, INC.
One Science Drive, Durham,
Carolina del Norte,
Estados Unidos de América.

IX. ANEXOS

- Formulario de modificaciones en solicitud pendiente.
- Recibo por concepto de presentación de modificaciones a las reivindicaciones por un valor de $132.000.
- Nuevo pliego reivindicatorio conformado por 20 reivindicaciones.
- Solicitud de división de una solicitud en trámite.
- Memoria descriptiva de la solicitud divisional.
- Pliego reivindicatorio divisional conformado por 50 reivindicaciones.
- Comprobante de tasa por la solicitud divisional por valor de $478.000
- Comprobante de pago por 40 reivindicaciones adicionales después de la décima por valor de $ 1.280.000 para la solicitud divisional.
- Copia del Poder.
- Maeshiba et al., Arzneimittelforsching, 47:29-30, 1997.
- Landreth, Neuropathics 3(3): 481-89, 2008.
- Heneka, et al. Actuate treatmetn with the PPAR agonist pioglitazone and ibuprofen reduces glial inflammation and AB1-42 levels in APPV717I transgenic mice, 2005.
- Perelson and Deeks, Drugs effectiveness explained: The mathematics of antiviral agents for HIV, 2012.
- Miyazaki et al. Dose-response effect of pioglitazone on insulin sensitivity and insulin secretion in type 2 diabetes, 2002.
- Geldmacher, et al. A randomized pilot clinical trial of the safety of pioglitazone in treatment of patients with Alzheimer disease, 2010.
- Patente estadounidense No. 9102666.
- Reivindicaciones aceptadas en Nueva Zelanda.

11

X. NOTIFICACIONES

Atentamente manifiesto a usted que recibiré notificaciones en la Secretaria de su Despacho o en mi oficina de abogada situada en la Carrera 4ª. No. 72-35, piso 4°, de esta ciudad de Bogotá, D.C.

Señor Superintendente,

LUZ CLEMENCIA DE PAEZ
C.C. 35.456.344 de Usaquén
T.P.A. No. 23.555

COLO-20376-0841-0001-1
COLO-20376-0264-0001-9
COLO-20376-0841-0002-9
CPT\CPT\ID-283071\WPC20376
No. M-2015-283071\CPT

Industria y Comercio
SUPERINTENDENCIA

Espacio reservado para el adhesivo de radicación

DIRECCIÓN DE NUEVAS CREACIONES
MODIFICACIONES Y/O CORRECCIONES

1. **Identificación del Tramite**

☐ **Error material** ☒ **Modificación a una Solicitud en trámite**

☒ Patente de Invención

☐ Patente de Modelo de Utilidad

☐ Registro de Diseño Industrial

☐ Esquema de Trazado de Circuitos Integrados

2. **Datos del solicitante**

Persona Natural ☐ Persona Jurídica ☒

ZINFANDEL PHARMACEUTICALS, INC. y TAKEDA PHARMACEUTICAL COMPANY LIMITED

Nombre o denominación / Nombre o razón social completa

Nombre representante legal

Tipo de empresa Micro ☐ Pequeña ☐ Mediana ☐ Otra ☐

Documento de identificación: ☐ C.C. ☐ C.E. ☐ NIT ☐ Otro Número_____

Nacionalidad/País de constitución	Dirección y domicilio del titular	Ciudad
Estados Unidos de América y Japón Respectivamente	One Science Drive, Durham, North Carolina 27708, Estados Unidos de América y 1-1, Doshomachi 4-chome, Chuo-ku, Osaka 541-0045, Japón Respectivamente	Durham y Osaka Respectivamente

Dirección electrónica	No. Fax	Número telefónico
clientes@cavelier.com	2 11 86 50	3 47 36 11

☐ **Autorizo expresamente a la Superintendencia de Industria y Comercio para que todas las comunicaciones sean enviadas a través de la dirección de correo electrónico**

13

3. Datos del apoderado:

Apellidos y Nombre	Documento de identificación	Tarjeta profesional
De Páez Luz Clemencia	C.C. 35.456.344	T.P.A. 23.555

Dirección y domicilio		Ciudad
Carrera 4ª No. 72 –35		Bogotá
Dirección electrónica	**No. Fax**	**Número telefónico**
cavelier@cavelier.com	2 11 86 50	3 47 36 11
En caso de haber presentado poder general para asuntos que se adelanten ante la Delegatura de Propiedad Industrial, sírvase indicar el número de su radicación o protocolo de poder general		

4. Datos del trámite

Corrección:

Expediente No 13,187,439

Aparece

Debe ser

Modificación:

☒ **Modificación al capítulo reivindicatorio.**
Presento nuevo capítulo reivindicatorio compuesto por 20 reivindicaciones y pido respetuosamente que el examen de patentabilidad sea realizado sobre estas nuevas reivindicaciones presentadas. Respetuosamente manifiesto que a pesar de eliminar materia del pliego reivindicatorio originalmente presentado, mi representada no renuncia a la protección que pueda obtener sobre dicha materia y además se reserva el derecho de presentar una solicitud divisional que la contenga durante el trámite de la presente solicitud, beneficiándose de la fecha de prioridad inicialmente reivindicada.

5. Anexos

☒ Comprobante de pago de la tasa para la presentación de la corrección y/o modificación por $132.000.

☒ Documento que contiene las modificaciones o correcciones.

☐ Comprobante de pago por reivindicaciones adicionales después de la décima reivindicación por.

6. Firma	
Nombre y apellidos	Firma
LUZ CLEMENCIA DE PAEZ	Luz Clemencia de Páez
C.C. 35.456.344 DE Usaquén	Tarjeta Profesional 23.555

CPT\3DC\ID-AF283089\WPC20376

14

Industria y Comercio SUPERINTENDENCIA	Espacio reservado para el adhesivo de radicación

DIRECCIÓN DE NUEVAS CREACIONES
CONVERSIÓN, DIVISIÓN Y FUSIÓN DE SOLICITUDES

1. Identificación del Tramite

☐ **Conversión** ☒ **División** ☐ **Fusión**

☒ Patente de Invención

☐ Patente de Modelo de Utilidad

☐ Registro de Diseño Industrial

☐ Esquema de Trazado de Circuitos Integrados

2. Datos del solicitante

Persona Natural ☐ Persona Jurídica ☒

ZINFANDEL PHARMACEUTICALS, INC. y TAKEDA PHARMACEUTICAL COMPANY LIMITED

Nombre o denominación / Nombre o razón social completa

Nombre representante legal

Tipo de empresa Micro ☐ Pequeña ☐ Mediana ☐ Otra ☐

Documento de identificación: ☐ C.C. ☐ C.E. ☐ NIT ☐ Otro Número_____

Nacionalidad/Pais de constitución	Dirección y domicilio del titular	Ciudad
Estados Unidos de América y Japón Respectivamente	One Science Drive, Durham, North Carolina 27708, Estados Unidos de América y 1-1, Doshomachi 4-chome, Chuo-ku, Osaka 541-0045, Japón Respectivamente	Durham y Osaka Respecticvamente

Dirección electrónica	No. Fax	Número telefónico
clientes@cavelier.com	2 11 86 50	3 47 36 11

☐ **Autorizo expresamente a la Superintendencia de Industria y Comercio para que todas las comunicaciones sean enviadas a través de la dirección de correo electrónico**

15

3. Datos del apoderado:

Apellidos y Nombre	Documento de identificación	Tarjeta profesional
De Páez Luz Clemencia	C.C. 35.456.344	T.P.A. 23.555

Dirección y domicilio		Ciudad
Carrera 4ª No. 72 –35		Bogotá
Dirección electrónica	**No. Fax**	**Número telefónico**
cavelier@cavelier.com	2 11 86 50	3 47 36 11
En caso de haber presentado poder general para asuntos que se adelanten ante la Delegatura de Propiedad Industrial, sírvase indicar el número de su radicación o protocolo de poder general		

4. Datos del trámite

CONVERSION	DIVISION	FUSION
Expediente_____	Expediente : **13.187.439**	Expediente_____
De: _____	De: _____	De: _____
A: _____	A: _____	A: _____

5. **Comprobante de Pago No.** 15-102274 **Fecha :** 2015/09/17
Comprobante de Pago No. 15-102271 **Fecha :** 2015/09/17

6. Anexos

- [x] Comprobante de pago de la tasa de presentación solicitud por $478.000.
- [x] Comprobante de pago por 40 reivindicaciones adicionales después de la décima reivindicación por $1.280.000
- [x] Poderes de **ZINFANDEL PHARMACEUTICALS, INC. y TAKEDA PHARMACEUTICAL COMPANY LIMITED**
- [x] Documento que contiene la conversión, división o fusión de la solicitud
- [ ] Copia de la solicitud y sus anexos en formato magnético

7. Firma	
Nombre y apellidos **LUZ CLEMENCIA DE PAEZ**	Firma Luz Clemencia de Páez
C.C. 35.456.344 DE Usaquén	Tarjeta Profesional 23.555

CPT\SDC\ID-AF283082\WPC20376

NOTA: Esta es una solicitud de división de la materia contenida originalmente en la solicitud de patente No. **13.187.439.** La solicitud de división de la materia se hace como consecuencia de la decisión proferida por ese Despacho por medio de la resolución No. **39046** notificada por fijación en lista del 04 de agosto de 2015. Por lo tanto pido que esta solicitud de división de materia sea tratada con el beneficio de presentación de la solicitud original, esto 06 de agosto de 2013 y la prioridad que allí se reivindica el 10 de enero de 2011.

Nota: La copia básica original se encuentra en el expediente No. **13.187.439**

REIVINDICACIONES MODIFICADAS

1. Un método in vitro para determinar el riesgo incrementado de desarrollar daño cognitivo del tipo Alzheimer en un sujeto humano en una edad o rango de edad predeterminado, en donde el método comprende:

detectar a partir de una muestra biológica del sujeto el genotipo rs10524523 del sujeto, en donde cada alelo del genotipo rs10524523 es asignado como:

(a) corto (S, menos de 19 residuos T);

(b) largo (L, 19 a 29 residuos); o

(c) muy largo (VL, 30 o más residuos); y

determinar a partir del genotipo rs10524523 si el sujeto está en riesgo incrementado de desarrollar daño cognitivo del tipo de Alzheimer en la edad o rango de edad predeterminada, en donde:

(1) una edad mayor a aproximadamente 62 y L,L o L,VL indica un riesgo incrementado;

(2) una edad mayor a aproximadamente 62 y VL,VL no indica un riesgo incrementado;

(3) una edad mayor a aproximadamente 74 y S,L indica un riesgo incrementado;

(4) una edad mayor a aproximadamente 77 y S,S indica un riesgo incrementado; y

(5) una edad mayor a aproximadamente 76 y S,VL indica un riesgo incrementado.

2. El método tal como se describe en la reivindicación 1, caracterizado porque la determinación comprende además detectar a partir de una muestra biológica del sujeto, el genotipo APOE del sujeto, en donde la presencia de un alelo APOE2 en el genotipo indica que el sujeto no está en riego incrementado.

3. Un método in vitro para determinar si se administra pioglitazona de dosis baja a un sujeto humano para el tratamiento de daño cognitivo del tipo

Alzheimer, donde la pioglitazona de dosis baja comprende de 0.5 a 9 mg de pioglitazona, caracterizado porque comprende:

detectar a partir de una muestra biológica del sujeto el genotipo rs10524523 del sujeto, en donde cada alelo es asignado como:

(a) corto (S, menos de 19 residuos T);

(b) largo (L, 19 a 29 residuos); o

(c) muy largo (VL, 30 o más residuos); y

determinar a partir del genotipo rs10524523 si de la edad del sujeto humano si se administra pioglitazona de dosis baja al sujeto para el tratamiento de daño cognitivo del tipo de Alzheimer, en donde:

(1) una edad mayor a aproximadamente 62 y L,L o L,VL indica tratamiento;

(2) una edad mayor a aproximadamente 62 y VL,VL no indica tratamiento;

(3) una edad mayor a aproximadamente 74 y S,L indica tratamiento;

(4) una edad mayor a aproximadamente 77 y S,S indica tratamiento; y

(5) una edad mayor a aproximadamente 76 y S,VL indica tratamiento.

4. El método tal como se describe en la reivindicación 3, caracterizado porque la determinación comprende además detectar a partir de una muestra biológica del sujeto, el genotipo APOE del sujeto, en donde la presencia de un alelo APOE2 en el genotipo no indica tratamiento.

5. El método tal como se describe en la reivindicación 3 o reivindicación 4, caracterizado porque el sujeto tiene cognición normal.

6. Una composición farmacéutica que comprende pioglitazona de dosis baja o una sal farmacéuticamente aceptable de la misma y un vehículo farmacéuticamente aceptable, donde la pioglitazona de dosis baja comprende de 0.5 a 9 mg de pioglitazona.

7. La composición farmacéutica de la reivindicación 6, en donde la composición farmacéutica es una tableta.

8. La composición farmacéutica de la reivindicación 6, en donde la composición farmacéutica es una cápsula.

9. La composición farmacéutica de la reivindicación 6, en donde la composición farmacéutica es una pastilla.

10. La composición farmacéutica de la reivindicación 6, en donde la composición farmacéutica es un líquido.

11. La composición farmacéutica de la reivindicación 6, en donde la composición farmacéutica es un semisólido.

12. La composición farmacéutica de la reivindicación 6, en donde la composición farmacéutica es un sólido.

13. La composición farmacéutica de la reivindicación 7 en donde dicha tableta es una tableta que se desintegra oralmente.

14. La composición farmacéutica de la reivindicación 11 en donde dicha formulación farmacéutica semisólida es seleccionada de un grupo de formulaciones farmacéuticas semisólidas que consisten de un gel, crema, loción, ungüento, bálsamo y salve.

15. La composición farmacéutica de la reivindicación 6, en donde la composición farmacéutica es un polvo.

16. La composición farmacéutica de la reivindicación 6, en donde la composición farmacéutica es una formulación bioequivalente.

17. La composición farmacéutica de la reivindicación 6, en donde la composición farmacéutica es una formulación farmacéuticamente equivalente.

18. La composición farmacéutica de la reivindicación 6, en donde la composición farmacéutica es una formulación terapéuticamente equivalente.

19. La composición farmacéutica de la reivindicación 6, en donde la composición comprende de 0.5 a 6 mg de pioglitazona.

20. La composición farmacéutica de la reivindicación 6, en donde la composición comprende de 0.5 a 1.5 mg de pioglitazona.

ONLINE FIRST

A Randomized Pilot Clinical Trial of the Safety of Pioglitazone in Treatment of Patients With Alzheimer Disease

David S. Geldmacher, MD; Thomas Fritsch, PhD; McKee J. McClendon, PhD; Gary Landreth, PhD

Objectives: To evaluate the safety of the peroxisome proliferator–activated receptor gamma agonist pioglitazone in nondiabetic patients with Alzheimer disease (AD) and to explore treatment effect sizes on clinical outcomes.

Design: Double-blind, placebo-controlled randomized controlled trial of 18-month duration.

Setting: Two academic medical center outpatient clinics.

Patients: Nondiabetic patients meeting research criteria for probable AD were enrolled. Twenty-five of 29 subjects completed the study; no withdrawals were attributable to adverse effects.

Intervention: Subjects received pioglitazone (Actos), titrated to 45 mg daily, or matching placebo, and 200 IU of vitamin E daily. Patients maintained treatment with cholinesterase inhibitors and could begin memantine therapy when it became available during the study.

Main Outcome Measures: The primary outcome was frequency of reported adverse effects (AEs). Secondary outcomes were measures of cognition, activities of daily living, neuropsychiatric symptoms, and global function.

Results: Peripheral edema was the principal AE occurring more frequently in subjects taking pioglitazone than placebo (28.6% vs 0%). This is consistent with the known AE profile of pioglitazone. No group differences in laboratory measures were identified. No significant treatment effect was observed on exploratory analysis of clinical efficacy.

Conclusions: Pioglitazone was generally well tolerated in this pilot study. There were no serious or unanticipated adverse events or clinical laboratory changes attributable to pioglitazone over a long-term exposure in nondiabetic patients with AD. The tolerability of pioglitazone in this population and peroxisome proliferator–activated receptor gamma effects in laboratory models of AD support further study of this drug class in earlier disease stages.

Trial Registration: clinicaltrials.gov Identifier: NCT00982202.

Arch Neurol. 2011;68(1):45-50. Published online September 13, 2010. doi:10.1001/archneurol.2010.229

Author Affiliations: Department of Neurology, University of Virginia Health System, Charlottesville (Dr Geldmacher); Parkinson Research Institute, Aurora Sinai Medical Center, Milwaukee, Wisconsin (Dr Fritsch); University Memory and Aging Center, University Hospitals (Dr McClendon), and Alzheimer's Research Laboratory, Department of Neuroscience (Dr Landreth), Case Western Reserve University, Cleveland, Ohio.

ALZHEIMER DISEASE (AD) IS an immense and growing public health problem. Although prescription drug therapy for the symptoms of AD has been available since 1993, these agents do not fundamentally alter the pathological expression of the disease or its progressive course. The failure of several recent treatment trials directed at the β-amyloid peptide, a key pathological correlate of AD, suggests a need to explore alternative approaches to AD treatment that are not focused on β-amyloid metabolism.

The nuclear receptor peroxisome proliferator–activated receptor gamma (PPARγ) is a potential therapeutic target for the treatment of AD.[1] PPARγ acts principally to regulate glucose and lipid metabolism, both of which are abnormal in AD. A local microglia-mediated inflammatory response centers on the amyloid plaques in the AD brain. PPARγ activation robustly suppresses inflammation as well as expression of cytokines and other inflammatory mediators associated with activated microglia.

Drugs of the thiazolidinedione class, originally developed to reduce insulin resistance in type 2 diabetes mellitus, are potent PPARγ agonists; 2 are in clinical use for treatment of diabetes mellitus (pioglitazone [Actos] and rosiglitazone [Avandia]). A preliminary trial of rosiglitazone, 4 mg daily, vs placebo in 30 subjects with mild AD or amnestic mild cognitive impairment showed better scores on tests of delayed memory and selective attention after 6 months of rosiglitazone treatment.[2] A

©2011 American Medical Association. All rights reserved.
Downloaded From: http://archneur.jamanetwork.com/ by a Takeda Pharmaceuticals International User on 12/03/2014

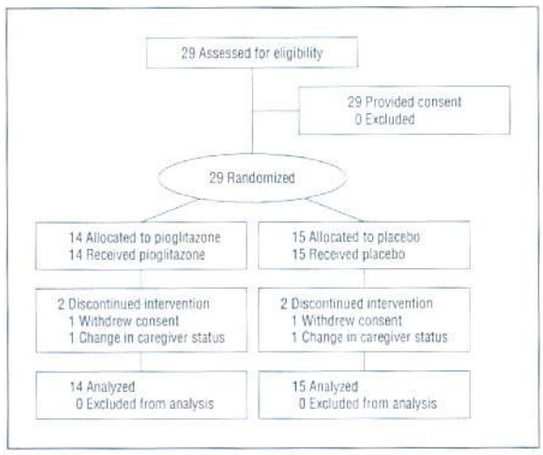


Figure. Patient flow.

subsequent double-blind, randomized, placebo-controlled study of rosiglitazone in 511 patients over 24 weeks revealed no significant improvement in the treated group overall; however, improved cognition was observed in a subset of patients who did not possess an apolipoprotein E ε4 (APOE4) allele.[3]

One potential explanation of the limited efficacy of rosiglitazone is poor bioavailability to the central nervous system. Although rosiglitazone passes the blood-brain barrier, it undergoes active efflux through P-glycoprotein–dependent transport, limiting its concentration in the brain.[4] Pioglitazone has demonstrated central nervous system penetration and relevant biological activity in a transgenic mouse model of AD.[5] Orally administered pioglitazone enters the brains of transgenic mice expressing AD pathology[6] in sufficient amounts to exert biologically relevant effects in reducing AD-related pathological burden and suppression of glial activation.[5,7] Pioglitazone treatment also reversed cerebrovascular dysfunction observed in aged animals with murine models of AD.[8] The combination of blood-brain barrier penetration and demonstrated activity on AD-related pathophysiology makes pioglitazone an attractive therapeutic candidate, even in light of the failure of rosiglitazone to demonstrate clinical efficacy in subjects with AD.

The specific aims of this study were to collect information on the safety and tolerability of long-term exposure to pioglitazone among nondiabetic, elderly patients with AD. Because there had been no prior experience with pioglitazone in this patient population, the study was also designed to explore treatment effect sizes to guide design of future clinical trials.

METHODS

This was a double-blind, randomized, placebo-controlled, group-comparison study of 18 months' duration. The study was conducted at University Hospitals of Cleveland/Case Western Reserve University and The University of Virginia Health System between 2001 and 2004. The study protocol and informed consent process were approved by the authorized human subjects committee at each institution. Fifteen-milligram pioglitazone and matching placebo tablets were supplied at no charge by Takeda Pharmaceuticals North America; the manufacturer had no other role in study conduct or analysis. Secure medication management and investigator blinding was provided by the investigational pharmacy service at each institution.

SUBJECTS

Twenty-nine subjects meeting National Institute of Neurological and Communicative Disorders and Stroke–the Alzheimer's Disease and Related Disorders Association criteria for probable AD were enrolled. Enrollment criteria included Mini-Mental State Examination[9] score between 12 and 26 and Clinical Dementia Rating[10] (CDR) score of 1 (mild severity) or 2 (moderate severity) at the time of treatment randomization and administration of the first dose of study medication. Potential subjects with medical conditions that would influence cognition or likelihood of study completion (including heart failure) were excluded, as were those without a reliable caregiver willing to participate and comply with protocol responsibilities. Patients with diabetes mellitus requiring treatment with oral medications or insulin were also excluded. All subjects who provided consent were randomized and received at least 1 dose of study medication. The patient flow is illustrated in the **Figure**.

Subjects received either 15-mg pioglitazone tablets or matched placebo beginning with 1 tablet daily. Daily dosing escalated by 1 tablet each week to 3 tablets daily to achieve a maximum dose of 45 mg of pioglitazone daily. Because of the potential for PPARγ activity by high-dose vitamin E supplementation, enrolled subjects discontinued all use of prior vitamin E supplements and were provided with 200-IU vitamin E capsules to be taken once daily. Medication compliance of more than 85% was required for continued participation and was assessed at each visit by pill counts.

Subjects could take prescribed cholinesterase inhibitor medications, provided they maintained a stable dose for 90 days prior to enrollment. Stable doses of antidepressant and antipsychotic drugs were also allowed if symptoms were adequately controlled. Memantine was approved for prescriptive use in the United States during this study. Based on subject demand, clinical equipoise, and the safety-oriented primary goal of the study, the protocol was modified to allow subjects to begin memantine therapy if prescribed. Memantine use was then incorporated as a planned covariate in the outcome analyses.

SAFETY MONITORING

Baseline health status was evaluated by physical and neurological examinations, routine blood tests, and electrocardiogram; these were repeated at study conclusion. Every 3 months, physical and neurological examinations, complete blood cell count, blood glucose level, hemoglobin A_{1C} level, and hepatic function markers (alanine aminotransferase and aspartate aminotransferase levels) were obtained. Clinical adverse event monitoring was conducted according to Food and Drug Administration regulations. An independent safety monitoring committee systematically reviewed adverse event reporting throughout the study.

EFFICACY OUTCOMES

One goal of the study was to explore the potential magnitude of treatment effects on outcomes used in dementia clinical trials. The study was not designed to demonstrate statistically significant effects on these outcomes. Outcome measures were collected every 3 months, with planned analyses for overall change over 18 months. If statistically significant differences were identified at 18 months, additional analyses of the 3-month data

©2011 American Medical Association. All rights reserved.
Downloaded From: http://archneur.jamanetwork.com/ by a Takeda Pharmaceuticals International User on 12/03/2014

Table 1. Subject Characteristics

	Mean (SD)	
	Pioglitazone (n=14)	Control (n=15)
Age, y[a]	74.9 (9.0)	67.0 (9.3)
Education, y	14.7 (3.0)	15.9 (2.5)
Baseline MMSE score	20.7 (3.5)	21.3 (3.4)
Male, %	36	40
Memantine Rx during trial, %	20	27

Abbreviations: MMSE, Mini-Mental State Examination; Rx, prescription.
[a] $P<.05$.

would be conducted to determine the time course of the treatment response. Clinical outcome measures were:

1. Clinical Dementia Rating sum of boxes (CDR-SB): This is an alternate scoring system, using the same data collection process as the CDR.[10] In contrast to its standard scoring, which provides ordinal-level data, CDR-SB provides interval-scale data, which were amenable to our planned statistical analyses.
2. Alzheimer's Disease Assessment Scale Cognitive Score (ADAS-COG): This is a very sensitive 70-point psychometric scale for measuring cognitive function with an emphasis on memory, language, and praxis.[11]
3. Neuropsychiatric Inventory: This was developed to assess behavioral disturbances occurring in patients with dementia. It rates severity and frequency of behavioral and psychiatric symptoms associated with dementia.[12]
4. Alzheimer's Disease Functional Assessment and Change Score: This scale assesses changes in instrumental and basic activities of daily living over time.[13]
5. Nurses' Observation Scale for Geriatric Patients: This is an easily administered scale designed to provide reliable assessments of multiple realms of function, namely memory, instrumental activities of daily living, self-care, mood, social behavior, and disturbing behavior. The instrument obtains caregiver ratings for each of 30 items on a 5-point scale according to frequency of occurrence. It provides a summary of the caregiver's interpretation of the impact of dementia on the subject's life.[14]

Additionally, the Clinician's Interview-Based Impression–Plus was evaluated at baseline and study conclusion. This is a global rating derived through an independent, comprehensive interview between the subject and caregiver by a clinician who is barred from knowledge of all psychometric test scores. Using the results from baseline for reference, the clinician interviewed the subject and caregiver at the final visit to obtain an "Impression of Change."[15]

ANALYSIS PLAN EFFICACY

Given the small sample size, efficacy analyses were intended to be exploratory. *t* Tests and χ^2 tests for independence were used, where appropriate, to test whether the 2 treatment groups (pioglitazone vs placebo) were similar or different in terms of age at baseline, education, sex, ethnicity (white vs minority), Mini-Mental State Examination score at baseline, presence of an APOE4 allele, and use of memantine during the study period.

The effects of pioglitazone on the clinical efficacy variables and on their rates of change over time were evaluated using multilevel models for repeated measures, except for Clinician's Interview-Based Impression–Plus Impression of Change for which only baseline and termination scores were obtained. Multilevel analysis, a statistical technique for analyzing data with nested variability,[16,17] is also commonly referred to as "hierarchical linear modeling" or "mixed models." It corrects for a lack of independence within clusters, such as several repeated observations within the same subject.

Table 2. Adverse Events Reported by 3 or More Pioglitazone-Treated Subjects

	No. (%)	
	Pioglitazone (n=14)	Placebo (n=15)
Cold symptoms	9 (64.3)	11 (73.3)
Glucose level low/asymptomatic	4 (28.6)	4 (26.7)
Muscle/skeletal pain	4 (28.6)	4 (26.7)
Nausea/vomiting	4 (28.6)	3 (20.0)
Swelling/edema of leg	4 (28.6)	0
Abdominal pain	3 (21.4)	1 (6.7)
Anemia	3 (21.4)	2 (13.3)
Diarrhea	3 (21.4)	1 (6.7)
Dizziness	3 (21.4)	4 (26.7)
Fatigue	3 (21.4)	5 (33.3)
Increased confusion	3 (21.4)	5 (33.3)

RESULTS

SUBJECT CHARACTERISTICS

Initial enrollment was 29 (14 pioglitazone, 15 placebo) subjects; 25 subjects (12 pioglitazone, 13 placebo) completed 18 months of therapy. Early discontinuations were associated with change in caregiver status (n=2) and withdrawal of consent (n=2). The sample characteristics are reported in **Table 1**. Women constituted 64% of the pioglitazone group and 60% of the placebo group. Patients receiving pioglitazone were older than those in the placebo group (mean, 74.9 years vs 67.0 years; $P<.05$); no other demographic variable differed between groups. No statistically significant differences for education, sex, ethnicity, APOE4 status, or Mini-Mental State Examination score at baseline were identified (all *P* values $>.05$). Seven patients began memantine therapy during the study (3 pioglitazone, 4 placebo). There was no difference in the time to onset of memantine therapy between treatment groups ($P>.05$).

SAFETY AND TOLERABILITY

No early discontinuations were attributed to adverse events. In general, pioglitazone was well tolerated, with no pattern of effect on blood glucose levels, hemoglobin A_{1C} levels, or other blood chemistry or hematologic measures. No serious adverse events were associated with pioglitazone treatment. Peripheral edema was the adverse effect most clearly different between groups, affecting 4 pioglitazone-treated and no placebo-treated subjects. Edema is a commonly recognized effect of pioglitazone in clinical use and this potential adverse treatment effect was anticipated. Adverse events affecting at least 3 pioglitazone-treated subjects are reported in **Table 2**; all were of mild or moderate severity.

©2011 American Medical Association. All rights reserved.
Downloaded From: http://archneur.jamanetwork.com/ by a Takeda Pharmaceuticals International User on 12/03/2014

Table 3. Means, Standard Deviations, and Sample Sizes by Treatment Group and Outcome Measure

	Baseline		6 mo		12 mo		18 mo	
Outcome Measure	Mean (SD)	Sample Size	Mean (SD)	Sample Size	Mean (SD)	Sample Size	Mean (SD)	Sample Size
ADAS-COG								
Pioglitazone	21.79 (7.3)	14	21.31 (9.64)	13	23.67 (10.64)	12	27.25 (11.92)	12
Placebo	20.2 (9.5)	15	18.43 (9.98)	14	23.5 (12.66)	14	26.08 (12.3)	13
NPI total score								
Pioglitazone	10.43 (9.68)	14	5.77 (4.68)	13	12 (12.46)	12	6.75 (8.55)	12
Placebo	6.67 (8.12)	15	11.79 (8.16)	14	7.71 (7.29)	14	10.85 (7.84)	13
NOSGER score								
Pioglitazone	92.71 (12.72)	14	90.92 (11.64)	13	89.25 (11.18)	12	88.42 (11.02)	12
Placebo	94.93 (14.21)	15	92.5 (12.7)	14	94.14 (10.66)	14	89.46 (15.06)	13
ADFACS total								
Pioglitazone	29.29 (10.42)	14	30.62 (8.95)	13	32.83 (9.44)	12	35.67 (8.6)	12
Placebo	25.67 (7.07)	15	28.64 (8.71)	14	31.29 (9.43)	14	31.08 (11.24)	13
CDR-SB								
Pioglitazone	6.44 (2.13)	14	7.12 (2.85)	13	8.17 (2.89)	12	8.92 (4.15)	12
Placebo	5.24 (1.32)	15	6.36 (2.59)	14	5.77 (2.24)	14	7.58 (3.24)	13

	Baseline		Termination	
Outcome Measure	Mean (SD)	Sample Size	Mean (SD)	Sample Size
CIBIC-Plus score				
Pioglitazone	3.71 (0.726)	14	4.15 (0.987)	13
Placebo	3.4 (0.507)	15	3.64 (0.841)	14

Abbreviations: ADAS-COG, Alzheimer's Disease Assessment Scale Cognitive Score; ADFACS, Alzheimer's Disease Functional Assessment and Change Score; CDR-SB, Clinical Dementia Rating sum of boxes; CIBIC-Plus, Clinician's Interview-Based Impression–Plus Impression of Change; NOSGER, Nurses' Observation Scale for Geriatric Patients; NPI, Neuropsychiatric Inventory.

Table 4. Regression Coefficients for Multilevel Growth Curve Model by Outcome

	NPI Total Score	ADAS-COG	ADFACS Total	CDR-SB	NOSGER Score
Constant	3.981	−3.108[a]	3.586	−1.189	−1.672
Time, mo	0.066	0.321[a]	0.322[a]	0.127[a]	0.127[a]
Pioglitazone	−1.139	−0.746	−1.468	−0.354	0.363
Outcome at baseline	0.580[a]	1.100[a]	0.894[a]	1.229[a]	1.321[a]
Between-subject variance	9.586	5.779[a]	7.425[a]	0.566	0.562
Within-subject variance	46.800[a]	13.849[a]	15.562[a]	2.088[a]	2.085[a]
−2×log (likelihood function)	731.319	611.533	626.379	398.581	398.331

Abbreviations: ADAS-COG, Alzheimer's Disease Assessment Scale Cognitive Score; ADFACS, Alzheimer's Disease Functional Assessment and Change Score; CDR-SB, Clinical Dementia Rating sum of boxes; CIBIC-Plus, Clinician's Interview-Based Impression–Plus Impression of Change; NOSGER, Nurses' Observation Scale for Geriatric Patients; NPI, Neuropsychiatric Inventory.
[a] $P<.05$.

EFFICACY

Observed mean scores at 6-month intervals, as well as entry and final Clinician's Interview-Based Impression–Plus Impression of Change scores, are shown in **Table 3**. Regression coefficients from the multilevel analysis are illustrated in **Table 4**. The coefficient for pioglitazone is the estimated difference in the adjusted mean for the outcome between the pioglitazone group and the placebo group. The coefficient of pioglitazone for ADAS-COG indicates that the adjusted mean for the ADAS-COG per month is −0.746 point less in the pioglitazone group than in the placebo group. As predicted by our small sample size, no significant effect of treatment was observed on any clinical outcome measure. All measures except Neuropsychiatric Inventory total score worsened over time ($P<.05$), consistent with the progressive course of AD.

EFFECT SIZE CALCULATIONS

An exploratory goal of this study was to estimate treatment effect size for pioglitazone. Sample size analyses were conducted to determine the number of subjects needed to detect significant differences between the pioglitazone and control group on 2 outcome measures typically used for regulatory approval, ADAS-COG and CDR-SB. We used Optimal Design software (J. Spybrook, S. W. Raudenbush, R. Congdon, A. Martinez, "Optimal Design for Longitudinal and Multilevel

©2011 American Medical Association. All rights reserved.
Downloaded From: http://archneur.jamanetwork.com/ by a Takeda Pharmaceuticals International User on 12/03/2014

Research," University of Michigan: Institute of Social Research, 2009) to compute the sample size needed to detect a significant difference of the magnitude of the regression coefficient for pioglitazone estimated in Table 4 (−0.746 for ADAS-COG and −0.354 for CDR-SB). For $\alpha = .05$ and power = 0.80, a sample size of 340 (170 pioglitazone, 170 placebo) would be needed to find the estimated effect (−0.746) of pioglitazone on ADAS-COG to be significant. For $\alpha = .05$ and power = 0.80, a sample size of 155 (78 pioglitazone, 77 placebo) would be needed to find the estimated effect (−0.354) of pioglitazone on CDR-SB to be significant. The needed sample size for CDR-SB is slightly less than half the needed sample size for ADAS-COG. Pivotal trials leading to Food and Drug Administration approval of currently available drugs typically enrolled 250 to 500 patients. Several ongoing clinical trials for disease-modifying agents will enroll more than 1000 subjects to test their hypotheses. These figures suggest that further studies to assess the clinical efficacy of pioglitazone or similar PPARγ agents would be feasible.

COMMENT

Pioglitazone was well tolerated, demonstrating no unanticipated safety problems in a sample of patients with AD without diabetes mellitus through an 18-month treatment trial. No efficacy was demonstrated on clinical outcome measures. Although marketed for the treatment of type 2 diabetes, long-term pioglitazone administration did not lead to clinically significant changes in blood glucose levels in these nondiabetic individuals. Edema is a frequent complication of thiazolidinedione use in clinical populations, affecting as much as 18% of treated individuals.[18] This rate is consistent with our observations (4 of 14 subjects, 28.6%), but much higher than prescribing information would predict, as well as higher than observed in the trial of rosiglitazone treatment in AD.[3] The risks for peripheral edema, heart failure, and other cardiovascular morbidities will need to be closely monitored if future trials of thiazolidinedione agents are undertaken for AD. Additionally, edema may limit blinding in studies of pioglitazone.

This study was not intended to determine treatment efficacy. At the time of its design (1999-2000), no human data existed regarding the magnitude of any potential treatment effect of thiazolidinediones in AD, nor was information published on the effects of thiazolidinediones on nondiabetic older adults. The efficacy measures were selected to cover a broad range of outcomes of both clinical relevance and regulatory impact. As expected, no treatment effects were observed on the efficacy outcomes. The small and nonsignificant differences suggest that mild to moderate AD is not likely to be an appropriate population for further study of thiazolidinediones.

The reasons why PPARγ agonists exert a beneficial effect in AD models but not in clinical samples remains unclear. Disease severity may play a role. Reducing systemic insulin resistance through PPARγ modulation has a salutary effect on neuronal function and memory formation,[19] which could contribute to the greater observed treatment effect in earlier phases of AD, like mild cognitive impairment. The amount of neuronal loss and synaptic dysfunction present by the time the full AD clinical syndrome is evident may overwhelm the functional benefits associated with treatment. It is also possible that the suppression of microglially mediated inflammation by thiazolidinediones is insufficient to exert a clinically relevant impact in humans. Furthermore, there may be endophenotypes of AD, such as APOE4-negative individuals or those with greater insulin resistance, who might selectively benefit from this drug class. Our study was too small to evaluate the clinical meaningfulness of such variables.

Disappointing results of treatment trials based on the amyloid hypothesis, and the reasonable degree of safety identified in this trial, suggest that exploratory studies of thiazolidinediones remain warranted. Future studies of this class should focus on earlier stages of disease progression and be augmented by biomarkers, such as nuclear imaging techniques, to measure changes in microglial activation associated with treatment.

Accepted for Publication: July 8, 2010.
Published Online: September 13, 2010. doi:10.1001/archneurol.2010.229
Correspondence: David S. Geldmacher, MD, Department of Neurology, PO Box 800394, Charlottesville, VA 22908 (dsg8n@virginia.edu).
Author Contributions: All authors had full access to all study data. *Study concept and design:* Geldmacher and Landreth. *Acquisition of data:* Geldmacher. *Analysis and interpretation of data:* Geldmacher, Fritsch, McClendon, and Landreth. *Drafting of the manuscript:* Geldmacher and Landreth. *Critical revision of the manuscript for important intellectual content:* Geldmacher, Fritsch, McClendon, and Landreth. *Statistical analysis:* Fritsch and McClendon. *Obtained funding:* Landreth. *Administrative, technical, and material support:* Geldmacher.
Financial Disclosure: Drs Geldmacher and Landreth have received consulting fees from Takeda Pharmaceuticals North America and consulting fees and research support from GlaxoSmithKline. Takeda Pharmaceuticals North America provided pioglitazone tablets and matching placebo free of charge. Case Western Reserve University has been issued a patent for the use of pioglitazone in treatment of central nervous system disorders including AD.
Funding/Support: This study was supported by National Institute on Aging grant R01AG18905.
Role of the Sponsors: The sponsors played no role in data analysis or interpretation nor in the preparation of the report.
Additional Contributions: We thank the clinical trials research staff at the University Memory and Aging Center (Cleveland, Ohio) and the Memory Disorders Program (Charlottesville, Virginia) for their dedication and excellence in carrying out the study. We also gratefully acknowledge the contributions of Alan Lerner, MD; Concepcion Santillan, MD; and Kathleen Smyth, PhD, to the execution, monitoring, and analysis of the study.

©2011 American Medical Association. All rights reserved.
Downloaded From: http://archneur.jamanetwork.com/ by a Takeda Pharmaceuticals International User on 12/03/2014

REFERENCES

1. Jiang Q, Heneka M, Landreth GE. The role of peroxisome proliferator-activated receptor-gamma (PPARgamma) in Alzheimer's disease: therapeutic implications. *CNS Drugs*. 2008;22(1):1-14.
2. Watson GS, Cholerton BA, Reger MA, et al. Preserved cognition in patients with early Alzheimer disease and amnestic mild cognitive impairment during treatment with rosiglitazone: a preliminary study. *Am J Geriatr Psychiatry*. 2005; 13(11):950-958.
3. Risner ME, Saunders AM, Altman JF, et al; Rosiglitazone in Alzheimer's Disease Study Group. Efficacy of rosiglitazone in a genetically defined population with mild-to-moderate Alzheimer's disease. *Pharmacogenomics J*. 2006;6(4):246-254.
4. Festuccia WT, Oztezcan S, Laplante M, et al. Peroxisome proliferator-activated receptor-gamma-mediated positive energy balance in the rat is associated with reduced sympathetic drive to adipose tissues and thyroid status. *Endocrinology*. 2008;149(5):2121-2130.
5. Heneka MT, Sastre M, Dumitrescu-Ozimek L, et al. Acute treatment with the PPARgamma agonist pioglitazone and ibuprofen reduces glial inflammation and Abeta1-42 levels in APPV717I transgenic mice. *Brain*. 2005;128(pt 6):1442-1453.
6. Maeshiba Y, Kiyota Y, Yamashita K, Yoshimura Y, Motohashi M, Tanayama S. Disposition of the new antidiabetic agent pioglitazone in rats, dogs, and monkeys. *Arzneimittelforschung*. 1997;47(1):29-35.
7. Roberts JC, Friel SL, Roman S, et al. Autoradiographical imaging of PPARgamma agonist effects on PBR/TSPO binding in TASTPM mice. *Exp Neurol*. 2009; 216(2):459-470.
8. Nicolakakis N, Aboulkassim T, Ongali B, et al. Complete rescue of cerebrovascular function in aged Alzheimer's disease transgenic mice by antioxidants and pioglitazone, a peroxisome proliferator-activated receptor gamma agonist. *J Neurosci*. 2008;28(37):9287-9296.
9. Folstein MF, Folstein SE, McHugh PR. "Mini-mental state": a practical method for grading the cognitive state of patients for the clinician. *J Psychiatr Res*. 1975; 12(3):189-198.
10. Morris JC. The Clinical Dementia Rating (CDR): current version and scoring rules. *Neurology*. 1993;43(11):2412-2414.
11. Rosen WG, Mohs RC, Davis KL. A new rating scale for Alzheimer's disease. *Am J Psychiatry*. 1984;141(11):1356-1364.
12. Cummings JL, Mega M, Gray K, Rosenberg-Thompson S, Carusi DA, Gornbein J. The Neuropsychiatric Inventory: comprehensive assessment of psychopathology in dementia. *Neurology*. 1994;44(12):2308-2314.
13. Mohs RC, Doody RS, Morris JC, et al; "312" Study Group. A 1-year, placebo-controlled preservation of function survival study of donepezil in AD patients. *Neurology*. 2001;57(3):481-488.
14. Spiegel R, Brunner C, Ermini-Fünfschilling D, et al. A new behavioral assessment scale for geriatric out- and in-patients: the NOSGER (Nurses' Observation Scale for Geriatric Patients). *J Am Geriatr Soc*. 1991;39(4):339-347.
15. Reisberg B, Schneider L, Doody R, et al. Clinical global measures of dementia: position paper from the International Working Group on Harmonization of Dementia Drug Guidelines. *Alzheimer Dis Assoc Disord*. 1997;11(suppl 3):8-18.
16. Bryk AS, Raudenbush SW. *Hierarchical Linear Models*. Newbury Park, CA: Sage; 1992.
17. Goldstein H. *Multilevel Statistical Models*. 2nd ed. New York, NY: Halstead; 1995.
18. Niemeyer NV, Janney LM. Thiazolidinedione-induced edema. *Pharmacotherapy*. 2002;22(7):924-929.
19. Craft S, Watson GS. Insulin and neurodegenerative disease: shared and specific mechanisms. *Lancet Neurol*. 2004;3(3):169-178.

Announcement

Sign Up for Alerts—It's Free! *Archives of Neurology* offers the ability to automatically receive the table of contents of *Archives* when it is published online. This also allows you to link to individual articles and view the abstract. It makes keeping up-to-date even easier! Go to http://pubs.ama-assn.org/misc/alerts.dtl to sign up for this free service.

©2011 American Medical Association. All rights reserved.
Downloaded From: http://archneur.jamanetwork.com/ by a Takeda Pharmaceuticals International User on 12/03/2014


US009102666B2

(12) **United States Patent**
Roses et al.

(10) **Patent No.: US 9,102,666 B2**
(45) **Date of Patent: Aug. 11, 2015**

(54) **METHODS AND DRUG PRODUCTS FOR TREATING ALZHEIMER'S DISEASE**

(75) Inventors: **Allen D. Roses**, Chapel Hill, NC (US); **Rajneesh Taneja**, Libertyville, IL (US)

(73) Assignees: **ZINFANDEL PHARMACEUTICALS, INC.**, Durham, NC (US); **TAKEDA PHARMACEUTICAL COMPANY LIMITED**, Osaka (JP)

(*) Notice: Subject to any disclaimer, the term of this patent is extended or adjusted under 35 U.S.C. 154(b) by 460 days.

(21) Appl. No.: **13/346,081**

(22) Filed: **Jan. 9, 2012**

(65) **Prior Publication Data**

US 2012/0184584 A1 Jul. 19, 2012

Related U.S. Application Data

(60) Provisional application No. 61/431,370, filed on Jan. 10, 2011.

(51) **Int. Cl.**

A61K 31/4439	(2006.01)
A61P 25/00	(2006.01)
A61P 25/28	(2006.01)
G01N 33/50	(2006.01)
C07D 417/12	(2006.01)
C12Q 1/68	(2006.01)

(52) **U.S. Cl.**

CPC ***C07D 417/12*** (2013.01); ***A61K 31/4439*** (2013.01); ***C12Q 1/6883*** (2013.01); *C12Q 2600/106* (2013.01); *C12Q 2600/118* (2013.01); *C12Q 2600/156* (2013.01); *C12Q 2600/172* (2013.01); *Y10T 436/143333* (2015.01)

(58) **Field of Classification Search**

CPC A61K 31/4439; A61P 25/00; A61P 25/28; G01N 33/50; C07D 417/12; C12Q 1/68

USPC 514/342; 546/269.7; 435/6.11; 436/94

See application file for complete search history.

(56) **References Cited**

U.S. PATENT DOCUMENTS

4,687,777	A	8/1987	Meguro et al.
5,002,953	A	3/1991	Hindley
5,112,460	A	5/1992	Karger et al.
5,171,750	A	12/1992	Brossi et al.
5,326,770	A	7/1994	Wilkerson
5,508,167	A	4/1996	Roses et al.
5,595,883	A	1/1997	Appleyard et al.
5,716,828	A	2/1998	Roses et al.
5,716,975	A	2/1998	Bue-Valleskey et al.
5,904,824	A	5/1999	Oh
5,965,569	A	10/1999	Camps Garcia et al.
5,965,584	A	10/1999	Ikeda et al.
5,990,126	A	11/1999	Park et al.
6,027,896	A	2/2000	Roses et al.
6,191,154	B1	2/2001	Landreth et al.
6,291,182	B1	9/2001	Schork et al.
6,303,633	B1	10/2001	Chen et al.
6,355,429	B1	3/2002	Nygren et al.
6,399,639	B1	6/2002	Matsui et al.
6,401,043	B1	6/2002	Stanton, Jr. et al.
6,432,985	B2	8/2002	Alanine et al.
6,532,467	B1	3/2003	Brocklebank et al.
6,642,267	B2	11/2003	Przewosny et al.
6,673,780	B2	1/2004	Dasseux et al.
6,680,299	B2	1/2004	Or et al.
6,699,910	B2	3/2004	Dasseux et al.
6,703,422	B2	3/2004	Dasseux et al.
6,811,988	B2	11/2004	Chojkier et al.
6,828,462	B2	12/2004	Henrich et al.
6,838,452	B2	1/2005	Harats et al.
6,956,055	B2	10/2005	Sundermann et al.
6,964,868	B1	11/2005	Williams et al.
7,052,849	B2	5/2006	Jackowski et al.
7,122,373	B1	10/2006	Williams et al.
7,127,466	B2	10/2006	Brocklebank et al.
7,132,244	B2	11/2006	Jackowski et al.
7,135,297	B2	11/2006	Jackowski et al.
7,186,704	B2	3/2007	Harats et al.

(Continued)

FOREIGN PATENT DOCUMENTS

EP	2172200 A1	4/2010
WO	WO 02/30860 A2	4/2002

(Continued)

OTHER PUBLICATIONS

Massimo Collino, Manuela Aragno, Raffaella Mastrocola, Margherita Gallicchio, Arianna Carolina Rosa, Chiara Dianzani, Oliviero Danni, Christopher Thiemermann, Roberto Fantozzi, Modulation of the oxidative stress and inflammatory response by PPAR-g agonists in the hippocampus of rats exposed to cerebral ischemia/reperfusion, European Journal of Phar.*

Office Action dated Apr. 16, 2013, in U.S. Appl. No. 13/058,724.

Reference SNP (refSNP) cluster report: rs10524523, printed on Apr. 10, 2013 from www.ncbi.nlm.nih.gov, 2 pages.

Hegele, Robert A., "SNP Judgments and Freedom of Association," Arterioscler. Thromb. Vasc. Biol., 2002, 22;1058-1061.

Jueppner, H., "Functional Properties of the PTH/PTHrP Receptor," Bone, Aug. 1995, 17(2)Supplement:39S-42S.

(Continued)

Primary Examiner — Sreeni Padmanabhan
Assistant Examiner — Jason A Deck
(74) *Attorney, Agent, or Firm* — Foley & Lardner LLP

(57) **ABSTRACT**

Provided herein are drug products with low dose pioglitazone for use in the treatment (e.g., delay of onset) of cognitive impairment of the Alzheimer's type. Methods of manufacture thereof are also provided. Further provided are methods of treatment for Alzheimer's disease including administering a drug product with low dose pioglitazone. The methods may include determining whether the subject is at risk of developing Alzheimer's disease based upon the subject's age and TOMM40 523 genotype.

24 Claims, 9 Drawing Sheets

(56) **References Cited**

U.S. PATENT DOCUMENTS

7,304,093	B2	12/2007	Dasseux et al.
7,329,501	B2	2/2008	Jackowski et al.
7,504,388	B2	3/2009	Harats et al.
7,608,412	B2	10/2009	Wooten et al.
7,625,882	B2	12/2009	Harats et al.
7,833,513	B2	11/2010	De la Monte et al.
7,888,035	B2	2/2011	Klass et al.
7,893,291	B2	2/2011	Harats et al.
7,897,356	B2	3/2011	Klass et al.
7,902,176	B2	3/2011	Harats et al.
7,973,023	B2	7/2011	Harats et al.
8,005,623	B2	8/2011	Hellerstein
2002/0077316	A1	6/2002	Dasseux et al.
2003/0022865	A1	1/2003	Dasseux et al.
2003/0078239	A1	4/2003	Dasseux et al.
2003/0096431	A1	5/2003	Jackowski et al.
2003/0100126	A1	5/2003	Jackowski et al.
2003/0220374	A1	11/2003	Needleman
2003/0225035	A1	12/2003	Harats et al.
2004/0060077	A1	3/2004	Esmond et al.
2004/0106677	A1	6/2004	Harats et al.
2004/0122091	A1	6/2004	Dasseux et al.
2004/0198814	A1	10/2004	Dasseux et al.
2004/0204502	A1	10/2004	Dasseux et al.
2004/0265849	A1	12/2004	Cargill et al.
2005/0004179	A1	1/2005	Pedersen
2005/0020694	A1	1/2005	Dasseux et al.
2005/0021236	A1	1/2005	Aston et al.
2005/0043242	A1	2/2005	Esmond et al.
2005/0272813	A1	12/2005	Harats et al.
2005/0277129	A1	12/2005	Aerssens et al.
2006/0020440	A1	1/2006	Hellerstein
2006/0194339	A1	8/2006	Jackowski et al.
2006/0205091	A1	9/2006	Jackowski et al.
2006/0211138	A1	9/2006	Jackowski et al.
2006/0211139	A1	9/2006	Jackowski et al.
2006/0211140	A1	9/2006	Jackowski et al.
2006/0211141	A1	9/2006	Jackowski et al.
2006/0211145	A1	9/2006	Jackowski et al.
2006/0211146	A1	9/2006	Jackowski et al.
2006/0228728	A1	10/2006	Cox et al.
2007/0010029	A1	1/2007	Jackowski et al.
2007/0099868	A1	5/2007	Harats et al.
2007/0105856	A1	5/2007	Carpino et al.
2007/0149615	A9	6/2007	Dasseux et al.
2007/0203083	A1	8/2007	Mootha et al.
2007/0238643	A1	10/2007	Wooten et al.
2008/0045582	A1	2/2008	Zineh et al.
2008/0051318	A1	2/2008	Li et al.
2008/0153088	A1	6/2008	Sun et al.
2008/0226719	A1	9/2008	Roses et al.
2008/0261865	A1	10/2008	Harats et al.
2008/0286876	A1	11/2008	Stephanie
2009/0042849	A1	2/2009	Birnbaum
2009/0143442	A1	6/2009	Colca et al.
2009/0209775	A1	8/2009	Harats et al.
2010/0048515	A1	2/2010	Harats et al.
2010/0092470	A1	4/2010	Bhatt et al.
2010/0105034	A1	4/2010	Hutton et al.
2010/0113290	A1	5/2010	Klass et al.
2010/0120842	A1	5/2010	Barlow et al.
2010/0136584	A1	6/2010	Bhatt et al.
2010/0184046	A1	7/2010	Klass et al.
2010/0203529	A1	8/2010	Kuslich et al.
2010/0256235	A1	10/2010	Puder et al.
2011/0082187	A1	4/2011	Campbell et al.
2011/0097350	A1	4/2011	Harats et al.
2011/0151460	A1	6/2011	Klass et al.
2011/0159506	A1	6/2011	Klass et al.
2011/0166185	A1	7/2011	Roses
2011/0189165	A1	8/2011	Roses
2011/0189212	A1	8/2011	Harats et al.
2011/0195394	A1	8/2011	Selinfreund et al.
2011/0195395	A1	8/2011	Selinfreund et al.
2011/0195396	A1	8/2011	Selinfreund et al.
2011/0195397	A1	8/2011	Selinfreund et al.
2011/0195398	A1	8/2011	Selinfreund et al.
2011/0195399	A1	8/2011	Selinfreund et al.
2011/0195400	A1	8/2011	Selinfreund et al.
2011/0195401	A1	8/2011	Selinfreund et al.
2011/0195402	A1	8/2011	Selinfreund et al.
2011/0195403	A1	8/2011	Selinfreund et al.
2011/0195404	A1	8/2011	Selinfreund et al.
2011/0195421	A1	8/2011	Selinfreund et al.
2011/0195422	A1	8/2011	Selinfreund et al.
2011/0195423	A1	8/2011	Selinfreund et al.
2011/0195424	A1	8/2011	Selinfreund et al.
2011/0195425	A1	8/2011	Selinfreund et al.
2011/0195427	A1	8/2011	Selinfreund et al.
2011/0195439	A1	8/2011	Selinfreund et al.
2011/0195440	A1	8/2011	Selinfreund et al.
2011/0195487	A1	8/2011	Selinfreund et al.
2011/0195488	A1	8/2011	Selinfreund et al.
2011/0195491	A1	8/2011	Selinfreund et al.
2011/0195508	A1	8/2011	Selinfreund et al.
2011/0195851	A1	8/2011	Selinfreund et al.
2011/0195855	A1	8/2011	Selinfreund et al.
2011/0195856	A1	8/2011	Selinfreund et al.
2011/0195857	A1	8/2011	Selinfreund et al.
2011/0195858	A1	8/2011	Selinfreund et al.
2011/0195859	A1	8/2011	Selinfreund et al.
2011/0195871	A1	8/2011	Selinfreund et al.
2011/0195872	A1	8/2011	Selinfreund et al.
2011/0195873	A1	8/2011	Selinfreund et al.
2011/0195874	A1	8/2011	Selinfreund et al.
2011/0196085	A1	8/2011	Selinfreund et al.
2011/0236317	A1	9/2011	Cravo et al.
2011/0237450	A1	9/2011	Klass et al.

FOREIGN PATENT DOCUMENTS

WO	WO 02/30882	A2	4/2002
WO	WO 02/30884	A2	4/2002
WO	WO 02/41827	A2	5/2002
WO	WO 03/046001	A2	6/2003
WO	WO 03/046005	A2	6/2003
WO	WO 03/046573	A2	6/2003
WO	WO 2004/005510	A1	1/2004
WO	WO 2004/106486	A2	12/2004
WO	WO 2005/003766	A2	1/2005
WO	WO 2005/047236	A1	5/2005
WO	WO 2005/081943	A2	9/2005
WO	WO 2006/054297	A2	5/2006
WO	WO 2007/038112	A2	4/2007
WO	WO 2007/038115	A2	4/2007
WO	WO 2007/044522	A1	4/2007
WO	WO 2007/109024	A2	9/2007
WO	WO 2008/019187	A2	2/2008
WO	WO 2008/036678	A2	3/2008
WO	WO 2008/147562	A2	12/2008
WO	WO 2010/019550	A2	2/2010
WO	WO 2010/033913	A1	3/2010
WO	WO 2010/053788	A1	5/2010
WO	WO 2010/056337	A2	5/2010
WO	WO 2010/062706	A2	6/2010
WO	WO 2010/066901	A2	6/2010
WO	WO 2010/100653	A2	9/2010
WO	WO 2010/123720	A1	10/2010
WO	WO 2011/109440	A1	9/2011
WO	WO 2011/127219	A1	10/2011

OTHER PUBLICATIONS

Fu, P.C., "The Effect and Mechanism Research of Pioglitazone to the Memory Impairment of Ad Rats," Globe Thesis [online] Sep. 22, 2010 (retrieved on Sep. 4, 2012), 2 page abstract.

Ponce-Lopez et al., "Lithium, phenserine, memantine and pioglitazone reverse memory deficit and restore phosphor-GSK3β decreased in hippocampus in intracerebroventricular streptozotocin induced memory deficit model," Brain Research, Oct. 1, 2011, 1426:73-85.

Doraiswamy et al., "Pharmacological strategies for the prevention of Alzheimer's disease," Expert Opinion on Pharmacotherapy, Jan. 2006, 7(1):1-10.

HIV

Drug Effectiveness Explained: The Mathematics of Antiviral Agents for HIV

Alan S. Perelson[1]* and Steven G. Deeks[2,3]

Antiretroviral therapy has improved the quality and length of life of millions of individuals affected by human immunodeficiency virus type 1 (HIV-1). The capacity of these drugs to indefinitely suppress HIV—which has a well-known capacity for escaping antiviral pressures—is surprising. In this issue of *Science Translational Medicine*, Shen *et al.* use a combination of mathematical modeling and experiment to examine the potency of anti-HIV drugs. They show that non-nucleoside reverse transcriptase inhibitors and protease inhibitors exhibit cooperative dose-response curves—a finding that has implications for the treatment of HIV as well as other viral infections, such as hepatitis C.

INTRODUCTION

Antiretroviral therapy has changed human immunodeficiency virus type 1 (HIV-1) infection from a death sentence to a treatable chronic illness. Since the mid-1990s when combination therapy first became available (*1*, *2*), the death rate from HIV has declined substantially (*3*). Although a cure has been elusive, long-lasting and perhaps lifelong control of HIV replication can be achieved in essentially all patients who have access to these drugs and who are able to adhere to the dosing requirements. The fact that therapy is so effective remains a puzzle. HIV replicates at a high titer and mutates constantly. Resistance to certain drugs given as monotherapy can emerge and dominate in the virus population in 14 days (*4*). The virus is known to replicate in several cellular and tissue sanctuaries; any one of these might serve as a source for low-level replication and eventual escape. Given the robust capacity for the virus to evolve in response to almost any antiviral pressure, many clinicians, researchers, and patients remain dubious about the prediction that antiretroviral drugs will work for everyone and for decades, yet the emerging clinical data suggest that this is indeed happening. In this issue of *Science Translational Medicine*, Shen and colleagues provide novel insights into the effectiveness of these drugs (*5*). This work might provide insights relevant to other antiviral strategies (including emerging work on the management of hepatitis C) and might even inform the future development of safer combination regimens for HIV as well as possibly provide insight into how to cure HIV infection.

DOSE RESPONSE

It was recognized around the 16th century that a drug's effect depended on its dose. A prescription written in 1562 for a mixture of hyoscyamus and opium stated that giving one dram to a person caused sleep, but added "If you want him to sleep less, give him less" (*6*). The notion that a drug's dose and effect are related is a basic tenet of pharmacology and is generally summarized by an experimentally derived dose-response curve. Determining the dose that gives 50% of the maximum response is one way to quantify the potency of a drug; For example, for an enzyme inhibitor such as a protease or reverse transcriptase inhibitor, one can determine the IC_{50} (the concentration of a drug needed to produce 50% of the maximal inhibitory effect in vitro) or the ED_{50} (the plasma concentration of a drug required to obtain 50% of the maximal effect in vivo). Frequently, the dose-response curve is an S-shaped curve, such as those shown in Fig. 1.

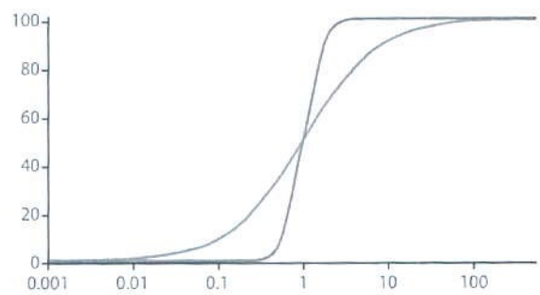


Fig. 1. Dose-response curves. A typical dose-response curve is shown in blue. The IC_{50} is the dose that leads to 50% of the maximal response; for both curves, the IC_{50} is 1. Each curve has a different slope m, which is also known as the Hill coefficient. For the blue curve, $m = 1$, whereas the red curve has a steeper slope of $m = 4$. In other words, the higher the Hill coefficient, the steeper the curve, and the more potent the drug at small increases in concentration above the IC_{50}. Curves with $m > 1$ usually arise from cooperative interactions.

Dose-response curves with the same IC_{50} can have varying steepness or slope (Fig. 1). Both the red and blue dose-response curves have an IC_{50} of 1; yet, for the red curve a dose of 5 generates 99.8% of the maximal response, whereas for the blue curve a dose of 5 yields 83% of the maximum response. A steep dose-response curve means that a drug concentration slightly above the IC_{50} can lead to extremely high levels of inhibition. Furthermore, if the maximum drug concentration that one can obtain in a patient is high (for example, 100 in Fig. 1) then the trough concentration can be 95% lower without any noticeable loss in drug effectiveness; this is true for the red dose-response curve, but not for the blue curve. Thus, the steepness of the dose-response curve has important clinical implications.

A function that describes many dose-response curves and has a long and venerable history in biochemistry was applied empirically by Hill in 1910 to describe the binding of oxygen to hemoglobin (*7*). This Hill equation—which has also been used to describe the effectiveness of a drug, such as interferon for the treatment of hepatitis C (*8*, *9*) or an antiretroviral for the treatment of HIV (*10*)—is written as

$$\varepsilon = \frac{D^m}{IC_{50}^m + D^m} \quad (1)$$

where D is the drug dose; m is the Hill coefficient; and ε is the response or the effectiveness of the drug, which varies between 0 (no effect of the drug) and 1 (the maximal effect). For the blue curve in Fig. 1, $m = 1$, whereas for the red curve $m = 4$. The higher the Hill coefficient, the steeper the dose-response curve. For oxygen binding to he-

[1]Los Alamos National Laboratory, Los Alamos, NM 87501, USA. [2]Department of Medicine, University of California–San Francisco, San Francisco, CA 94110, USA. [3]San Francisco General Hospital, San Francisco, CA 94110, USA.

*To whom correspondence should be addressed. E-mail: asp@lanl.gov

CREDIT: C. BICKEL/SCIENCE TRANSLATIONAL MEDICINE

Downloaded from stm.sciencemag.org on February 24, 2012

moglobin, the Hill coefficient is $m = 4$ and represents the fact that four oxygen molecules can bind to each hemoglobin molecule and that the binding is cooperative; in other words, the binding of one oxygen molecule makes it easier for the subsequent molecules to bind.

In this issue of *Science Translational Medicine*, Shen *et al.* (*5*) discuss the conceptual basis for dose-response curves for anti-HIV drugs that have slopes or Hill coefficients greater than 1. Rather than using the Hill equation which yields an S-shaped dose-response curve (Fig. 1), they used a logarithmic transformation to generate an equivalent linear plot called a median effects plot (*11*). In an earlier publication, Shen and colleagues measured the Hill coefficient—or, as described by the authors, the "slope parameter"—for a large number of anti-HIV compounds (*10*). They showed that the slope parameter of the dose-response curve was characteristic of a drug class, with $m = 1$ applying to nucleoside reverse transcriptase inhibitors (NRTIs) and integrase inhibitors, whereas $m > 1$ for non-nucleoside reverse transcriptase inhibitors (NNRTIs), fusion inhibitors, and protease inhibitors (PIs), with an m of approximately 1.7 for NNRTIs and fusion inhibitors and m between 1.8 and 4.5 for PIs (*10*). Thus, antiretroviral drugs acting through different mechanisms show distinct slopes of their dose-response curves. In classical ligand–receptor binding theory, slopes of m greater than 1 imply that the binding is cooperative. It is surprising that the binding of a small molecule, such as a PI, to an enzyme that contains a single drug-binding site follows a mathematical law that describes cooperative binding. Typically, small molecules that bind a target molecule with a single drug-binding site generate a dose-response curve that is noncooperative and that has a slope parameter of $m = 1$ (Fig. 1).

THE CRITICAL SUBSET MODEL

The new insight described by Shen *et al.* (*5*), which explains the cooperative dose-response curves of anti-HIV drugs in the PI and NNRTI classes, is that multiple copies of the target molecule within virions or infected cells need to be inactivated by a drug in order to block HIV infection. As an example, consider HIV-1 protease, which is the enzyme that processes the Gag and Gag-Pol polyproteins to yield mature, infectious HIV virions. If protease activity is lacking, then immature, noninfectious viral particles are produced. Rosé *et al.* showed that if wild-type HIV protease was replaced by a mutant form so that the protease activity was 25% of the wild-type activity, then the viral particles produced were morphologically similar to wild-type virions and only a slight reduction in infectivity was observed (*12*). However, if a mutant with only 2% of the wild-type protease activity was used, then noninfectious particles were produced. Thus, there appears to be a threshold level of protease activity required for processing HIV polyproteins and generating infectious particles.

In light of the work by Rosé *et al.* (*12*) and related work by Ambrose *et al.* (*13*), Shen and colleagues put forth the idea that a critical number of HIV enzymes would need to be inhibited by a drug in order to reduce HIV infectivity. Using the law of mass-action, they formulated this idea mathematically and called it the "critical subset model." Applying the model to PIs, the authors considered a virion containing a total of n_T protease enzymes. The binding of a PI to any one enzyme renders it inactive. If a critical subset c, or more of the protease molecules remain active (that is, have no drug bound), then they assume the virus is infectious; conversely, if fewer than c protease molecules remained active, then the virus was assumed to be noninfectious. In the experiment by Rosé *et al.* (*12*), the critical subset would have been between 2 and 25% of the protease molecules. Because the number of protease enzymes in a virion might not be the same in all virions, Shen *et al.* considered the effect of allowing n_T to vary among virions. They also showed that the slope of a dose-response curve is determined by n_T and c. Further, for PIs and NNRTIs they demonstrated that the dose-response curve they had predicted using the critical subset model was able to well-approximate experimental data measuring the infectivity of HIV versus drug dose in single-round infectivity assays (*5*). The model was further tested experimentally by modulating the number of functional drug targets per virus. Dose-response curves generated by the model again fit the data well.

Both theory and experiment also showed that as the number of functional enzymes was decreased, it was easier to inhibit viral replication at the same drug dose. Thus, the IC_{50} of a drug was not only a property of the drug but also the number of drug targets available in the cell or virion. If there were fewer reverse transcriptase (RT) enzyme molecules in a cell, then fewer need to be bound by a drug to reduce the number of active (unbound) molecules below the critical threshold c. A related argument goes as follows: Assume at drug concentration D of a reverse transcriptase inhibitor (RTI) there is a 99% probability of an RT enzyme being inhibited. Thus, if there is a single RT enzyme in a cell the chance of it not being inhibited (remaining unbound) is 1%; however, if there are 10 RT enzymes in the cell and each has a 99% chance of being inhibited, then the chance that at least one fails to be inhibited is $1 - (0.99)^{10} = 9.6\%$. In other words, the more enzymes there are, the higher the chance that some remain functional. Importantly, for drugs whose targets are abundant biomolecules—such as proteases and RT enzymes in virions and cells, but not integrase (for which only the single molecule bound to the viral genome in cells is the relevant target)—a cooperative dose-response curve exists (Fig. 1, red line).

FAR-REACHING CLINICAL IMPLICATIONS

The observation that drug-mediated inhibition of an enzyme depends on the number of copies of that enzyme has clinical implications beyond those discussed in the article by Shen *et al.* For example, HIV can spread by cell-to-cell transmission, potentially making it harder to inhibit viral replication. During such transmission events, several viral particles can be transferred (*14*, *15*). The presumably higher efficiency of cell-to-cell transfer of HIV might explain recent observations suggesting that, if virus replication persists during therapy, it is happening in areas that may support this type of replication, including the densely packed T cell zones of inductive lymphoid structures (*16*). Inhibiting all replication will probably be a necessary (albeit not sufficient) first step in curing HIV infection, and efforts aimed at enhancing the potency of current regimens will likely be needed. The work by Shen and colleagues (*5*) can and should inform the design of novel curative strategies.

Another, perhaps more practical implication for this work is the design of novel regimens for HIV management. Industry and clinical investigators have long pursued a strategy that avoids the use of nucleoside analogs (which are thought to be toxic). To date, no such strategy has emerged that is both well-tolerated and effective (*17*), and most such strategies have failed owing to efficacy concerns. There are too many pos-

Downloaded from stm.sciencemag.org on February 24, 2012

sible drug combinations to test them all in HIV clinical trials; as such, regimens that are selected in part on the basis of having a cooperative dose-response curve ($m > 1$) may play a role in optimizing regimens, both for treatment of naïve patients and for patients who have failed the standard well-characterized, first-line regimens.

The Hill coefficient (slope parameter) is only one component that explains the relative effectiveness of antiretroviral drugs and hence is not able to fully predict what happens in vivo. For example, the drug raltegravir—which has a Hill coefficient of approximately 1—is very effective in treating HIV when administered twice per day. Also, protease inhibitors have the highest Hill coefficient, yet there are some data suggesting that they are less effective than NNRTIs in completely suppressing HIV replication (*17*, *18*). These inconsistencies suggest that other factors, such as tolerability, favorable pharmacologic properties, and where the drugs act during the viral life cycle (*1*), might dominate in defining which regimens are the most effective options for patients.

The critical subset model (*5*) provides an appealing explanation of how steep dose-response curves arise. The steep slope of such dose-response curves implies that small increases of drug concentration can produce a large increase in antiviral activity and, further, that extremely high potencies can be obtained at physiologically relevant concentrations. More importantly, it implies that when drugs with a steep dose-response curve ($m > 1$) are delivered at concentrations greater than their IC_{50}, the drug potency will persist as long as the minimum concentration stays a few fold above the IC_{50}. The work by Shen *et al.* (*5*) suggests why some anti-HIV drugs, specifically the PIs and NNRTIs, have more in vivo potency than others and why some drugs, such as the PI class, might even work as monotherapy (*19*). More broadly, this study might have implications for other antiviral drugs and explain the potency of agents such as the PIs boceprevir and telaprevir for hepatitis C virus (*20*, *21*) and explain why the NS5A molecule of HCV appears to be a good drug target (*22*). Drug developers should take heed of this model in choosing future drug targets.

REFERENCES AND NOTES

1. S. M. Hammer, K. E. Squires, M. D. Hughes, J. M. Grimes, L. M. Demeter, J. S. Currier, J. J. Eron Jr., J. E. Feinberg, H. H. Balfour Jr., L. R. Deyton, J. A. Chodakewitz, M. A. Fischl, J. P. Phair, L. Pedneault, B.-Y. Nguyen, J. C. Cook, A controlled trial of two nucleoside analogues plus indinavir in persons with human immunodeficiency virus infection and CD4 cell counts of 200 per cubic millimeter or less. AIDS Clinical Trials Group 320 Study Team. *N. Engl. J. Med.* **337**, 725–733 (1997).
2. A. S. Perelson, P. Essunger, Y. Cao, M. Vesanen, A. Hurley, K. Saksela, M. Markowitz, D. D. Ho, Decay characteristics of HIV-1-infected compartments during combination therapy. *Nature* **387**, 188–191 (1997).
3. A. Mocroft, B. Ledergerber, C. Katlama, O. Kirk, P. Reiss, A. d'Arminio Monforte, B. Knysz, M. Dietrich, A. N. Phillips, J. D. Lundgren; EuroSIDA study group, Decline in the AIDS and death rates in the EuroSIDA study: An observational study. *Lancet* **362**, 22–29 (2003).
4. J. Lu, S. G. Deeks, R. Hoh, G. Beatty, B. A. Kuritzkes, J. N. Martin, D. R. Kuritzkes, Rapid emergence of enfuvirtide resistance in HIV-1-infected patients: Results of a clonal analysis. *J. Acquir. Immune Defic. Syndr.* **43**, 60–64 (2006).
5. L. Shen, S. A. Rabi, A. R. Sedaghat, L. Shan, J. Lai, S. Xing, R. F. Siliciano, A critical subset model provides a conceptual basis for dose-response relationships of HIV drugs. *Sci. Transl. Med.* **3**, 91ra63 (2011).
6. S. Norton, The origins of pharmacology in the 16th century. *Mol. Interv.* **5**, 144–149 (2005).
7. A. Hill, A new mathematical treatment of changes of ionic concentration in muscle and nerve under the action of electric currents, with a theory as to their mode of excitation. *J. Physiol.* **40**, 190–224 (1910).
8. N. H. Holford, L. B. Sheiner, Kinetics of pharmacologic response. *Pharmacol. Ther.* **16**, 143–166 (1982).
9. A. H. Talal, R. M. Ribeiro, K. A. Powers, M. Grace, C. Cullen, M. Hussain, M. Markatou, A. S. Perelson, Pharmacodynamics of PEG-IFN alpha differentiate HIV/HCV coinfected sustained virological responders from nonresponders. *Hepatology* **43**, 943–953 (2006).
10. L. Shen, S. Peterson, A. R. Sedaghat, M. A. McMahon, M. Callender, H. Zhang, Y. Zhou, E. Pitt, K. S. Anderson, E. P. Acosta, R. F. Siliciano, Dose-response curve slope sets class-specific limits on inhibitory potential of anti-HIV drugs. *Nat. Med.* **14**, 762–766 (2008).
11. T. C. Chou, Theoretical basis, experimental design, and computerized simulation of synergism and antagonism in drug combination studies. *Pharmacol. Rev.* **58**, 621–681 (2006).
12. J. R. Rosé, L. M. Babé, C. S. Craik, Defining the level of human immunodeficiency virus type 1 (HIV-1) protease activity required for HIV-1 particle maturation and infectivity. *J. Virol.* **69**, 2751–2758 (1995).
13. Z. Ambrose, J. G. Julias, P. L. Boyer, V. N. Kewalramani, S. H. Hughes, The level of reverse transcriptase (RT) in human immunodeficiency virus type 1 particles affects susceptibility to nonnucleoside RT inhibitors but not to lamivudine. *J. Virol.* **80**, 2578–2581 (2006).
14. Q. Dang, J. Chen, D. Unutmaz, J. M. Coffin, V. K. Pathak, D. Powell, V. N. KewalRamani, F. Maldarelli, W. S. Hu, Nonrandom HIV-1 infection and double infection via direct and cell-mediated pathways. *Proc. Natl. Acad. Sci. U.S.A.* **101**, 632–637 (2004).
15. N. M. Dixit, A. S. Perelson, Multiplicity of human immunodeficiency virus infections in lymphoid tissue. *J. Virol.* **78**, 8942–8945 (2004).
16. S. A. Yukl, A. K. Shergill, K. McQuaid, S. Gianella, H. Lampiris, C. B. Hare, M. Pandori, E. Sinclair, H. F. Günthard, M. Fischer, J. K. Wong, D. V. Havlir, Effect of raltegravir-containing intensification on HIV burden and T-cell activation in multiple gut sites of HIV-positive adults on suppressive antiretroviral therapy. *AIDS* **24**, 2451–2460 (2010).
17. S. A. Riddler, R. Haubrich, A. G. DiRienzo, L. Peeples, W. G. Powderly, K. L. Klingman, K. W. Garren, T. George, J. F. Rooney, B. Brizz, U. G. Lalloo, R. L. Murphy, S. Swindells, D. Havlir, J. W. Mellors; AIDS Clinical Trials Group Study A5142 Team, Class-sparing regimens for initial treatment of HIV-1 infection. *N. Engl. J. Med.* **358**, 2095–2106 (2008).
18. M. J. Buzón, M. Massanella, J. M. Llibre, A. Esteve, V. Dahl, M. C. Puertas, J. M. Gatell, P. Domingo, R. Paredes, M. Sharkey, S. Palmer, M. Stevenson, B. Clotet, J. Blanco, J. Martinez-Picado, HIV-1 replication and immune dynamics are affected by raltegravir intensification of HAART-suppressed subjects. *Nat. Med.* **16**, 460–465 (2010).
19. J. R. Arribas, A. Horban, J. Gerstoft, G. Fätkenheuer, M. Nelson, N. Clumeck, F. Pulido, A. Hill, Y. van Delft, T. Stark, C. Moecklinghoff, The MONET trial: Darunavir/ritonavir with or without nucleoside analogues, for patients with HIV RNA below 50 copies/ml. *AIDS* **24**, 223–230 (2010).
20. J. G. McHutchison, G. T. Everson, S. C. Gordon, I. M. Jacobson, M. Sulkowski, R. Kauffman, L. McNair, J. Alam, A. J. Muir; PROVE1 Study Team, Telaprevir with peginterferon and ribavirin for chronic HCV genotype 1 infection. *N. Engl. J. Med.* **360**, 1827–1838 (2009).
21. F. Poordad, J. McCone Jr., B. R. Bacon, S. Bruno, M. P. Manns, M. S. Sulkowski, I. M. Jacobson, K. R. Reddy, Z. D. Goodman, N. Boparai, M. J. DiNubile, V. Sniukiene, C. A. Brass, J. K. Albrecht, J. P. Bronowicki; SPRINT-2 Investigators, Boceprevir for untreated chronic HCV genotype 1 infection. *N. Engl. J. Med.* **364**, 1195–1206 (2011).
22. M. Gao, R. E. Nettles, M. Belema, L. B. Snyder, V. N. Nguyen, R. A. Fridell, M. H. Serrano-Wu, D. R. Langley, J. H. Sun, D. R. O'Boyle 2nd, J. A. Lemm, C. Wang, J. O. Knipe, C. Chien, R. J. Colonno, D. M. Grasela, N. A. Meanwell, L. G. Hamann, Chemical genetics strategy identifies an HCV NS5A inhibitor with a potent clinical effect. *Nature* **465**, 96–100 (2010).

23. **Funding:** Portions of this work were done under the auspices of the U.S. Department of Energy under contract DE-AC52-06NA25396 and supported by NIH grants R37 AI028433, P20 RR018754, and R01 RR006555 (A.S.P.). S.G.D. was supported in part by the National Institute of Allergy and Infectious Diseases (RO1 AI087145, K24AI069994). **Competing Interests:** The authors declare no competing interests.

10.1126/scitranslmed.3002656

Citation: A. S. Perelson, S. G. Deeks, Drug effectiveness explained: The mathematics of antiviral agents for HIV. *Sci. Transl. Med.* **3**, 91ps30 (2011).

Downloaded from stm.sciencemag.org on February 24, 2012

HIV

Drug Effectiveness Explained: The Mathematics of Antiviral Agents for HIV

Alan S. Perelson[1]* and Steven G. Deeks[2,3]

Antiretroviral therapy has improved the quality and length of life of millions of individuals affected by human immunodeficiency virus type 1 (HIV-1). The capacity of these drugs to indefinitely suppress HIV—which has a well-known capacity for escaping antiviral pressures—is surprising. In this issue of *Science Translational Medicine*, Shen *et al.* use a combination of mathematical modeling and experiment to examine the potency of anti-HIV drugs. They show that non-nucleoside reverse transcriptase inhibitors and protease inhibitors exhibit cooperative dose-response curves—a finding that has implications for the treatment of HIV as well as other viral infections, such as hepatitis C.

INTRODUCTION

Antiretroviral therapy has changed human immunodeficiency virus type 1 (HIV-1) infection from a death sentence to a treatable chronic illness. Since the mid-1990s when combination therapy first became available (*1*, *2*), the death rate from HIV has declined substantially (*3*). Although a cure has been elusive, long-lasting and perhaps lifelong control of HIV replication can be achieved in essentially all patients who have access to these drugs and who are able to adhere to the dosing requirements. The fact that therapy is so effective remains a puzzle. HIV replicates at a high titer and mutates constantly. Resistance to certain drugs given as monotherapy can emerge and dominate in the virus population in 14 days (*4*). The virus is known to replicate in several cellular and tissue sanctuaries; any one of these might serve as a source for low-level replication and eventual escape. Given the robust capacity for the virus to evolve in response to almost any antiviral pressure, many clinicians, researchers, and patients remain dubious about the prediction that antiretroviral drugs will work for everyone and for decades, yet the emerging clinical data suggest that this is indeed happening. In this issue of *Science Translational Medicine*, Shen and colleagues provide novel insights into the effectiveness of these drugs (*5*). This work might provide insights relevant to other antiviral strategies (including emerging work on the management of hepatitis C) and might even inform the future development of safer combination regimens for HIV as well as possibly provide insight into how to cure HIV infection.

[1]Los Alamos National Laboratory, Los Alamos, NM 87501, USA. [2]Department of Medicine, University of California–San Francisco, San Francisco, CA 94110, USA. [3]San Francisco General Hospital, San Francisco, CA 94110, USA.

*To whom correspondence should be addressed. E-mail: asp@lanl.gov

CREDIT: C. BICKEL/*SCIENCE TRANSLATIONAL MEDICINE*

DOSE RESPONSE

It was recognized around the 16th century that a drug's effect depended on its dose. A prescription written in 1562 for a mixture of hyoscyamus and opium stated that giving one dram to a person caused sleep, but added "If you want him to sleep less, give him less" (*6*). The notion that a drug's dose and effect are related is a basic tenet of pharmacology and is generally summarized by an experimentally derived dose-response curve. Determining the dose that gives 50% of the maximum response is one way to quantify the potency of a drug; For example, for an enzyme inhibitor such as a protease or reverse transcriptase inhibitor, one can determine the IC_{50} (the concentration of a drug needed to produce 50% of the maximal inhibitory effect in vitro) or the ED_{50} (the plasma concentration of a drug required to obtain 50% of the maximal effect in vivo). Frequently, the dose-response curve is an S-shaped curve, such as those shown in Fig. 1.

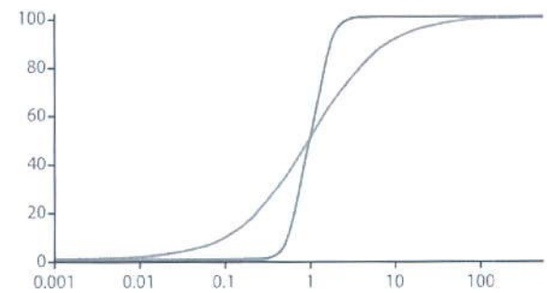


Fig. 1. Dose-response curves. A typical dose-response curve is shown in blue. The IC_{50} is the dose that leads to 50% of the maximal response; for both curves, the IC_{50} is 1. Each curve has a different slope m, which is also known as the Hill coefficient. For the blue curve, $m = 1$, whereas the red curve has a steeper slope of $m = 4$. In other words, the higher the Hill coefficient, the steeper the curve, and the more potent the drug at small increases in concentration above the IC_{50}. Curves with $m > 1$ usually arise from cooperative interactions.

Dose-response curves with the same IC_{50} can have varying steepness or slope (Fig. 1). Both the red and blue dose-response curves have an IC_{50} of 1; yet, for the red curve a dose of 5 generates 99.8% of the maximal response, whereas for the blue curve a dose of 5 yields 83% of the maximum response. A steep dose-response curve means that a drug concentration slightly above the IC_{50} can lead to extremely high levels of inhibition. Furthermore, if the maximum drug concentration that one can obtain in a patient is high (for example, 100 in Fig. 1) then the trough concentration can be 95% lower without any noticeable loss in drug effectiveness; this is true for the red dose-response curve, but not for the blue curve. Thus, the steepness of the dose-response curve has important clinical implications.

A function that describes many dose-response curves and has a long and venerable history in biochemistry was applied empirically by Hill in 1910 to describe the binding of oxygen to hemoglobin (*7*). This Hill equation—which has also been used to describe the effectiveness of a drug, such as interferon for the treatment of hepatitis C (*8*, *9*) or an antiretroviral for the treatment of HIV (*10*)—is written as

$$\varepsilon = \frac{D^m}{IC_{50}^m + D^m} \quad (1)$$

where D is the drug dose; m is the Hill coefficient; and ε is the response or the effectiveness of the drug, which varies between 0 (no effect of the drug) and 1 (the maximal effect). For the blue curve in Fig. 1, $m = 1$, whereas for the red curve $m = 4$. The higher the Hill coefficient, the steeper the dose-response curve. For oxygen binding to he-

Downloaded from stm.sciencemag.org on February 24, 2012

moglobin, the Hill coefficient is $m = 4$ and represents the fact that four oxygen molecules can bind to each hemoglobin molecule and that the binding is cooperative; in other words, the binding of one oxygen molecule makes it easier for the subsequent molecules to bind.

In this issue of *Science Translational Medicine*, Shen *et al.* (*5*) discuss the conceptual basis for dose-response curves for anti-HIV drugs that have slopes or Hill coefficients greater than 1. Rather than using the Hill equation which yields an S-shaped dose-response curve (Fig. 1), they used a logarithmic transformation to generate an equivalent linear plot called a median effects plot (*11*). In an earlier publication, Shen and colleagues measured the Hill coefficient—or, as described by the authors, the "slope parameter"—for a large number of anti-HIV compounds (*10*). They showed that the slope parameter of the dose-response curve was characteristic of a drug class, with $m = 1$ applying to nucleoside reverse transcriptase inhibitors (NRTIs) and integrase inhibitors, whereas $m > 1$ for non-nucleoside reverse transcriptase inhibitors (NNRTIs), fusion inhibitors, and protease inhibitors (PIs), with an m of approximately 1.7 for NNRTIs and fusion inhibitors and m between 1.8 and 4.5 for PIs (*10*). Thus, antiretroviral drugs acting through different mechanisms show distinct slopes of their dose-response curves. In classical ligand–receptor binding theory, slopes of m greater than 1 imply that the binding is cooperative. It is surprising that the binding of a small molecule, such as a PI, to an enzyme that contains a single drug-binding site follows a mathematical law that describes cooperative binding. Typically, small molecules that bind a target molecule with a single drug-binding site generate a dose-response curve that is noncooperative and that has a slope parameter of $m = 1$ (Fig. 1).

THE CRITICAL SUBSET MODEL

The new insight described by Shen *et al.* (*5*), which explains the cooperative dose-response curves of anti-HIV drugs in the PI and NNRTI classes, is that multiple copies of the target molecule within virions or infected cells need to be inactivated by a drug in order to block HIV infection. As an example, consider HIV-1 protease, which is the enzyme that processes the Gag and Gag-Pol polyproteins to yield mature, infectious HIV virions. If protease activity is lacking, then immature, noninfectious viral particles are produced. Rosé *et al.* showed that if wild-type HIV protease was replaced by a mutant form so that the protease activity was 25% of the wild-type activity, then the viral particles produced were morphologically similar to wild-type virions and only a slight reduction in infectivity was observed (*12*). However, if a mutant with only 2% of the wild-type protease activity was used, then noninfectious particles were produced. Thus, there appears to be a threshold level of protease activity required for processing HIV polyproteins and generating infectious particles.

In light of the work by Rosé *et al.* (*12*) and related work by Ambrose *et al.* (*13*), Shen and colleagues put forth the idea that a critical number of HIV enzymes would need to be inhibited by a drug in order to reduce HIV infectivity. Using the law of mass-action, they formulated this idea mathematically and called it the "critical subset model." Applying the model to PIs, the authors considered a virion containing a total of n_T protease enzymes. The binding of a PI to any one enzyme renders it inactive. If a critical subset c, or more of the protease molecules remain active (that is, have no drug bound), then they assume the virus is infectious; conversely, if fewer than c protease molecules remained active, then the virus was assumed to be noninfectious. In the experiment by Rosé *et al.* (*12*), the critical subset would have been between 2 and 25% of the protease molecules. Because the number of protease enzymes in a virion might not be the same in all virions, Shen *et al.* considered the effect of allowing n_T to vary among virions. They also showed that the slope of a dose-response curve is determined by n_T and c. Further, for PIs and NNRTIs they demonstrated that the dose-response curve they had predicted using the critical subset model was able to well-approximate experimental data measuring the infectivity of HIV versus drug dose in single-round infectivity assays (*5*). The model was further tested experimentally by modulating the number of functional drug targets per virus. Dose-response curves generated by the model again fit the data well.

Both theory and experiment also showed that as the number of functional enzymes was decreased, it was easier to inhibit viral replication at the same drug dose. Thus, the IC_{50} of a drug was not only a property of the drug but also the number of drug targets available in the cell or virion. If there were fewer reverse transcriptase (RT) enzyme molecules in a cell, then fewer need to be bound by a drug to reduce the number of active (unbound) molecules below the critical threshold c. A related argument goes as follows: Assume at drug concentration D of a reverse transcriptase inhibitor (RTI) there is a 99% probability of an RT enzyme being inhibited. Thus, if there is a single RT enzyme in a cell the chance of it not being inhibited (remaining unbound) is 1%; however, if there are 10 RT enzymes in the cell and each has a 99% chance of being inhibited, then the chance that at least one fails to be inhibited is $1 - (0.99)^{10} = 9.6\%$. In other words, the more enzymes there are, the higher the chance that some remain functional. Importantly, for drugs whose targets are abundant biomolecules—such as proteases and RT enzymes in virions and cells, but not integrase (for which only the single molecule bound to the viral genome in cells is the relevant target)—a cooperative dose-response curve exists (Fig. 1, red line).

FAR-REACHING CLINICAL IMPLICATIONS

The observation that drug-mediated inhibition of an enzyme depends on the number of copies of that enzyme has clinical implications beyond those discussed in the article by Shen *et al.* For example, HIV can spread by cell-to-cell transmission, potentially making it harder to inhibit viral replication. During such transmission events, several viral particles can be transferred (*14*, *15*). The presumably higher efficiency of cell-to-cell transfer of HIV might explain recent observations suggesting that, if virus replication persists during therapy, it is happening in areas that may support this type of replication, including the densely packed T cell zones of inductive lymphoid structures (*16*). Inhibiting all replication will probably be a necessary (albeit not sufficient) first step in curing HIV infection, and efforts aimed at enhancing the potency of current regimens will likely be needed. The work by Shen and colleagues (*5*) can and should inform the design of novel curative strategies.

Another, perhaps more practical implication for this work is the design of novel regimens for HIV management. Industry and clinical investigators have long pursued a strategy that avoids the use of nucleoside analogs (which are thought to be toxic). To date, no such strategy has emerged that is both well-tolerated and effective (*17*), and most such strategies have failed owing to efficacy concerns. There are too many pos-

Downloaded from stm.sciencemag.org on February 24, 2012

sible drug combinations to test them all in HIV clinical trials; as such, regimens that are selected in part on the basis of having a cooperative dose-response curve ($m > 1$) may play a role in optimizing regimens, both for treatment of naïve patients and for patients who have failed the standard well-characterized, first-line regimens.

The Hill coefficient (slope parameter) is only one component that explains the relative effectiveness of antiretroviral drugs and hence is not able to fully predict what happens in vivo. For example, the drug raltegravir—which has a Hill coefficient of approximately 1—is very effective in treating HIV when administered twice per day. Also, protease inhibitors have the highest Hill coefficient, yet there are some data suggesting that they are less effective than NNRTIs in completely suppressing HIV replication (*17, 18*). These inconsistencies suggest that other factors, such as tolerability, favorable pharmacologic properties, and where the drugs act during the viral life cycle (*1*), might dominate in defining which regimens are the most effective options for patients.

The critical subset model (*5*) provides an appealing explanation of how steep dose-response curves arise. The steep slope of such dose-response curves implies that small increases of drug concentration can produce a large increase in antiviral activity and, further, that extremely high potencies can be obtained at physiologically relevant concentrations. More importantly, it implies that when drugs with a steep dose-response curve ($m > 1$) are delivered at concentrations greater than their IC_{50}, the drug potency will persist as long as the minimum concentration stays a few fold above the IC_{50}. The work by Shen *et al.* (*5*) suggests why some anti-HIV drugs, specifically the PIs and NNRTIs, have more in vivo potency than others and why some drugs, such as the PI class, might even work as monotherapy (*19*). More broadly, this study might have implications for other antiviral drugs and explain the potency of agents such as the PIs boceprevir and telaprevir for hepatitis C virus (*20, 21*) and explain why the NS5A molecule of HCV appears to be a good drug target (*22*). Drug developers should take heed of this model in choosing future drug targets.

REFERENCES AND NOTES

1. S. M. Hammer, K. E. Squires, M. D. Hughes, J. M. Grimes, L. M. Demeter, J. S. Currier, J. J. Eron Jr., J. E. Feinberg, H. H. Balfour Jr., L. R. Deyton, J. A. Chodakewitz, M. A. Fischl, J. P. Phair, L. Pedneault, B.-Y. Nguyen, J. C. Cook, A controlled trial of two nucleoside analogues plus indinavir in persons with human immunodeficiency virus infection and CD4 cell counts of 200 per cubic millimeter or less. AIDS Clinical Trials Group 320 Study Team. *N. Engl. J. Med.* **337**, 725–733 (1997).
2. A. S. Perelson, P. Essunger, Y. Cao, M. Vesanen, A. Hurley, K. Saksela, M. Markowitz, D. D. Ho, Decay characteristics of HIV-1–infected compartments during combination therapy. *Nature* **387**, 188–191 (1997).
3. A. Mocroft, B. Ledergerber, C. Katlama, O. Kirk, P. Reiss, A. d'Arminio Monforte, B. Knysz, M. Dietrich, A. N. Phillips, J. D. Lundgren; EuroSIDA study group, Decline in the AIDS and death rates in the EuroSIDA study: An observational study. *Lancet* **362**, 22–29 (2003).
4. J. Lu, S. G. Deeks, R. Hoh, G. Beatty, B. A. Kuritzkes, J. N. Martin, D. R. Kuritzkes, Rapid emergence of enfuvirtide resistance in HIV-1-infected patients: Results of a clonal analysis. *J. Acquir. Immune Defic. Syndr.* **43**, 60–64 (2006).
5. L. Shen, S. A. Rabi, A. R. Sedaghat, L. Shan, J. Lai, S. Xing, R. F. Siliciano, A critical subset model provides a conceptual basis for dose-response relationships of HIV drugs. *Sci. Transl. Med.* **3**, 91ra63 (2011).
6. S. Norton, The origins of pharmacology in the 16th century. *Mol. Interv.* **5**, 144–149 (2005).
7. A. Hill, A new mathematical treatment of changes of ionic concentration in muscle and nerve under the action of electric currents, with a theory as to their mode of excitation. *J. Physiol.* **40**, 190–224 (1910).
8. N. H. Holford, L. B. Sheiner, Kinetics of pharmacologic response. *Pharmacol. Ther.* **16**, 143–166 (1982).
9. A. H. Talal, R. M. Ribeiro, K. A. Powers, M. Grace, C. Cullen, M. Hussain, M. Markatou, A. S. Perelson, Pharmacodynamics of PEG-IFN alpha differentiate HIV/HCV coinfected sustained virological responders from nonresponders. *Hepatology* **43**, 943–953 (2006).
10. L. Shen, S. Peterson, A. R. Sedaghat, M. A. McMahon, M. Callender, H. Zhang, Y. Zhou, E. Pitt, K. S. Anderson, E. P. Acosta, R. F. Siliciano, Dose-response curve slope sets class-specific limits on inhibitory potential of anti-HIV drugs. *Nat. Med.* **14**, 762–766 (2008).
11. T. C. Chou, Theoretical basis, experimental design, and computerized simulation of synergism and antagonism in drug combination studies. *Pharmacol. Rev.* **58**, 621–681 (2006).
12. J. R. Rosé, L. M. Babé, C. S. Craik, Defining the level of human immunodeficiency virus type 1 (HIV-1) protease activity required for HIV-1 particle maturation and infectivity. *J. Virol.* **69**, 2751–2758 (1995).
13. Z. Ambrose, J. G. Julias, P. L. Boyer, V. N. Kewalramani, S. H. Hughes, The level of reverse transcriptase (RT) in human immunodeficiency virus type 1 particles affects susceptibility to nonnucleoside RT inhibitors but not to lamivudine. *J. Virol.* **80**, 2578–2581 (2006).
14. Q. Dang, J. Chen, D. Unutmaz, J. M. Coffin, V. K. Pathak, D. Powell, V. N. KewalRamani, F. Maldarelli, W. S. Hu, Nonrandom HIV-1 infection and double infection via direct and cell-mediated pathways. *Proc. Natl. Acad. Sci. U.S.A.* **101**, 632–637 (2004).
15. N. M. Dixit, A. S. Perelson, Multiplicity of human immunodeficiency virus infections in lymphoid tissue. *J. Virol.* **78**, 8942–8945 (2004).
16. S. A. Yuki, A. K. Shergill, K. McQuaid, S. Gianella, H. Lampiris, C. B. Hare, M. Pandori, E. Sinclair, H. F. Günthard, M. Fischer, J. K. Wong, D. V. Havlir, Effect of raltegravir-containing intensification on HIV burden and T-cell activation in multiple gut sites of HIV-positive adults on suppressive antiretroviral therapy. *AIDS* **24**, 2451–2460 (2010).
17. S. A. Riddler, R. Haubrich, A. G. DiRienzo, L. Peeples, W. G. Powderly, K. L. Klingman, K. W. Garren, T. George, J. F. Rooney, B. Brizz, U. G. Lalloo, R. L. Murphy, S. Swindells, D. Havlir, J. W. Mellors; AIDS Clinical Trials Group Study A5142 Team, Class-sparing regimens for initial treatment of HIV-1 infection. *N. Engl. J. Med.* **358**, 2095–2106 (2008).
18. M. J. Buzón, M. Massanella, J. M. Llibre, A. Esteve, V. Dahl, M. C. Puertas, J. M. Gatell, P. Domingo, R. Paredes, M. Sharkey, S. Palmer, M. Stevenson, B. Clotet, J. Blanco, J. Martinez-Picado, HIV-1 replication and immune dynamics are affected by raltegravir intensification of HAART-suppressed subjects. *Nat. Med.* **16**, 460–465 (2010).
19. J. R. Arribas, A. Horban, J. Gerstoft, G. Fätkenheuer, M. Nelson, N. Clumeck, F. Pulido, A. Hill, Y. van Delft, T. Stark, C. Moecklinghoff, The MONET trial: Darunavir/ritonavir with or without nucleoside analogues, for patients with HIV RNA below 50 copies/ml. *AIDS* **24**, 223–230 (2010).
20. J. G. McHutchison, G. T. Everson, S. C. Gordon, I. M. Jacobson, M. Sulkowski, R. Kauffman, L. McNair, J. Alam, A. J. Muir; PROVE1 Study Team, Telaprevir with peginterferon and ribavirin for chronic HCV genotype 1 infection. *N. Engl. J. Med.* **360**, 1827–1838 (2009).
21. F. Poordad, J. McCone Jr., B. R. Bacon, S. Bruno, M. P. Manns, M. S. Sulkowski, I. M. Jacobson, K. R. Reddy, Z. D. Goodman, N. Boparai, M. J. DiNubile, V. Sniukiene, C. A. Brass, J. K. Albrecht, J. P. Bronowicki; SPRINT-2 Investigators, Boceprevir for untreated chronic HCV genotype 1 infection. *N. Engl. J. Med.* **364**, 1195–1206 (2011).
22. M. Gao, R. E. Nettles, M. Belema, L. B. Snyder, V. N. Nguyen, R. A. Fridell, M. H. Serrano-Wu, D. R. Langley, J. H. Sun, D. R. O'Boyle 2nd, J. A. Lemm, C. Wang, J. O. Knipe, C. Chien, R. J. Colonno, D. M. Grasela, N. A. Meanwell, L. G. Hamann, Chemical genetics strategy identifies an HCV NS5A inhibitor with a potent clinical effect. *Nature* **465**, 96–100 (2010).

23. **Funding:** Portions of this work were done under the auspices of the U.S. Department of Energy under contract DE-AC52-06NA25396 and supported by NIH grants R37 AI028433, P20 RR018754, and R01 RR006555 (A.S.P.). S.G.D. was supported in part by the National Institute of Allergy and Infectious Diseases (RO1 AI087145, K24AI069994). **Competing Interests:** The authors declare no competing interests.

10.1126/scitranslmed.3002656

Citation: A. S. Perelson, S. G. Deeks, Drug effectiveness explained: The mathematics of antiviral agents for HIV. *Sci. Transl. Med.* **3**, 91ps30 (2011).

Downloaded from stm.sciencemag.org on February 24, 2012

Emerging Treatments and Technologies
ORIGINAL ARTICLE

Dose-Response Effect of Pioglitazone on Insulin Sensitivity and Insulin Secretion in Type 2 Diabetes

YOSHINORI MIYAZAKI, MD, PHD
MASAFUMI MATSUDA, MD, PHD
RALPH A. DEFRONZO, MD

OBJECTIVE — To investigate the dose-response effects of pioglitazone on glycemic control, insulin sensitivity, and insulin secretion in patients with type 2 diabetes.

RESEARCH DESIGN AND METHODS — A total of 58 diet-treated patients with type 2 diabetes (aged 54 ± 1 years; 34 men and 24 women; BMI 31.5 ± 0.6 kg/m^2) were randomly assigned to receive placebo (n = 11) or 7.5 mg (n = 13), 15 mg (n = 12), 30 mg (n = 11), or 45 mg (n = 11) of pioglitazone per day for 26 weeks. Before and after 26 weeks, subjects underwent a 75-g oral glucose tolerance test (OGTT).

RESULTS — Patients treated with 7.5 or 15 mg/day of pioglitazone had no change in fasting plasma glucose (FPG) and fasting plasma insulin (FPI) concentrations or in plasma glucose (PG) and insulin concentrations during the OGTT. Patients treated with 30 and 45 mg/day of pioglitazone, respectively, had significant decreases from placebo in HbA_{1c} (Δ = –2.0 and –2.9%), FPG (Δ = –66 and –97 mg/dl), and mean PG during OGTT (Δ = –84 and –107 mg/dl). Fasting plasma insulin decreased significantly in the 45-mg/day pioglitazone group, but the mean plasma insulin during the OGTT did not change. The insulinogenic index (Δ area under the curve [AUC] insulin/ΔAUC glucose) during the OGTT increased significantly in the 30- and 45-mg/day pioglitazone groups (0.13 ± 0.03 to 0.27 ± 0.05, $P < 0.05$). From the OGTT, we previously have derived a composite whole-body insulin sensitivity index (ISI) that correlates well with that measured directly with the insulin clamp technique. Whole-body ISI [ISI = $10{,}000/\sqrt{(FPG \times FPI) \times (\overline{PG} \times \overline{PI})}$, where $\overline{PG}$ and $\overline{PI}$ equal mean plasma glucose and insulin concentrations during OGTT] increased significantly in patients treated with 30 mg (1.8 ± 0.3 to 2.5 ± 0.3, $P < 0.05$) or 45 mg (1.6 ± 0.2 to 2.7 ± 0.6, $P < 0.05$) per day of pioglitazone. In the basal state, the hepatic ISI [k/(FPG × FPI)[k/(FPG × FPI)], which agrees closely with that measured directly with tritiated glucose, increased in patients treated with 30 mg (0.13 ± 0.02 to 0.21 ± 0.03, $P < 0.05$) and 45 mg (0.11 ± 0.02 to 0.24 ± 0.06, $P < 0.05$) per day of pioglitazone. Significant correlations between the dose of pioglitazone and the changes in HbA_{1c} (r = −0.58), FPG (r = −0.47), mean PG during the OGTT (r = −0.46), insulinogenic index (r = 0.34), hepatic ISI (r = 0.44), and whole-body ISI (r = 0.36) were observed.

CONCLUSIONS — Pioglitazone improves glycemic control through the dose-dependent enhancement of β-cell function and improved whole-body and hepatic insulin sensitivity.

Diabetes Care 25:517–523, 2002

Thiazolidinediones, a new class of insulin-sensitizing agents, recently have been introduced for the treatment of patients with type 2 diabetes. Early studies showed that troglitazone ameliorates insulin resistance and improves hyperglycemia and hyperinsulinemia in type 2 diabetes (1,2). Thiazolidinediones activate a specific nuclear receptor, termed peroxisome proliferator–activated receptor-γ (PPARγ) (3), causing preadipocytes to differentiate into mature fat cells and inducing key lipogenic enzymes (3,4). A close relationship exists between the ability of various thiazolidinediones to activate PPARγ and their hypoglycemic action (5). Pioglitazone, a relatively new member of the thiazolidinedione class, improves hyperglycemia, reduces hyperinsulinemia, and ameliorates hypertriglyceridemia in a variety of insulin-resistant animal models of impaired glucose tolerance (6). Recently, Aronoff et al. (7) demonstrated a dose-dependent beneficial effect of pioglitazone monotherapy on glycemic control in type 2 diabetic patients in a large-scale multicenter trial. However, only one previous study has examined the effect of pioglitazone on insulin sensitivity in diabetic humans (8), and no clinical study has examined the dose-dependent effect of pioglitazone on insulin sensitivity in vivo. Previously, we derived a composite index of whole-body insulin sensitivity during 75-g oral glucose tolerance testing (OGTT) and demonstrated that this index correlates well with that measured directly with the insulin clamp technique (9). Using this insulin sensitivity index (ISI), we have examined the dose-dependent effect of pioglitazone on whole-body insulin sensitivity and insulin secretion in 58 patients with type 2 diabetes after 26 weeks of treatment with pioglitazone or placebo. This analysis provides important new information about the mechanism, as well as the dose-response characteristics of pioglitazone, in the treatment of patients with type 2 diabetes.

From the University of Texas Health Science Center and Texas Diabetes Institute, San Antonio, Texas.
Address correspondence and reprint requests to Ralph A. DeFronzo, MD, University of Texas Health Science Center, Diabetes Division, Room #3.380S, 7703 Floyd Curl Dr., San Antonio, TX 78229-3900.
Received for publication 18 June 2001 and accepted in revised form 6 November 2001.
R.A.D. has received a research grant from and is on the advisory board and the National Speakers Bureau of Takeda Pharmaceuticals.
Abbreviations: AUC, area under the curve; FPG, fasting plasma glucose; FPI, fasting plasma insulin; ISI, insulin sensitivity index; OGTT, oral glucose tolerance test; PG, plasma glucose; PPARγ, peroxisome proliferator–activated receptor-γ.
A table elsewhere in this issue shows conventional and Système International (SI) units and conversion factors for many substances.

RESEARCH DESIGN AND METHODS

Study design

A total of 58 patients with type 2 diabetes underwent 75-g OGTT before and after 26 weeks of pioglitazone therapy in a randomized, double-blind, placebo-control, multicenter clinical trial. To be eligible, patients were required to have HbA_{1c} ≥7.0%, fasting plasma glucose (FPG) ≥140 mg/dl, and fasting C-peptide >1 ng/ml. Patients who used insulin or who had unstable proliferative retinopathy, impaired liver function (aspartate aminotransferase or alanine aminotransferase >2.5 × upper limit of normal), impaired kidney function (serum creatinine >1.8 mg/dl), or anemia were excluded. Patients taking previous antidiabetic therapy (sulfonylureas or metformin) underwent a 6- to 8-week single-blind washout period before the baseline OGTT was performed. After the washout period, only patients with HbA_{1c} ≥7.0% were enrolled. Patients were randomized to one of five parallel treatment groups: pioglitazone 7.5, 15, 30, or 45 mg/day or placebo. During the double-blind period, patients were seen every 2 weeks for the first 6 weeks and every 4 weeks for the remaining 20 weeks. At 26 weeks, all subjects underwent repeat 75-g OGTT. To minimize the confounding effect of weight loss on metabolic changes, no specific dietary modifications were recommended during the study.

Measurements

During the OGTT, plasma glucose (PG) concentration was measured at 0, 1, and 2 h by the hexokinase method (Hitachi 747-200 Analyzer; Roche, Indianapolis, IN). Plasma insulin concentration was measured at 0, 1, and 2 h during OGTT by an automated enzyme immunoassay (Tosoh AIA-1200; Tosoh Medicus, South San Francisco, CA). HbA_{1c} was measured by automated ion-exchange high-performance liquid chromatography (Bio-Rad Variant Analyzer; Bio-Rad Diagnostics, Hercules, CA). Fasting serum lipid levels (total cholesterol, HDL cholesterol, and triglycerides) were determined enzymatically (Hitachi 747 Analyzer; Roche, Indianapolis, IN). LDL cholesterol was calculated from the Friedewald equation.

Calculations

The whole-body ISI was determined from the OGTT as follows (9):

$$\frac{10{,}000}{\sqrt{(FPG \times FPI) \times (\overline{PG} \times \overline{PI})}}$$

where FPI = fasting plasma insulin (μU/ml), FPG = fasting plasma glucose (mg/dl), and $\overline{PG}$ and $\overline{PI}$ represent the mean plasma glucose and plasma insulin concentrations during OGTT. This index provides a composite measure of the combined effects of hyperinsulinemia plus hyperglycemia on muscle and hepatic glucose metabolism and is highly correlated with insulin sensitivity measured with the euglycemic insulin clamp technique (9). In the previous study (9), whole-body ISI was calculated from PG and insulin concentrations measured every 30 min during OGTT. In the present study, PG and insulin were measured every hour during the OGTT. Therefore, using the previously published data (9), we reanalyzed the relationship between insulin sensitivity obtained from euglycemic insulin clamp and ISI derived from PG and insulin concentrations at 0, 1, and 2 h during OGTT. A highly significant correlation between these parameters was observed in nondiabetic ($r = 0.74$, $P < 0.001$) and type 2 diabetic ($r = 0.67$, $P < 0.001$) individuals.

Hepatic insulin sensitivity can be estimated from the FPG and FPI as follows (9,10):

$$\frac{k}{FPG \times FPI}$$

This equation is mathematically equivalent to the reduced formula of the homeostasis model assessment (HOMA) (10), where $k = 22.5 \times 18$, and the index of hepatic insulin sensitivity correlates closely with that measured directly with tritiated glucose (9).

Statistical analysis

Statistical calculations were performed using StatView for Windows software (version 5.0; SAS Institute, Cary, NC). Values before and after treatment within each group were analyzed using paired Student's *t* test. Comparison between groups was performed using ANOVA with Bonferroni/Dunn post-hoc testing. Comparisons over time were made using repeated measures ANOVA. Pearson's correlations between continuous variables were used as a measure of association. For the association between the five groups and changes in metabolic variables after treatment with pioglitazone or placebo, we also reevaluated the significance using Spearman's correlation coefficient by rank. All data are presented as the mean ± SEM. $P < 0.05$ was considered statistically significant.

RESULTS

Patient characteristics, HbA_{1c}, glucose, insulin, and lipids

Fifty-eight patients were randomized to receive placebo ($n = 11$) or 7.5 ($n = 13$), 15 ($n = 12$), 30 ($n = 11$), or 45 ($n = 11$) mg/day of pioglitazone. At baseline, there were no significant differences in age, ethnicity, sex, BMI, HbA_{1c}, FPG, or insulin concentrations between the placebo and four pioglitazone-treated groups (Table 1). There tended to be more men than women in the pioglitazone-treated groups compared with the placebo group. Within the four pioglitazone-treated groups, the distribution of men and women was similar. It is known that men respond less well to thiazolidinediones than women because of their lower percentage of body fat (11). Plasma lipid levels were similar in the pioglitazone and placebo groups (Table 1).

After 26 weeks of treatment, there was a dose-dependent increase in body weight and BMI in the pioglitazone-treated groups (Table 1). The increments in body weight (4.5 ± 0.7 kg) and BMI (1.6 ± 0.3 kg/m^2) were significantly greater ($P < 0.01$) in the 45-mg/day pioglitazone group than in the placebo group. Plasma HbA_{1c} and FPG also demonstrated a dose-dependent decrease, with significant decrements in HbA_{1c} in the 15-, 30-, and 45-mg/day pioglitazone groups ($P < 0.05$–0.001 versus placebo) (Table 1). The increase in HbA_{1c} in the placebo group most likely reflects the lack of equilibration of HbA_{1c} during the 6- to 8-week washout period and, to a lesser extent, the progressive nature of type 2 diabetes. A highly significant inverse relationship was observed between change in body weight and change in HbA_{1c} ($n = 58$, $r = -0.527$, $P < 0.0001$). Fasting plasma insulin concentration decreased slightly in all pioglitazone-treated groups,

Table 1—*Changes in metabolic and laboratory parameters at 26 weeks compared with baseline*

		Pioglitazone			
	Placebo	7.5 mg/day	15 mg/day	30 mg/day	45 mg/day
Men/Women	3/8	10/3	8/4	8/3	5/6
Ethnicity (C/AA/MA/A/others)	9/1/1/0/0	10/1/0/2/0	10/1/1/0/0	6/0/4/0/1	7/1/2/0/1
Age (years)	58 ± 3	51 ± 3	57 ± 4	51 ± 2	55 ± 2
Weight (kg)					
Baseline	90 ± 4	93 ± 5	93 ± 5	97 ± 4	86 ± 3
Week 26	90 ± 4	93 ± 5	95 ± 7*	100 ± 4*	91 ± 3†
Change	−0.4 ± 1.4	0.2 ± 0.5	2.0 ± 0.9	3.0 ± 1.1	4.5 ± 0.7
P value versus placebo		0.7	0.17	0.07	0.006
BMI (kg/m^2)					
Baseline	32.8 ± 1.6	31.3 ± 1.2	30.8 ± 1.3	32.2 ± 1.6	30.4 ± 1.0
Week 26	32.7 ± 1.9	31.3 ± 1.3	31.6 ± 1.5*	33.2 ± 1.8*	32.0 ± 1.3†
Change	−0.1 ± 0.5	0.1 ± 0.2	0.7 ± 0.3	1.0 ± 0.4	1.0 ± 0.3
P value versus placebo		0.8	0.18	0.11	0.006
HbA_{1c} (%)					
Baseline	8.6 ± 0.5	8.9 ± 0.4	8.0 ± 0.3	8.5 ± 0.5	9.1 ± 0.3
Week 26	9.8 ± 0.8	9.2 ± 0.4	7.9 ± 0.5	7.6 ± 0.5*	7.4 ± 0.3†
Change	1.2 ± 0.5	0.3 ± 0.4	−0.1 ± 0.4	−0.8 ± 0.3	1.8 ± 0.4
P value versus placebo		0.14	0.05	0.003	0.002
FPG (mg/dl)					
Baseline	198 ± 22	231 ± 13	192 ± 13	213 ± 18	230 ± 14
Week 26	218 ± 23	217 ± 18	182 ± 15	167 ± 14*	154 ± 7†
Change	21 ± 25	13 ± 17	10 ± 0.8	−46 ± 19	−77 ± 13
P value versus placebo		0.3	0.2	0.04	0.002
FPI (μU/ml)					
Baseline	18 ± 3	25 ± 5	20 ± 4	20 ± 3	21 ± 3
Week 26	20 ± 4	20 ± 3	17 ± 4	14 ± 2	16 ± 2*
Change	2 ± 2	−5 ± 4	−3 ± 1	−5 ± 3	−5 ± 2
P value versus placebo		0.14	0.07	0.05	0.02
Total cholesterol (mg/dl)					
Baseline	230 ± 2	193 ± 7	205 ± 10	223 ± 14	209 ± 15
Week 26	231 ± 6	198 ± 5	207 ± 11	215 ± 9	214 ± 14
Change	1 ± 14	4 ± 5	3 ± 7	−8 ± 10	5 ± 7
P value versus placebo		0.8	0.9	0.6	0.8
HDL cholesterol (mg/dl)					
Baseline	43 ± 3	40 ± 3	40 ± 2	37 ± 2	41 ± 3
Week 26	46 ± 3	42 ± 3	45 ± 3	42 ± 3†	46 ± 3†
Change	3 ± 2	2 ± 1	5 ± 2	6 ± 1	5 ± 1
P value versus placebo		0.7	0.6	0.2	0.3
LDL cholesterol (mg/dl)					
Baseline	143 ± 14	120 ± 5	123 ± 10	139 ± 12	129 ± 12
Week 26	131 ± 7	119 ± 7	120 ± 9	132 ± 8	133 ± 12
Change	−12 ± 13	−1 ± 6	−3 ± 5	−6 ± 1	5 ± 8
P value versus placebo		0.4	0.5	0.7	0.3
Triglycerides (mg/dl)					
Baseline	248 ± 34	169 ± 7	224 ± 48	256 ± 33	198 ± 24
Week 26	301 ± 56	185 ± 22	205 ± 36	204 ± 39	174 ± 17
Change	53 ± 56	16 ± 17	−19 ± 21	−53 ± 39	−24 ± 22
P value versus placebo		0.3	0.09	0.05	0.08

Data are means ± SEM or *n*. $P < 0.05$ vs. baseline; †$P < 0.01$ vs. baseline. $P < 0.01$ vs. baseline C, Caucasian; AA, African-American; MA, Mexican-American; A, Asian.

reaching significance in the 45-mg/day group (Table 1). In the 30- and 45-mg/day pioglitazone groups, plasma HDL cholesterol increased significantly from baseline, and plasma triglyceride concentration tended to decrease compared with placebo (Table 1). Plasma total and LDL cholesterol did not change significantly from baseline or from the placebo group.

Table 2—*Changes in plasma glucose and insulin concentration, insulinogenic index, and hepatic and whole-body ISI during OGTT at baseline and after 26 weeks of pioglitazone treatment*

		Pioglitazone			
	Placebo	7.5 mg/day	15 mg/day	30 mg/day	45 mg/day
Mean PG (mg/dl)					
Baseline	322 ± 28	341 ± 16	293 ± 16	342 ± 21	351 ± 19
Week 26	336 ± 35	327 ± 19	290 ± 23	271 ± 19†	258 ± 12*
Change	14 ± 34	−14 ± 19	−3 ± 17	−70 ± 19	−94 ± 21
P value versus placebo		0.5	0.6	0.04	0.01
Mean PI (μU/ml)					
Baseline	43 ± 7	40 ± 5	46 ± 7	38 ± 8	36 ± 6
Week 26	39 ± 9	37 ± 4	42 ± 8	38 ± 8	43 ± 7
Change	−5 ± 6	−3 ± 5	−4 ± 7	0 ± 1	7 ± 4
P value versus placebo		0.9	0.9	0.4	0.095
ΔAUC glucose (mg/dl × min)					
Baseline	14,890 ± 925	13,216 ± 849	12,598 ± 897	15,434 ± 650	14,566 ± 745
Week 26	14,125 ± 1,745	13,152 ± 692	12,100 ± 538	12,545 ± 898†	12,529 ± 687*
Change	−766 ± 1,734	−65 ± 636	−498 ± 893	−2,888 ± 604	−2,037 ± 1,113
P value versus placebo		0.7	0.9	0.3	0.5
ΔAUC insulin (μU/ml × min)					
Baseline	3,064 ± 655	1,788 ± 274	3,172 ± 691	2,137 ± 682	1,833 ± 481
Week 26	2,222 ± 691	1,957 ± 472	3,069 ± 557	2,854 ± 847	3,260 ± 540†
Change	−842 ± 564	169 ± 510	−103 ± 703	717 ± 413	1,427 ± 424
P value versus placebo		0.2	0.4	0.03	0.004
IGI (120 min)					
Baseline	0.22 ± 0.05	0.14 ± 0.02	0.28 ± 0.07	0.15 ± 0.06	0.13 ± 0.03
Week 26	0.21 ± 0.07	0.16 ± 0.04	0.26 ± 0.05	0.27 ± 0.10*	0.27 ± 0.05†
Change	−0.01 ± 0.04	0.02 ± 0.04	−0.02 ± 0.06	0.12 ± 0.05	0.14 ± 0.04
P value versus placebo		0.6	0.9	0.07	0.02
Hepatic ISI					
Baseline	0.15 ± 0.02	0.11 ± 0.02	0.15 ± 0.02	0.13 ± 0.02	0.11 ± 0.02
Week 26	0.13 ± 0.02	0.13 ± 0.03	0.21 ± 0.04	0.21 ± 0.03*	0.24 ± 0.06*
Change	−0.01 ± 0.02	0.02 ± 0.01	0.06 ± 0.03	0.08 ± 0.03	0.13 ± 0.05
P value versus placebo		0.08	0.05	0.02	0.009
Whole-body ISI					
Baseline	1.93 ± 0.29	1.52 ± 0.25	1.92 ± 0.28	1.82 ± 0.26	1.61 ± 0.19
Week 26	2.03 ± 0.39	1.84 ± 0.32	2.34 ± 0.30	2.49 ± 0.29*	2.69 ± 0.57*
Change	0.09 ± 0.19	0.32 ± 0.15	0.42 ± 0.23	0.67 ± 0.25	1.08 ± 0.44
P value versus placebo		0.4	0.3	0.08	0.05

Data are *n* or means ± SEM. $P < 0.05$ versus baseline. †$P < 0.01$ versus baseline. Mean PG, mean plasma glucose concentration during OGTT; Mean PI, mean plasma insulin concentration during OGTT; ΔAUC glucose, (mean PG during OGTT − FPG) × 120 min; ΔAUC insulin, (mean PI during OGTT − fasting PI) × 120 min; IGI (120 min), insulinogenic index = ΔAUC insulin/ΔAUC glucose from 0 to 120 min during OGTT.

OGTT

During the baseline study, there were no statistically significant differences in FPG or FPI concentrations, the incremental area under the plasma glucose curve (ΔAUC glucose) and the incremental area under the plasma insulin curve (ΔAUC insulin) during the OGTT, the insulinogenic index (ΔAUC insulin/ΔAUC glucose) from 0 to 120 min, the hepatic insulin sensitivity index, or the whole-body ISI between the placebo and each pioglitazone group (Table 2). After 26 weeks of treatment with 30 and 45 mg/day of pioglitazone, the PG concentration during OGTT was significantly reduced from baseline ($P < 0.01$–0.05) and from placebo ($P < 0.01$–0.05) (Table 2). In both the 30- and 45-mg/day pioglitazone groups, the ΔAUC glucose was also significantly reduced compared with the pretreatment OGTT (Table 2). After 26 weeks, the incremental plasma insulin responses during the OGTT were similar in the placebo, 7.5-mg pioglitazone, and 15-mg/day pioglitazone groups. However, the ΔAUC insulin increased significantly in the 30-mg/day pioglitazone group ($P = 0.03$ versus placebo) and the 45-mg/day pioglitazone group ($P < 0.01$ versus placebo and versus baseline). After 26 weeks of pioglitazone treatment, the insulinogenic index (ΔAUC insulin/ΔAUC glucose from 0 to 120 min) increased significantly in the 30-mg/day pioglitazone group ($P < 0.05$ versus baseline and $P = 0.07$ versus placebo) and the 45-mg/day pioglitazone group ($P \leq 0.02$ versus placebo and baseline) (Table 2). The hepatic ISI increased significantly versus placebo in the 15-, 30-, and 45-mg/day pioglitazone treatment groups (Table 2).

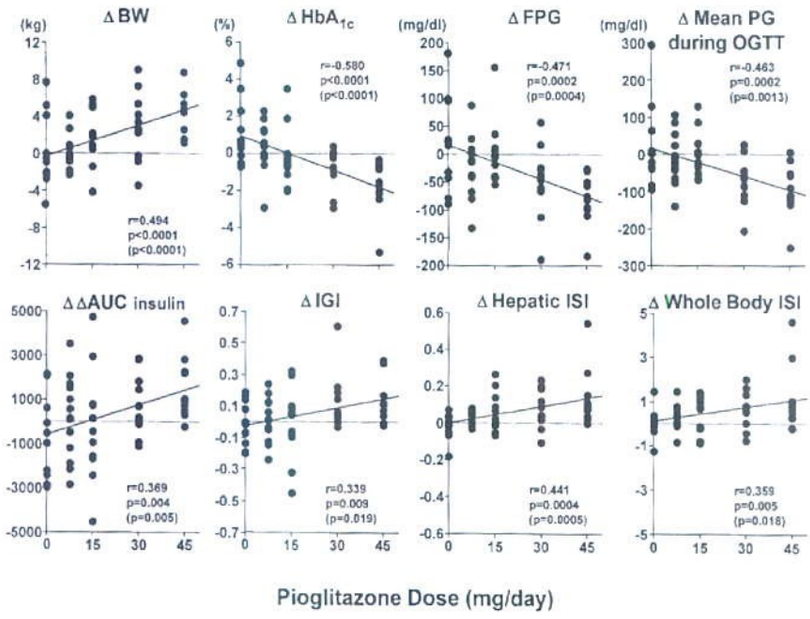


Figure 1—*Dose-response relation between pioglitazone and the changes in body weight (BW), HbA_{1c}, FPG, mean PG during the OGTT, the incremental insulin area during the OGTT (ΔAUC insulin), insulinogenic index from 0 to 120 min [IGI (120 min)], hepatic ISI, and whole-body ISI in patients with type 2 diabetes. The Pearson's correlation coefficient and associated P value are shown. The Spearman's correlation coefficient is shown in parentheses.*

The whole-body ISI increased in the 30- and 45-mg/day pioglitazone treatment groups compared with baseline and placebo (Table 2).

Correlation analyses

The relationships between pioglitazone dose and change in the selected variables during the 26-week pioglitazone treatment period are shown in Fig. 1. Using Pearson's correlation coefficient, significant positive associations were observed between the pioglitazone dose and increases in body weight, plasma insulin response during OGTT, insulinogenic index, hepatic ISI, and whole-body ISI. Significant negative associations were observed between the pioglitazone dose and decrements in HbA_{1c}, FPG, and mean PG concentration during OGTT. Using Spearman's correlation coefficient, we also examined the association by rank among the five groups (placebo and four pioglitazone groups) and the change in the same selected variables. Highly significant associations between the pioglitazone dose and change in each variable were also observed (Fig. 1; see *P* values within parentheses).

CONCLUSIONS — This dose-ranging study demonstrates that pioglitazone, given as monotherapy in doses of 30 and 45 mg/day, reduces FPG concentration and glucose excursion during OGTT. The decreases in fasting and post-OGTT PG were associated with decrements in HbA_{1c} of 0.8 and 1.6%, respectively, from baseline and 2.0 and 2.9%, respectively, from placebo. In the diabetic group treated with 15 mg/day of pioglitazone, there was a significant decrease in HbA_{1c} compared with placebo (1.3%, $P < 0.05$) but not compared with baseline (Table 1).

The ΔAUC glucose during OGTT decreased significantly from baseline in the 30- and 45-mg/day pioglitazone groups (Table 1). This beneficial effect of pioglitazone on postprandial hyperglycemia is quite distinct from sulfonylureas (12) and metformin (13), which exert their primary effect on the FPG concentration. Although the meglitinides reduce the postprandial glucose excursion, their effect on FPG is quite modest (14). The improvement in postprandial hyperglycemia after pioglitazone treatment could result from 1) increased insulin secretion, 2) enhanced tissue (peripheral and/or hepatic) sensitivity to insulin, or 3) an improvement in the combined effects of hyperglycemia plus hyperinsulinemia to promote glucose metabolism.

The effect of thiazolidinedione treatment on insulin secretion in patients with type 2 diabetes is controversial (1,11,15,16). Some studies have reported a decrease in plasma insulin response to a glucose challenge (1,11), whereas others have failed to observe any significant change (15,16). We found an increase in plasma insulin response during OGTT in diabetic patients treated with 30 and 45 mg/day of pioglitazone (Table 2). An increased or maintained plasma insulin response in the presence of a decreased PG concentration suggests an improvement in β-cell function. Consistent with this, pioglitazone (30- and 45-mg/day dose) increased the insulinogenic index (ΔAUC insulin/ΔAUC glucose) (Table 2). We believe that the variable effect of thiazolidinediones on the plasma insulin response to a glucose challenge is explained by two opposing effects: 1) a decrease in fasting and postprandial glucose concentrations, leading to reduced glucose toxicity (17); and 2) an increase in insulin sensitivity, leading to reduced insulin secretion (18).

Previous studies with thiazolidinediones in patients with type 2 diabetes concluded that their primary mechanism of action is related to improved insulin sensitivity (1,16,19,20). However, each of these insulin clamp studies used pharmacologic insulin infusion rates (80,120, or 300 mU · m^{-2} · min^{-1}), which produced supraphysiologic plasma insulin concentrations. In a recent study (8) using more physiologic plasma insulin concentrations, pioglitazone had only a very modest effect to enhance insulin sensitivity in patients with type 2 diabetes. In the present study, 26 weeks of pioglitazone treatment (30 and 45 mg/day) significantly increased the whole-body ISI compared with baseline and compared with placebo (Table 2). This improvement in whole-body ISI was observed with mean plasma insulin concentrations of 36–46 μU/ml (Table 2). It is important to note that there are significant differences between the OGTT and euglycemic insulin clamp, including the presence (OGTT) or absence (euglycemic insulin clamp) of hyperglycemia and the route of glucose administration (oral ver-

sus intravenous). Moreover, in contrast to the insulin clamp, the whole-body ISI during OGTT is greatly influenced by *1*) glucose-mediated glucose uptake and the combined effects of hyperinsulinemia plus hyperglycemia to augment glucose disposal, 2) less effective suppression of hepatic glucose production (21), and 3) splanchnic uptake of 30–40% of the ingested glucose load (21). With regard to the latter, Kawamori et al. (22) have suggested that pioglitazone augments splanchnic glucose uptake after glucose ingestion. These considerations suggest that mechanisms, in addition to improved insulin sensitivity in muscle, contribute to the improvement in whole-body insulin sensitivity during OGTT after pioglitazone therapy.

From the dose-response standpoint, the insulin-sensitizing effect of pioglitazone is clearly evident at doses of 30 and 45 mg/day (Table 2). There was a tendency for whole-body insulin sensitivity to increase at 15 mg/day, but this did not reach statistical significance. Although whole-body insulin sensitivity and dose of pioglitazone were linearly related (Fig. 1), the threshold for a clinically significant insulin-sensitizing effect on glucose homeostasis is ~15 mg/day of pioglitazone.

The product of basal hepatic glucose production (measured with tritiated glucose) and the FPI concentration provides a direct measure of hepatic insulin resistance under postabsorptive conditions, whereas the inverse provides a measure of hepatic insulin sensitivity (9). Because basal hepatic glucose production is closely correlated with FPG concentration (23), the inverse of the product of FPG and insulin concentrations provides an index of hepatic insulin sensitivity (9). The hepatic ISI increased in the 15-, 30-, and 45-mg/day pioglitazone groups ($P < 0.05$–0.01 versus placebo). Previous studies examining the effect of troglitazone on basal hepatic glucose production provided apparently contradictory results (1,16,20). In two studies, troglitazone reduced hepatic glucose production (1,20), whereas one study (16) found no effect of troglitazone on basal glucose output by the liver. However, these studies failed to relate the basal rate of hepatic glucose production to the fasting plasma insulin concentration. Because troglitazone treatment was associated with a decrease in FPI, a decreased or even unchanged rate of hepatic glucose production implies an improvement in hepatic insulin sensitivity.

In type 2 diabetic subjects, weight gain causes worsening of insulin resistance and deterioration of glycemic control. In the present study, pioglitazone treatment (15–45 mg/day) for 26 weeks was associated with mean weight gain of 2.0–4.5 kg, which was significantly and inversely correlated with decreases in HbA_{1c} ($r = -0.527$, $P < 0.0001$), FPG ($r = -0.381$, $P = 0.03$), and mean PG concentration during OGTT ($r = -0.462$, $P < 0.001$). Improved glycemic control, despite weight gain, has been reported with other thiazolidinediones, including rosiglitazone and troglitazone (11,15). Although decreased glucosuria (associated with improved glycemic control) could contribute to the weight gain, this would not be expected to enhance insulin sensitivity. The seemingly paradoxical relationship between weight gain and improved glucose homeostasis/insulin sensitivity most likely is explained by the basic cellular mechanism of action of the thiazolidinediones, which exert their effects through the PPARγ (3,4). PPARγ receptors are found primarily in adipose tissue (3), and their activation causes preadipocytes to differentiate into mature small fat cells (3,4). PPARγ activation also induces key enzymes involved in lipogenesis in these newly formed adipocytes (3,4). Plasma free fatty acids provide the major source of lipid for triglyceride synthesis in these newly formed adipocytes (3). Although PPARγ receptors are present in both visceral and subcutaneous adipose tissue in humans, thiazolidinediones cause the differentiation of preadipocytes into mature adipocytes only in subcutaneous fat depots (24). This most likely explains the finding that thiazolidinedione-induced weight gain is associated with an increase in subcutaneous fat tissue and a decrease in visceral abdominal fat content (15,25). Because increased visceral fat is associated with insulin resistance (26), a reduction in visceral fat would be expected to lead to an enhancement in insulin sensitivity. Moreover, elevated plasma free fatty acid concentrations/oxidation are common in type 2 diabetic patients and cause insulin resistance in both liver and muscle (27,28). Because thiazolidinedione treatment consistently reduces plasma free fatty acid levels (11,20,29), this may provide another explanation for the improvement in insulin sensitivity despite weight gain.

Dose-response analyses demonstrated significant linear, positive associations between the pioglitazone dose and decrements in HbA_{1c}, FPG, and mean PG concentration during OGTT, as well as between pioglitazone dose and increases in body weight, ΔAUC insulin, insulinogenic index, and hepatic and whole-body ISI (Fig. 1). These significant associations were observed whether or not the placebo group was included in the analysis. Although we cannot determine the maximally effective dose of pioglitazone from the present study, it can be concluded that pioglitazone (at doses ranging from 15 to 45 mg/day) causes a dose-dependent decrease in fasting and postprandial PG concentrations through improvements in hepatic/whole-body insulin sensitivity and in β-cell function in type 2 diabetic patients. For most metabolic parameters, statistically significant changes from baseline and from placebo are evident with pioglitazone doses of 30 and 45 mg/day, with a tendency for the changes to become significant at 15 mg/day. Although some type 2 diabetic patients may respond to a pioglitazone dose of 15 mg/day when given as monotherapy, most will require ≥30 mg/day to see clinically significant effects on insulin sensitivity, enhanced β-cell function, and improved glucose homeostasis.

Acknowledgments— Support for the multicenter trial was provided by Takeda.

We thank Elva Chapa and Lorrie Albarado for expert secretarial assistance in preparing the manuscript.

References

1. Maggs DG, Buchanan TA, Burant CF, Cline G, Gumbiner B, Hsueh WA, Inzucchi S, Kelley D, Nolan J, Olefsky JM, Polonsky KS, Silver D, Valiquett TR, Shulman GI: Metabolic effects of troglitazone monotherapy in type 2 diabetes mellitus: a randomized, double-blind, placebo-controlled trial. *Ann Intern Med* 128:176–185, 1998
2. Fonseca VA, Valiquett TR, Huang SM, Ghazzi MN, Whitcomb RW, and the Troglitazone Study Group: Troglitazone monotherapy improves glycemic control in patients with type 2 diabetes mellitus: a randomized, controlled study. *J Clin En-*

doi:10.1093/brain/awh452 *Brain* (2005), **128**, 1442–1453

Acute treatment with the PPARγ agonist pioglitazone and ibuprofen reduces glial inflammation and Aβ1–42 levels in APPV717I transgenic mice

Michael T. Heneka,[1] Magdalena Sastre,[1] Lucia Dumitrescu-Ozimek,[1] Anne Hanke,[1] Ilse Dewachter,[2] Cuno Kuiperi,[2] Kerry O'Banion,[3] Thomas Klockgether,[1] Fred Van Leuven[2] and Gary E. Landreth[4]

[1]*Department of Neurology, University of Bonn, Bonn, Germany,* [2]*Experimental Genetics Group, Department of Human Genetics, K.U. Leuven, Leuven, Belgium,* [3]*Department of Neurobiology and Anatomy, University of Rochester Medical Center, Rochester, NY and* [4]*Department of Neurosciences, Alzheimer Research Laboratory, Case Western Reserve University, Cleveland, OH, USA*

Correspondence to: Michael T. Heneka, Department of Neurology, University of Münster, Albert-Schweitzer-Str. 33, Münster, Germany
E-mail: heneka@uni-muenster.de

Summary

Neuritic plaques in the brain of Alzheimer's disease patients are characterized by β-amyloid deposits associated with a glia-mediated inflammatory response. Non-steroidal anti-inflammatory drug (NSAID) therapy reduces Alzheimer's disease risk and ameliorates microglial reactivity in Alzheimer's disease brains; however, the molecular mechanisms subserving this effect are not yet clear. Since several NSAIDs bind to and activate the nuclear receptor peroxisome proliferator-activated receptor-γ (PPARγ) which acts to inhibit the expression of proinflammatory genes, this receptor appears a good candidate to mediate the observed anti-inflammatory effects. Recent data *in vitro* suggested that NSAIDs negatively regulate microglial activation and immunostimulated amyloid precursor protein processing via PPARγ activation. We report that an acute 7 day oral treatment of 10-month-old APPV717I mice with the PPARγ agonist pioglitazone or the NSAID ibuprofen resulted in a reduction in the number of activated microglia and reactive astrocytes in the hippocampus and cortex. Drug treatment reduced the expression of the proinflammatory enzymes cyclooxygenase 2 (COX2) and inducible nitric oxide synthase (iNOS). In parallel to the suppression of inflammatory markers, pioglitazone and ibuprofen treatment decreased β-secretase-1 (BACE1) mRNA and protein levels. Importantly, we observed a significant reduction of the total area and staining intensity of Aβ1–42-positive amyloid deposits in the hippocampus and cortex. Additionally, animals treated with pioglitazone revealed a 27% reduction in the levels of soluble Aβ1–42 peptide. These findings demonstrate that anti-inflammatory drugs can act rapidly to inhibit inflammatory responses in the brain and negatively modulate amyloidogenesis.

Keywords: Alzheimer's disease; PPAR; inflammation; NSAID; neurodegeneration

Abbreviations: Aβ = amyloid β; APP = amyloid precursor protein; COX = cyclooxygenase; BACE-1 = β-secretase-1; GAPDH = glyceraldehyde-3-phosphate dehydrogenase; GFAP = glial fibrillary acidic protein; IB4 = isolectin B4; iNOS = inducible nitric oxide synthase; NSAID = non-steroidal anti-inflammatory drug; PPARγ = peroxisome proliferator-activated receptor-γ; PCR = polymerase chain reaction

Received August 31, 2004. Revised October 19, 2004. Accepted January 21, 2005. Advance Access publication April 7, 2005

© The Author (2005). Published by Oxford University Press on behalf of the Guarantors of Brain. All rights reserved. For Permissions, please email: journals.permissions@oupjournals.org

Downloaded from brain.oxfordjournals.org at Medical Center Library, Duke University on September 7, 2010

Introduction

Inflammation plays an important role in the pathogenesis of a number of neurodegenerative diseases and arises as a consequence of the primary disease process. Alzheimer's disease is clinically characterized by progressive memory loss and decline of cognitive functions. Its classical histopathological hallmarks include extracellular amyloid peptide (Aβ) deposition in neuritic plaques, and intracellular deposits of hyperphosphorylated tau, causing formation of neurofibrillary tangles and finally neuronal death. Aβ peptides are generated from the amyloid precursor protein (APP) by sequential actions of two proteolytic enzymes, the β-secretase 1 (BACE1) and the γ-secretase (Dingwall, 2001; Esler and Wolfe, 2001). Formation and aggregation of Aβ represent a key feature and possibly a triggering mechanism of Alzheimer's disease. The importance of Aβ formation is supported by dominantly inherited familial forms of Alzheimer's disease that are linked to APP mutations in or close to the β- and γ-secretase cleavage sites (Hardy and Allsop, 1991). This made it possible to generate transgenic mouse models of cerebral amyloidosis and Alzheimer-like histopathology, i.e. amyloid plaques and cerebral amyloid angiopathy (Hsiao *et al.*, 1995; Sturchler-Pierrat *et al.*, 1997; Lamb *et al.*, 1999; Moechars *et al.*, 1999; Van Dorpe *et al.*, 2000).

Next to neurodegeneration, Alzheimer's disease shows a significant inflammatory component that is characterized by the presence of abundant and activated glial cells associated with fibrillar deposits of Aβ that comprise the senile plaque (Akiyama *et al.*, 2000; Wyss-Coray and Mucke, 2002). Once initiated, inflammatory processes may contribute independently to neural dysfunction and cell death, thereby establishing a self-perpetuating vicious cycle (Griffin *et al.*, 1998), by which the inflammation may represent the primary cause of further neurodegeneration.

In the CNS, the cellular mediators of the innate immune response are the microglia cells whose activation results in the production of a diverse range of inflammatory molecules. Once activated, microglia release a diverse range of cytokines and other proinflammatory products, which contribute to neurodegeneration and exacerbation of the inflammatory reaction by recruiting and stimulating astrocytes. The recognition that a robust inflammatory response is a component of the disease process led to the discovery that long-term treatment with non-steroidal anti-inflammatory drugs (NSAIDs) dramatically reduced the risk for Alzheimer's disease, delayed disease onset, ameliorated symptomatic severity and slowed cognitive decline (McGeer *et al.*, 1996; Stewart *et al.*, 1997; In t'Veld *et al.*, 2001). In addition, NSAID treatment was positively correlated with a reduction of plaque-associated, activated microglia in humans (Mackenzie and Munoz, 1998; Alafuzoff *et al.*, 2000). This observation is supported by two recent studies which demonstrate that the NSAID ibuprofen acts to reduce microglial activation and cytokine production in transgenic mice overexpressing APP (Lim *et al.*, 2000; Yan *et al.*, 2003). Importantly, a 6 month oral ibuprofen treatment also reduced the amount of Aβ deposited in the brains of these animals.

The mechanisms by which NSAIDs act to reduce inflammation in Alzheimer's disease are controversial. The established targets of NSAIDs are cyclooxygenases (COXs) 1 and 2, and experimental data using a neuronal COX2 overexpression paradigm in APP transgenic mice support the hypothesis of a detrimental role for elevated COX2 expression in brains of Alzheimer's disease patients (Xiang *et al.*, 2002). While it has been shown that prostaglandin E_2 levels are increased 5-fold in the CSF of probable Alzheimer's disease patients (Montine *et al.*, 1999), the role of COX products for Alzheimer's disease pathophysiology has not been fully elucidated yet (Akiyama *et al.*, 2000), raising the question of whether the COXs are indeed the biologically relevant target of NSAIDs responsible for the reduced risk of Alzheimer's disease. Moreover, recent clinical trials of COX2 selective inhibitors in Alzheimer's disease patients showed that they are ineffective in treating the disease (Aisen *et al.*, 2003). Therefore, alternative targets of NSAID action have to be considered. A novel action of a subset of commonly used NSAIDs was reported recently by Weggen *et al.* (2001) who found that these drugs selectively reduce the production of Aβ1–42 due to alteration of the preferred γ-secretase cleavage site in APP.

A subset of NSAIDs directly regulate gene expression through their ability to bind and activate the nuclear receptor peroxisome proliferator-actived receptor-γ (PPARγ) (Lehmann *et al.*, 1997). In microglia and macrophages, PPARγ activation results in the inhibition of proinflammatory gene expression through silencing the action of the transcription factors nuclear factor-κB and AP-1 on the promoters of these genes (Jiang *et al.*, 1998; Ricote *et al.*, 1998; Daynes and Jones, 2002). We have demonstrated that PPARγ agonists reduce Aβ- and cytokine-mediated neuroinflammation and neurotoxicity both *in vitro* (Heneka *et al.*, 1999; Combs *et al.*, 2000) and *in vivo* (Heneka *et al.*, 2000). Moreover, we were able to show *in vitro* that NSAIDs, such as indomethacin and ibuprofen, as well as several structurally different PPARγ agonists, reduce immunostimulated Aβ production in a PPARγ-dependent manner (Sastre *et al.*, 2003). We report here that acute treatment of APP-overexpressing mice with ibuprofen or the specific PPARγ agonist, pioglitazone, results in reduction of microglial activation, inflammatory gene expression, BACE1 levels and Aβ deposition in the brain.

Material and methods

Animals

The transgenic mice used in this study were of the FVB/N genetic background and expressed APPV717I under the control of the mouse thy1 gene promoter. The generation of these APPV717I transgenic mice has been described previously (Moechars *et al.*, 1999). Mice (n = 6 per group) of 10 months of age were used for experiments

Downloaded from brain.oxfordjournals.org at Medical Center Library, Duke University on September 7, 2010

since APPV717I mice begin to deposit amyloid peptides in the subiculum at this age, with an accompanying profound inflammatory component becoming apparent. Mice were fed Purina 5002 rodent chow *ad libitum* supplemented with either 375 p.p.m. ibuprofen (Sigma, St Louis, MO) or 240 p.p.m. pioglitazone (Actos™ Takeda Pharmaceuticals, Osaka, Japan). The latter drug concentration was chosen since only ~18% of pioglitazone crosses the blood–brain barrier in mammals (Maeshiba *et al.*, 1997), and a previous experiment using a lower drug dosage failed to show statistically significant results (Yan *et al.*, 2003). Animals were treated for 7 days, since this time period was believed to allow the detection of both anti-inflammatory and amyloid-lowering effects. The final dosage of drug was computed to be 62.5 mg/kg/day of ibuprofen and 40 mg/kg/day of pioglitazone based on an average daily food consumption of 5 g of chow per mouse. There were no significant changes in body weight between or within groups of mice. Of note, pioglitazone did not affect blood glucose levels in APP mice as determined in a set of pilot experiments using the identical treatment protocol in accordance with previous observations in non-diabetic mice (Shiomi *et al.*, 2002). During the experimental treatment, animals were housed singly to allow monitoring of drug intake by weighing the animal daily as well as weighing the remaining food pellets at the same time. In all instances, animals lived under standard conditions of 22°C with a 12 h light–dark cycle and with free access to food and water. At the time of sacrifice, animals received a short inhalation anaesthesia using isoflurane. Animals were transcardially perfused with heparinized sodium chloride (0.9%). The brains were removed and brain regions were dissected from one hemisphere. One hemisphere was placed into an acryl brain block lined up with the interaural line at 0 mm. Subsequently, coronal slices were cut to obtain cortical, hippocampal, cerebellar and brainstem sections, which were dissected, snap-frozen in liquid nitrogen and stored at −80°C until further analysis by reverse transcription–polymerase chain reaction (RT–PCR) within 2 weeks. The remaining brain hemisphere was either fixed in 4% paraformaldehyde followed by paraffin embedding according to standard protocols and sectioning for immunohistochemistry, or underwent cryofixation. For the latter purpose, brains were mounted with Jung tissue freezing medium (Leica Mircosystems, Nussloch, Germany), frozen in melting isopentane and stored in liquid nitrogen until further processing. Animal care and handling was performed according to the Declaration of Helsinki and was approved by the local ethics committees (approval #50.203.2BN33,34/00).

Biochemical analysis of transgenic mouse brain

The individual hemispheres were homogenized in 6.5 volumes of ice-cold buffer containing 20 mM Tris–HCl (pH 8.5) and a cocktail of proteinase inhibitors (Roche Mannheim, Germany), using a small Potter-type mechanical homogenizer. After centrifugation (135 000 *g* for 1 h at 4°C), a portion of the supernatant was centrifuged again (200 000 *g* for 2 h at 4°C) and soluble amyloid peptides were quantified by enzyme-linked immunosorbent assay (ELISA).

ELISA for soluble and plaque-associated amyloid peptides

The extracted protein fractions were applied to small C18-Sep-Pack reverse phase columns (Waters, Massachusetts, MA) and washed with increasing concentrations of acetonitrile (5, 25 and 50%) containing 0.1% trifluoroacetic acid (TFA). The last fraction, containing the amyloid peptides, was dried under vacuum overnight. The samples were assayed using a sandwich ELISA for Aβ1–40 and Aβ1–42 peptides. The capture antisera were CFA3340 (Barelli *et al.*, 1997) and 21F12. The reaction was developed with the biotinylated monoclonal antibody 6F3D.

Immunohistochemistry

Serial sagittal sections of paraffin-embedded or cryofixed tissue were cut (7 μm thick, Leica microtome 2155 or Leica Cryostat CM3050S) and mounted (poly-L-lysine-coated slides, Histobond adhesion slides, Marienfeld, Germany). Retrieval of antigen sites, blocking of endogenous peroxidase activity and blocking of non-specific binding sites were performed according to standard protocols. After washing in phosphate-buffered saline (PBS), sections were incubated overnight at 4°C with primary antibodies. The antibodies and dilutions used were: (i) rabbit anti-glial fibrillary acidic protein (GFAP) polyclonal antibody (pAb; Z 334; 1 : 800, DAKO, Hamburg, Germany); (ii) rabbit pAb against inducible nitric oxide synthase (iNOS) (32030; 1 : 150, Transduction Laboratories, Bioscience, Heidelberg, Germany); (iii) anti-COX2 affinity-purified antibody (160126; 1 : 1000; Cayman Chemical, Ann Arbor, MI); (iv) rabbit pAb against Aβ1–42 (#44-344; 1 : 50, Biosource International, Inc., USA); (v) a pAb 7520 directed against the C-terminal domain of BACE1 (a gift from Dr Christian Haass, Adolf-Butenandt-Institute, University of Munich); and (vi) a mouse monoclonal antibody against neuronal nuclei (neuN, #MAB 377; 1 : 500, Chemicon, Hofheim, Germany). Microglial cells were identified by means of biotin-labelled isolectin B4 (IB4), from *Bandeiraea simplicifolia* as described by others (Naujoks-Manteuffel and Niemann, 1994) (1 : 50, Sigma Taufkirchen, Germany). Immunohistochemistry was performed using the avidin–biotin–peroxidase complex method (ABC-Kit, Vector Labs) with 3,3′-diaminobenzidine tetrahydrochloride as chromogen.

All fluorescent double immunostaining was performed on cryofixed sections cut (6 μm) and mounted as described above. Sections were dried at room temperature for 1 h and then fixed in 4% PFA or methanol for 15 min at room temperature. After washing with PBS, the double staining was performed by adding simultaneously both first antibodies, and followed by overnight incubation at 4°C. The goat secondary antibodies (fluorescein DTAF-conjugated anti-rabbit 1 : 150, Texas red-conjugated anti-mouse 1 : 80, Texas red-conjugated anti-rat 1 : 80, Jackson Immuno Research Laboratories, West Grove, PA) were applied sequentially after washing in PBS. Negative controls included non-specific IgG instead of primary antibodies, pre-absorption with the respective cognate peptides (150–200 μg of peptide/ml of antibody working solution), omission of the secondary antibody and absence of immunoreactivity in non-transgenic controls of the respective age.

Confocal laser scanning microscopy

Double-labelled specimens were analysed with a confocal laser scanning microscope (Multiprobe 2001; Molecular Probes, Inc., Eugene, OR) equipped with an Ar/Kr laser with balanced emission at 488, 568 and 647 nm. To achieve an optimal signal-to-noise ratio for each fluorophore, sequential scanning with 568 and 488 nm was used. The digitalized images were then processed with ImageSpace 3.10 software (Molecular Probes, Inc.) on a Silicon Graphics

Downloaded from brain.oxfordjournals.org at Medical Center Library, Duke University on September 7, 2010

(Mountain View, CA) power series 310GTX work station. Original section series were subjected to Gaussian filtration to reduce noise and enhance weakly but specifically labelled structures. Original and filtered sections were projected on one plane using a maximum intensity algorithm and in some cases using depth-coding and surface-rendering algorithms.

Quantification of immunohistochemistry

For quantitative image analysis of hippocampal and cortical immunostaining, serial sagittal sections of one hemisphere taken from lateral (+0.5 to +2.25) were examined. IB4, GFAP, iNOS, COX2 and Aβ1–42 immunostaining was evaluated on sagittal brain sections of six animals from each group. For each animal, antigens were detected in 10 parallel sections having a defined distance of 70 μm and showing both the hippocampus and cortex. In each section, the hippocampus and the frontal cortex were evaluated. The total stained area (real area) and integral staining density (sum of all individual optical densities of each pixel in the area being measured) were determined and given as stained area in $\mu m^2/mm^2$ (IB4 and GFAP) or percentage of stained surface per region (Aβ1–42). For iNOS and COX2, plaque areas were excluded and the number of stained cells was counted and is shown as immunopositive cells per mm^2. All images were acquired using a standard light and immunofluorescence microscope (Nikon, Eclipse E-800) connected to a digital camera (Sony, model DXC-9100P, Sony, Köln, Germany) and to a PC system with LUCIA imaging software (LUCIA 32G, version 4.11; Laboratory Imaging, Düsseldorf, Germany). For each animal, average values from all sections were determined. These data were analysed by ANOVA with Tukey's post-tests using SYSTAT software (Systat, Evanston, IL).

RNA preparation and RT–PCR

Total RNA was extracted from brain samples using Trizol reagent according to the manufacturer's procedures (Sigma, St Louis, MO), and RT–PCR was carried out as described (Heneka *et al.*, 2002). The primers used were: iNOS forward 5′-TGG GAG CCA CAG CAA TAT AG-3′ and iNOS reverse 5′-ACA GTT TGG TGT GGT GTA GG-3′; GFAP forward 5′-TCC GCG GCA CGA ACG AGT C-3′ and GFAP reverse 5′-CAC CAT CCC GCA TCT CCA CAG TCT-3′; COX2 forward 5′-AAC ATC CCC TTC CTG CGA AG-3′ and COX2 reverse 5′-AAG TCC ACT CCA TGG CCC AG-3′; BACE1 forward 5′-GGCGGGAGTGGTATTATGAGGTGA-3′ and BACE1 reverse 5′-TATTGCTGCGGAAGGATGGTGA-3′; GAPDH forward 5′-TCA CCA GGG CTG CCA TTT GC-3′ and GAPDH reverse 5′-GAC TCC ACG ACA TAC TCA GC-3′. PCRs were carried out on RNA prepared from the individual animals in each group, and representative gels of two different animals per group are shown. PCR conditions were 35 cycles of denaturation at 95°C for 30 s, annealing at 63°C for 45 s, and extension at 72°C for 45 s using a PX2 thermocycler (ThermoHybaid, Ulm, Germany). PCR products were separated by electrophoresis through 2% agarose containing 0.5 μg/ml ethidium bromide, imaged using an Alpha Inotech imaging system (Temecula, CA), and band intensities determined using ImageJ public domain software from NIH. The data were analysed by ANOVA with Tukey's post-tests (Systat, Evanston, IL).

Results

Anti-inflammatory drug treatment reduces glial activation

The 10-month-old APPV717I transgenic mice received an oral treatment with either standard chow, or chow containing the PPARγ agonist pioglitazone or with ibuprofen for a period of 7 days. At 10 months of age, the APPV717I mice are starting to exhibit focal deposits of amyloid, accompanied by a glia-mediated inflammatory response. Analysis of sections of the hippocampus and frontal cortex revealed that treatment with ibuprofen or pioglitazone reduced the area covered by IB4-positive microglia by 30 and 40%, respectively. Additionally, both drugs reduced the integral staining intensity of immunopositive cells (Fig. 1A). Confocal immunolabelling showed that clusters of IB4-stained microglia were closely surrounded by GFAP-positive astrocytes (Fig. 1B). Within these clusters, arborized as well as rounded IB4-positive microglia, indicating different stages of inflammatory activation, were found. A subset of IB4-positive microglial cells also expressed COX2 as determined by confocal laser microscopy (Fig. 1C). The vast majority of COX2-positive microglial cells showed a round to oval morphology, indicating an inflammatory activated state. Quantitative counting of activated and COX2-positive microglial cells in the hippocampus and frontal cortex of placebo- and drug-treated APPV717I mice showed that both ibuprofen and pioglitazone treatment effectively reduced the number of COX2-positive microglia in both brain regions. In parallel, COX2 mRNA levels in hippocampal lysates were significantly decreased by ibuprofen and pioglitazone treatment (Fig. 1C).

To determine whether astrocyte activation is influenced by drug treatment, immunohistochemical analysis of GFAP, an astrocyte-specific intermediate filament component, was performed. GFAP expression previously has been reported to be upregulated in APP-overexpressing mice by ~50% (Lim *et al.*, 2000) and is associated with astrocytosis accompanying amyloid deposition in these animals (Bondolfi *et al.*, 2002). Evaluation of sections of the hippocampus and frontal cortex showed that the area covered by GFAP-positive astrocytes and the respective integral staining intensities were reduced by ibuprofen and pioglitazone treatment (Fig. 2A and B). Co-staining of GFAP and Aβ1–42 confirmed that astrocyte activation could be observed predominantly at sites of amyloid deposition (Fig. 2C). Confocal immunostaining for iNOS and GFAP showed that a subset of astrocytes expressed iNOS. These iNOS-positive cells were found in close contact with amyloid plaques (not shown). In addition, an increased immunostaining against nitrotyrosine, indicating NO-dependent peroxynitrite generation, was found near to amyloid deposits (not shown). Detection of GFAP mRNA levels showed that both ibuprofen and pioglitazone reduced GFAP mRNA by ~60%. Pioglitazone-treated animals exhibited a statistically significant 40% decrease in iNOS mRNA, whereas ibuprofen treatment did not reduce iNOS mRNA

Downloaded from brain.oxfordjournals.org at Medical Center Library, Duke University on September 7, 2010

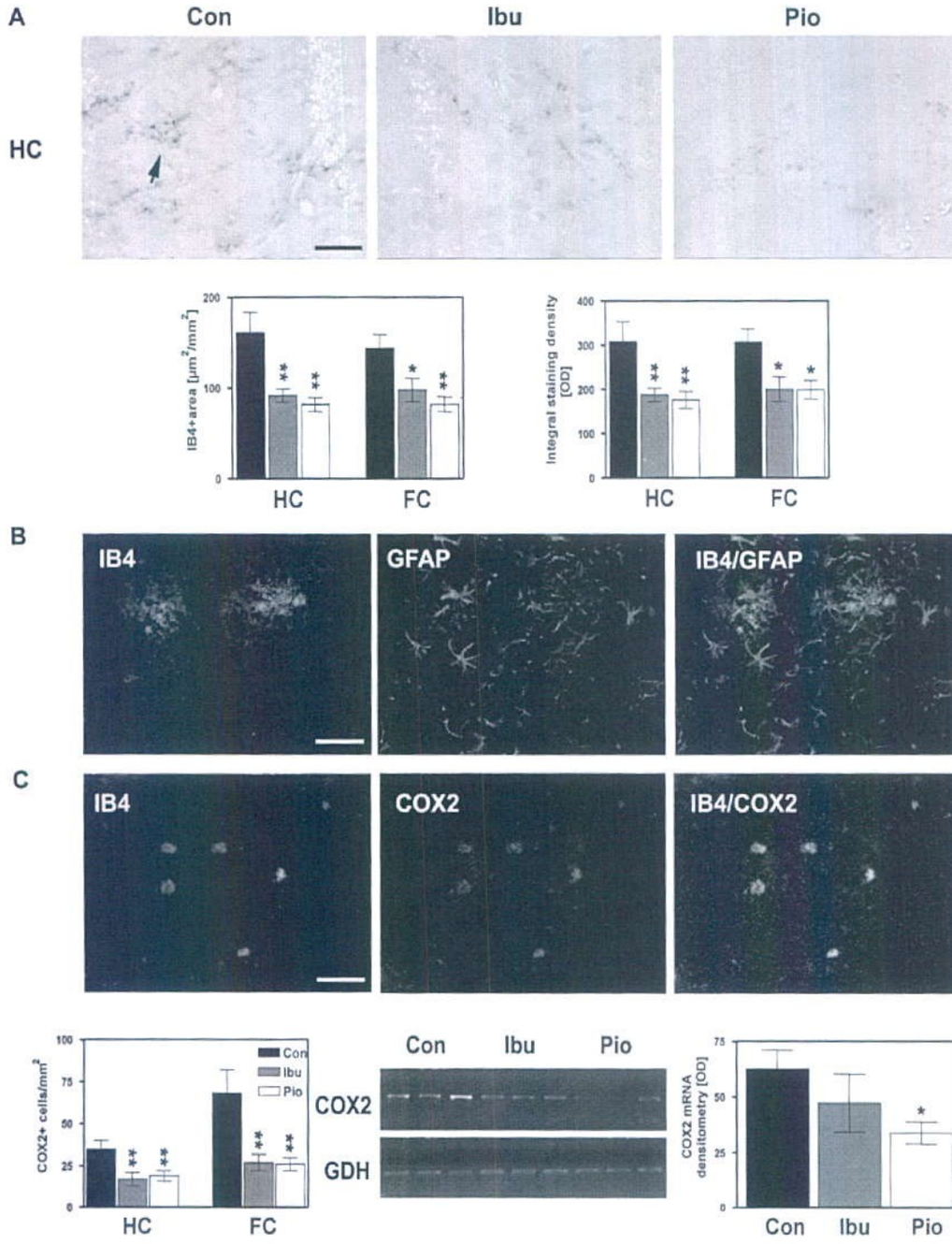


Fig. 1 Anti-inflammatory drug treatment reduces the number of reactive microglia in the hippocampus of APPV717I mice. APPV717I transgenic mice (10 months of age) received either control chow (Con), or chow supplemented with ibuprofen (Ibu) or pioglitazone (Pio) for 7 days. Activated microglia were visualized by staining with IB4 and are shown in the hippocampus (**A**). Arrows indicate clusters of microglia cells. For quantitation, the total area covered by IB4 and the integral IB4 staining intensity were determined in serial sections of the hippocampus (HC) and frontal cortex (FC) (**A**). Confocal analysis of IB4 and the astrocytic marker GFAP revealed that clusters of microglia were closely surrounded by GFAP-positive astrocytes (**B**). Further co-staining showed that a subset of IB4-positive microglial cells were also expressing cyclooxygenase 2 (COX2), and the number of COX2-positive cells was quantified in the HC and FC (**C**). COX2 mRNA levels were determine by RT–PCR in hippocampal lysates of all animal groups (displayed as triplicates) and subsequently analysed by densitometry. GAPDH (GDH) served as control (**C**). Asterisks indicate sign ficant differences between control and drug-treated groups ($^{*}P < 0.05$, $^{**}P < 0.01$, SEM, ANOVA followed by a Tukey test). (**A**) Bar = 25 µm, (**B**) bar = 50 µm, (**C**) bar = 25 µm.

Downloaded from brain.oxfordjournals.org at Medical Center Library, Duke University on September 7, 2010

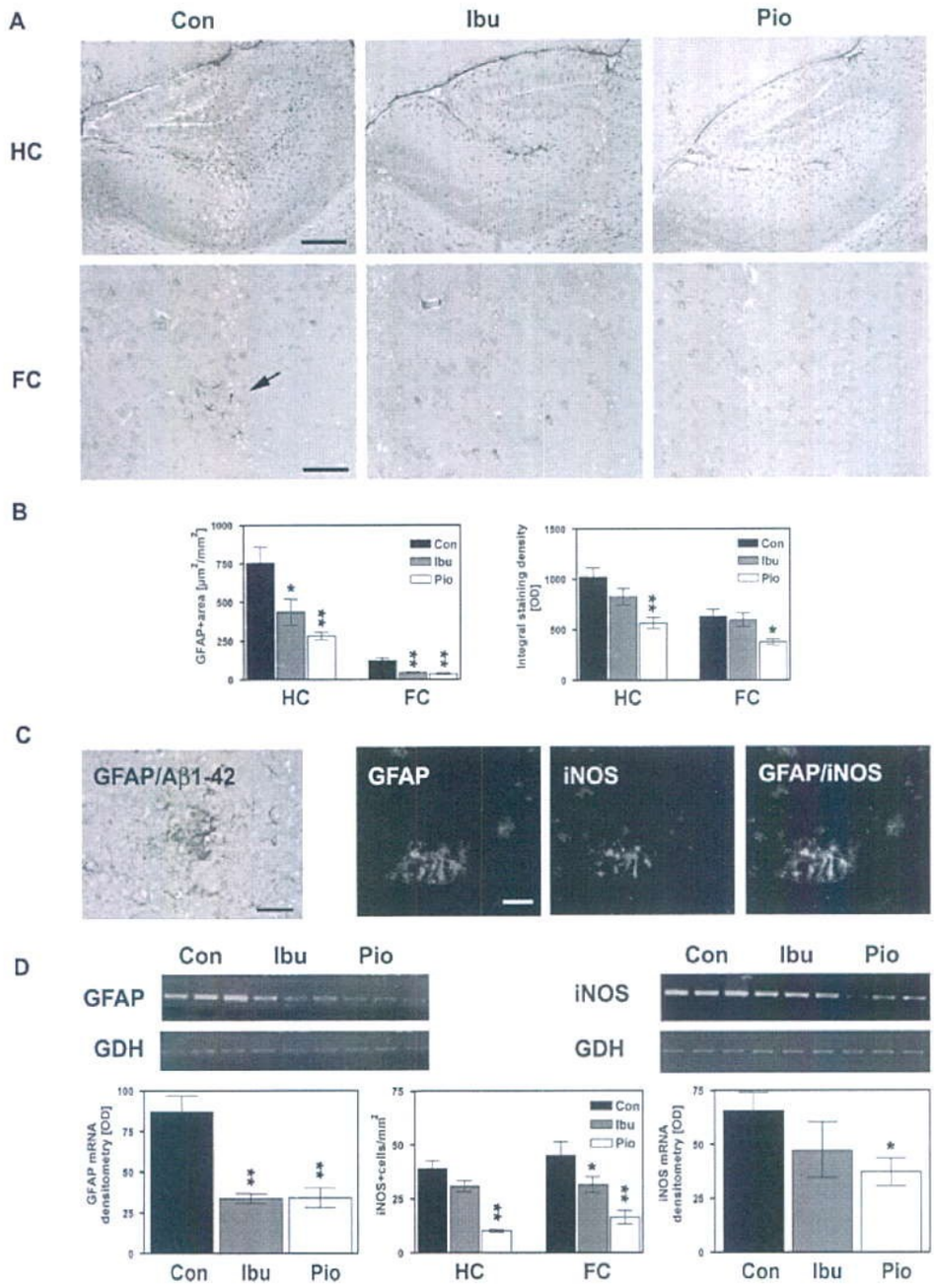


Fig. 2 Downregulation of GFAP expression in 10-month-old APPV717I transgenic mice by anti-inflammatory drug treatment. GFAP expression was analysed immunohistochemically in the hippocampus (HC) and frontal cortex (FC) of 10-month-old APPV717I transgenic mice treated with either control chow (Con), or chow supplemented with ibuprofen (Ibu) or pioglitazone (Pio) for 7 days (**A**). Arrows indicate clusters of GFAP-positive astrocytes in the FC. For quantitation, the total area covered by GFAP and the integral GFAP staining intensity were determined for both areas, the HC and FC, in serial sections (**B**). Representative picture of a section co-stained for GFAP (brown) and Aβ1–42 (blue), revealing that astrocytes assembled predominantly at sites of amyloid plaque deposition (**C**). Confocal staining of GFAP and inducible nitric oxide synthase (iNOS) showed that a subset of GFAP-positive cells expressed iNOS (**C**) and the number of iNOS positive astrocytes was quantified (**D**). iNOS and GFAP mRNA levels were then determined by RT–PCR in hippocampal lysates of all animal groups (displayed as triplicates) and subsequently analysed by densitometry. GAPDH (GDH) served as control (**D**). Asterisks indicate significant differences between placebo- and drug-treated groups ($*P < 0.05$, $**P < 0.01$, SEM, ANOVA followed by Tukey test). (**A**) Bar = 250 µm (HC) and 100 µm (FC). (**C**) bar = 50 µm (GFAP/Aβ1–42) and 25 µm (GFAP/iNOS).

Downloaded from brain.oxfordjournals.org at Medical Center Library, Duke University on September 7, 2010

levels to a comparable extent but tended to be lower than in control animals. The variation observed in the degree of GFAP and iNOS mRNA inhibition upon ibuprofen or pioglitazone treatment between single animals may be due to inter-animal variability in this particular assay but may also result from different drug concentrations at the time of sacrifice. Because chronic amyloid deposition will result in a constant inflammatory stimulus, the degree of inhibition may depend on the individual food intake, especially in food-based treatment protocols. However, immunohistochemical quantification of iNOS-positive cells found a corresponding reduction of the number of iNOS-positive astrocytes in response to drug treatment (Fig. 2D).

Reduced levels of BACE1 protein and mRNA in pioglitazone-treated APPV717I mice

We previously have reported that treatment of neuroblastoma cells with several proinflammatory cytokines resulted in an increased BACE1 expression and that ibuprofen and pioglitazone reduced immunostimulated BACE1 levels *in vitro* (Sastre *et al.*, 2003). These data prompted us to perform an immunohistochemical analysis of BACE1 expression and detection of BACE1 mRNA levels. BACE1-positive cells were immunohistochemically detected in the frontal cortex (Fig. 3A) and hippocampus of 10-month-old APPV717I

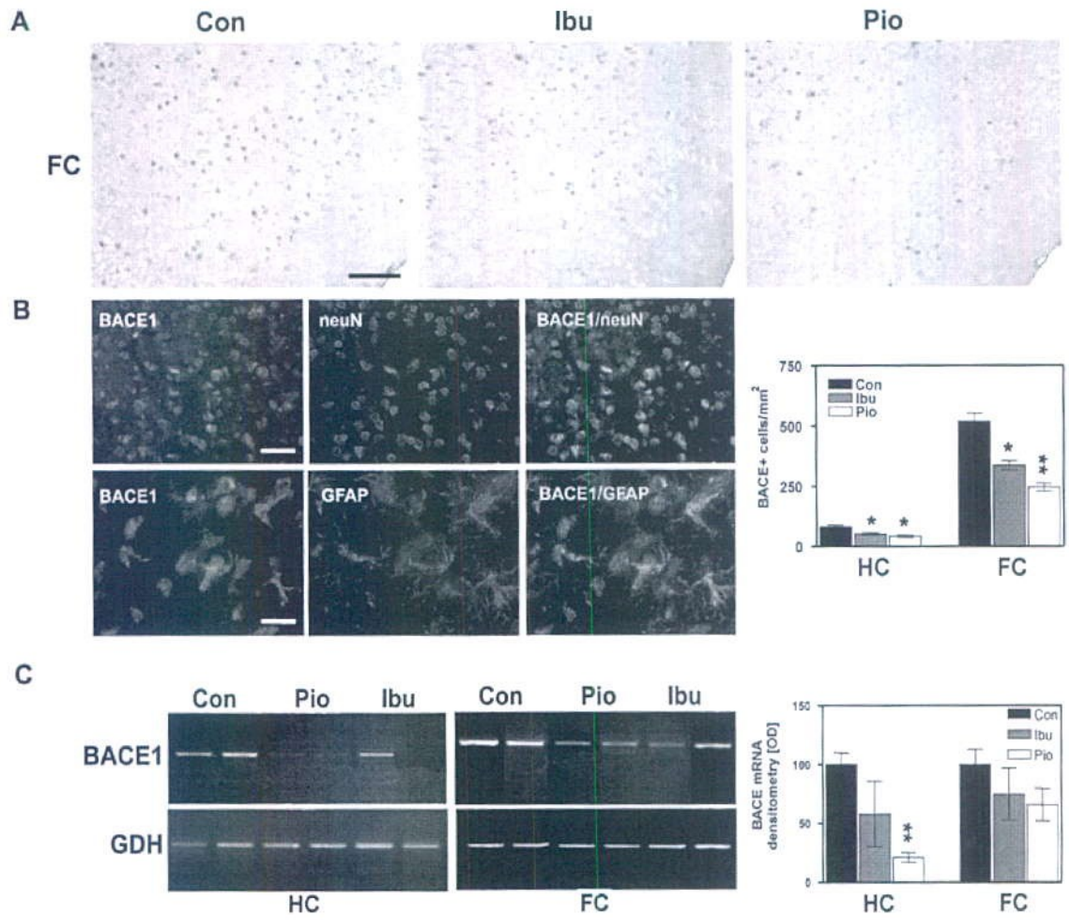


Fig. 3 Pioglitazone decreases the level of BACE1 mRNA and protein in APPV717I-transgenic mice. Immunohistochemical detection of β-secretase (BACE1) in the frontal cortex (FC) of 10-month-old APPV717I transgenic mice treated with either control chow (Con), or chow supplemented with ibuprofen (Ibu) or pioglitazone (Pio) for 7 days (**A**). Confocal immunostaining of BACE1 and the neuronal marker neuN revealed that BACE1 was mostly expressed by neurons in 10-month-old APPV717I mice (**B**). However, co-staining of BACE1 and GFAP showed that a subset of astrocytes also expressed BACE1 (**B**). Quantification of BACE1-positive cells showed a significant reduction in response to both pioglitazone and ibuprofen treatment (**B**). BACE1 mRNA levels were determined in lysates of the hippocampus (HC) and subsequently analysed by densitometry (**C**). Asterisks indicate significant differences between the control and drug-treated groups ($P < 0.05$, $^{**}P < 0.01$, SEM, ANOVA followed by Tukey test). (**A**) Bar = 250 μm, (**B**) bar = 50 μm (BACE/neuN) and 25 μm (BACE1/GFAP).

Downloaded from brain.oxfordjournals.org at Medical Center Library, Duke University on September 7, 2010

transgenic mice. At this age, APPV717I mice expressed BACE1 mainly in neurons as determined by confocal immunohistochemistry for the neuronal marker neuN and BACE1 (Fig. 3B). In addition, co-staining of sections with GFAP revealed that activated astrocytes were found in focal clusters, with a subset of astrocytes also expressing BACE1 (Fig. 3B). Quantification of BACE1-positive neurons in ibuprofen- or pioglitazone-treated animals revealed a marked reduction in the frontal cortex and hippocampus when compared with non-treated APP mice (Fig. 3B). Analysis of BACE1 mRNA levels in whole brain lysates from the respective brain regions showed that pioglitazone, and to a lesser extent ibuprofen, downregulated BACE1 mRNA (Fig. 3C).

Pioglitazone and ibuprofen drug treatment alters Aβ levels and deposition

Anti-inflammatory drug treatment has been reported to reduce Aβ levels in the brain of APP-expressing mice (Lim *et al.*, 2000, 2001; Weggen *et al.*, 2001; Yan *et al.*, 2003). The APPV717I-transgenic mice investigated in the present study start to exhibit Aβ deposition at 10 months of age (Moechars *et al.*, 1999; Van Dorpe *et al.*, 2000). Immunohistochemical analysis of Aβ deposits in the hippocampus and frontal cortex was performed using an antibody specific for Aβ1–42 (Fig. 4A). Compared with non-treated APP mice, pioglitazone reduced the percentage of Aβ1–42-stained plaque area by ~25 and 33% in the hippocampus and frontal cortex, respectively (Fig. 4B). Ibuprofen exerted a similar reduction in the hippocampus; however, it was less efficient in reducing amyloid deposition in the frontal cortex. In addition, there was a corresponding significant reduction of Aβ1–42 staining intensity in the pioglitazone-treated animals (Fig. 4B). We measured soluble levels of Aβ1–40 and Aβ1–42 by ELISA and found that treatment with pioglitazone significantly reduced cerebral levels of soluble Aβ1–42 by 27% (Fig. 4C). There was a smaller and statistically insignificant reduction in ibuprofen-treated mice. Soluble AB1–40 levels were not significantly altered by drug treatment over this interval (Fig. 4C). The Aβ42/40 ratio was reduced 22% in pioglitazone-treated animals (Fig. 4C).

Discussion

There recently has been an increased appreciation of the role that inflammation plays in the pathogenesis of Alzheimer's disease that has arisen principally from epidemiological studies showing a dramatic effect of long-term NSAID treatment on Alzheimer's disease risk. However, the molecuar mechanisms by which NSAIDs intervene in the pathological processes that underlie cognitive decline and neuronal loss remain unclear (Stewart *et al.*, 1997; In t'Veld *et al.*, 2001).

We show that a brief and oral treatment of 10-month-old APPV717I-overexpressing mice with the PPARγ agonist pioglitazone and with the NSAID ibuprofen decreased amyloid-associated microglial and astroglial activation in the hippocampus and frontal cortex. In particular, microglial COX2 expression as well as astrocytic expression of iNOS were potently reduced by both treatments. BACE1, a key enzyme of the APP processing pathway, was detected predominantly in neurons and to a minor extent in clustered astrocytes, and found to be significantly reduced by both pioglitazone and ibuprofen treatment. In parallel to BACE1 reduction, pioglitazone, and to a lesser extent ibuprofen, were able to decrease the total Aβ1–42-positive amyloid plaque area and the respective staining intensity. Additionally, soluble levels of Aβ1–42 were significantly attenuated by pioglitazone treatment.

Animal models of Alzheimer's disease which develop extensive amyloid deposits in the brain also exhibit reactive astrocytosis and abundant plaque-associated, activated microglia with elevated levels of proinflammatory secretory products (Frautschy *et al.*, 1998; Benzing *et al.*, 1999; Stalder *et al.*, 1999; Mehlhorn *et al.*, 2000; Bornemann *et al.*, 2001; Matsuoka *et al.*, 2001). Two recent studies in Tg2576 animals have demonstrated that ibuprofen treatment over a period of several months dramatically reduces glial activation and proinflammatory gene expression (Lim *et al.*, 2000; Yan *et al.*, 2003). These studies suggest that anti-inflammatory treatment strategies may offer substantial clinical benefit. However, several recent clinical trials using COX2-specific inhibitors (Aisen, 2002; Aisen *et al.*, 2003) and traditional NSAIDs alone or in combination (Aisen, 2002) have failed, suggesting that we do not yet fully understand the biology underlying the inflammatory processes in Alzheimer's disease or the relevant mechanisms of protective drug actions, and suggesting that alternative mechanisms of NSAID drug action have to be considered.

It has been recognized recently that a subset of NSAIDs can bind to and activate the nuclear hormone receptor PPARγ (Lehmann *et al.*, 1997; Jaradat *et al.*, 2001). In myeloid lineage cells, including microglia, the principal effect of PPARγ activation is to transcriptionally silence proinflammatory gene expression (Jiang *et al.*, 1998; Ricote *et al.*, 1998; Daynes and Jones, 2002). We have argued that the anti-inflammatory effects of NSAIDs may be partly mediated through the activation of this transcription factor (Landreth and Heneka, 2001). Anti-inflammatory effects of PPARγ agonists and ibuprofen have been shown to protect neurons from cytokine-mediated death (Heneka *et al.*, 1999) and were also observed following infusion of immunostimulants into rodent brain (Heneka *et al.*, 2000). Studying Aβ-mediated microglial activation and neurotoxicity *in vitro*, Combs *et al.* reported that PPARγ agonists, including ibuprofen, were neuroprotective (Combs *et al.*, 2000). These findings led us to investigate the effects of a highly specific PPARγ agonist and ibuprofen in APPV717I-overexpressing mice, a murine model of the amlyoid pathology in Alzheimer's disease (Van Leuven, 2000). We found that acute treatment of these animals with the PPARγ agonist pioglitazone resulted in a significant reduction in the number of IB4-positive microglia

Downloaded from brain.oxfordjournals.org at Medical Center Library, Duke University on September 7, 2010

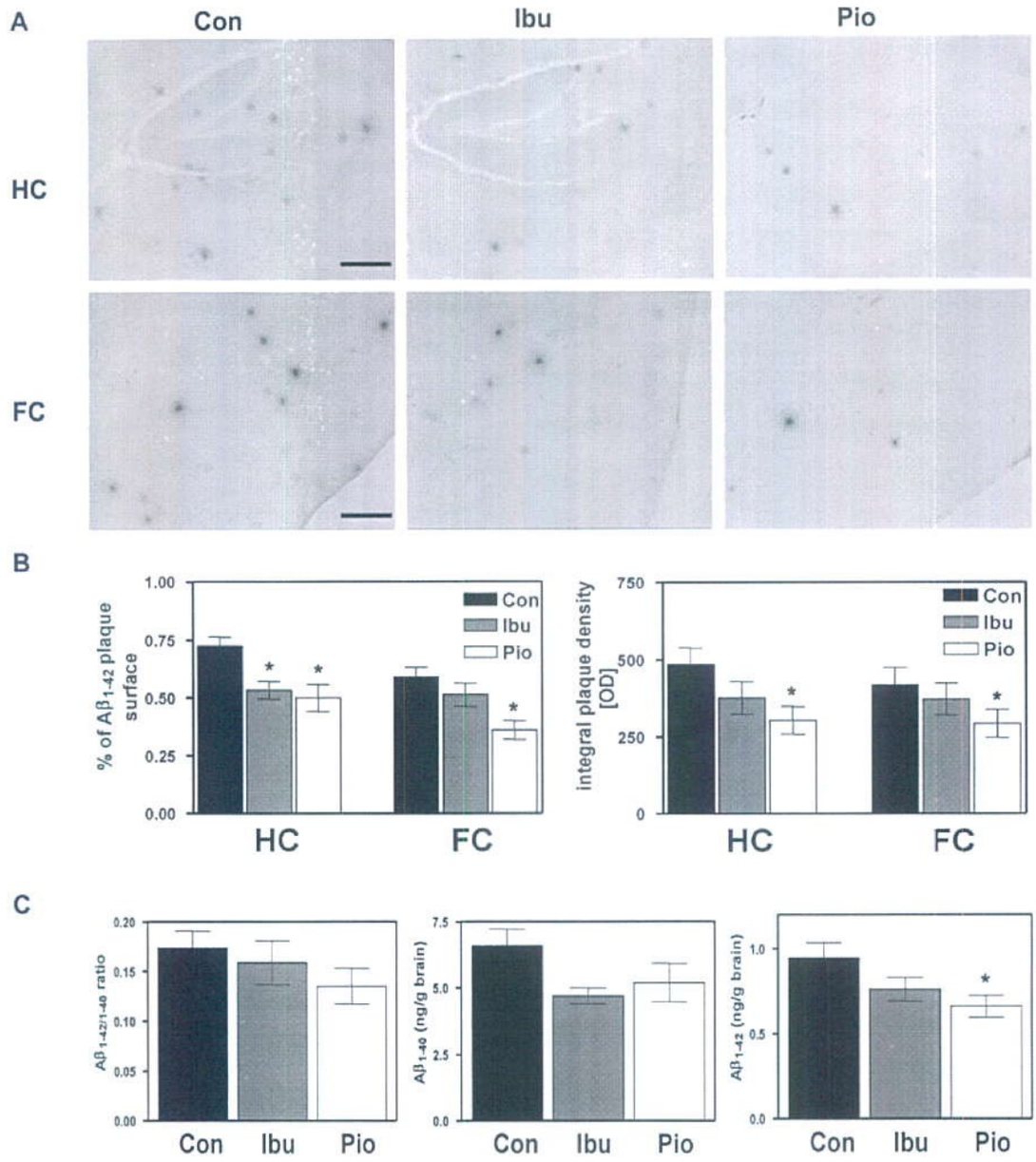


Fig. 4 Effect of anti-inflammatory drug treatment on Aβ levels in 10-month-old APPV717I transgenic mice. Immunohistochemical analysis of Aβ1–42 deposition in the hippocampus (HC) and frontal cortex (FC) was performed in 10-month-old APPV717I transgenic mice treated with either control chow (Con), or chow supplemented with ibuprofen (Ibu) or pioglitazone (Pio) for 7 days (**A**). Serial sections were evaluated for the total plaque surface (given as a percentage of Aβ1–42-stained surface/region) and for the integral Aβ1–42 staining density in the HC and FC (**B**). Levels of soluble Aβ1–42, Aβ1–40 and the ratio Aβ1–42/Aβ1–40 were quantitated by ELISA (**C**). Aβ levels are given as ng/g brain tissue. Asterisks indicate significant differences between the control and drug-treated groups (*$P < 0.05$, SEM, ANOVA followed by Tukey test). (**A**) Bar = 250 μm.

and GFAP-positive astrocytes in the hippocampus and the frontal cortex. Moreover, the brief anti-inflammatory drug treatment inhibited the transcription and expression of COX2 and iNOS in both brain areas. COX2 was expressed predominantly in activated microglial cells, whereas iNOS was strictly co-localized with GFAP, indicating that activated astrocytes served as a major source of iNOS-dependent NO. Inhibition of both COX2 and iNOS has been proven beneficial in several other models of neurodegeneration and inflammation including amyotrophic lateral sclerosis, brain trauma

Downloaded from brain.oxfordjournals.org at Medical Center Library, Duke University on September 7, 2010

and experimental stroke (Zhang *et al.*, 1996; Iadecola *et al.*, 2001; Parmentier-Batteur *et al.*, 2001; Hurley *et al.*, 2002; Pompl *et al.*, 2003; Manabe *et al.*, 2004), suggesting that pioglitazone, and to a lesser extent ibuprofen, can exert neuroprotective effects. Similar results showing that ibuprofen treatment reduced activated, plaque-associated microglia as well as interleukin (IL)-1β levels were obtained after an oral treatment of APP-overexpressing mice for 6 months (Lim *et al.*, 2000). One of the most important outcomes of the present study is that short intervals of drug treatment inhibit the expression of inflammatory markers and reduce the activation status of microglia and astrocytes. In this respect, it seems noteworthy that similarly to the findings in previous studies and the present study, evaluation of human pathological material indicates that NSAID treatment results in a reduction of glial activation that accompanies amyloid deposition and plaque formation in the brains of Alzheimer's disease patients (Mackenzie and Munoz, 1998; Alafuzoff *et al.*, 2000). While pioglitazone and ibuprofen share the pharmacological mechanism of PPARγ activation, it is not clear whether both drugs exert their beneficial effects through activation of this receptor. Pioglitazone and other thiazolidinediones have also been suggested to exert their anti-inflammatory effects through PPARγ-independent mechanisms (Chawla *et al.*, 2001) and ibuprofen has been shown to inhibit protein kinases that are elements of inflammatory signalling cascades and nuclear factor-κB (Tegeder *et al.*, 2001).

Inflammation plays a role in amyloidogenesis and Aβ deposition; however, the mechanistic relationship between these processes remains to be resolved. The capacity of inflammatory stimuli to promote the generation of amyloidogenic Aβ species has not been examined extensively; however, Blasko and colleagues have reported that neuronal Aβ secretion is enhanced by cytokine exposure (Blasko *et al.*, 2001). These findings were recently extended by showing that several cytokines including IL-1β and tumour necrosis factor-α, alone or in concert, effectively increase the generation of the fibrillogenic Aβ1–40 and Aβ1–42 peptides *in vitro* (Sastre *et al.*, 2003). The observed increase of amyloid secretion was paralleled *in vitro* by an upregulation of BACE1, one of two key secretases of the APP processing pathway. In the present study, BACE1 was mainly expressed by neurons but was also focally found in astrocytes as revealed by confocal immunostaining. Treatment of animals with pioglitazone and ibuprofen reduced the number of BACE1-positive neurons and astrocytes and BACE1 mRNA levels in both brain regions, the hippocampus and frontal cortex.

In the present study, a 7 day treatment with pioglitazone and ibuprofen decreased the area of focal Aβ1–42-positive amyloid deposits and their respective staining intensity in the hippocampus and frontal cortex. This latter finding confirms previous reports in ibuprofen- and indomethacin-treated animals. However, in all previous studies, treatment intervals were considerably longer (Lim *et al.*, 2000; Jantzen *et al.*, 2002; Quinn *et al.*, 2003; Yan *et al.*, 2003). While PPARγ-independent mechanisms need to be considered, *in vitro* data showing that ibuprofen and pioglitazone as well as other NSAIDs and structurally different PPARγ agonists share a common and PPARγ-dependent mechanism in reducing immunostimulated BACE1 and Aβ production (Sastre *et al.* 2003) suggest that at least one dimension of NSAID-mediated protection is mediated by PPARγ.

An unexpected finding was the observation that acute treatment with pioglitzone resulted in a significant 27% reduction of brain soluble Aβ1–42 levels. The only comparable data on acute effects of anti-inflammatory drugs on Aβ levels in transgenic mice are those of Weggen *et al.* (Weggen *et al.*, 2001; Eriksen *et al.*, 2003). These authors reported that oral treatment of 3-month-old Tg2576 mice with ibuprofen (50 mg/kg/day) for only 3 days resulted in a reduction of SDS-soluble Aβ1–42 levels by ~40% without a change in Aβ1–40. In the present study, we observed a reduction in soluble Aβ levels with 7 days of ibuprofen treatment; however, this effect did not reach statistical significance. Weggen and colleagues have shown that ibuprofen and other NSAIDs can alter APP processing, and this effect is correlated with the ability of ibuprofen to reduce Aβ1–42 levels acutely in APP-expressing transgenic mice (Weggen *et al.*, 2001; Sagi *et al.*, 2003; Yan *et al.*, 2003). These findings support the view that these drugs act on γ-secretase to alter its specificity. The effects of pioglitazone on Aβ deposition are not likely to arise from a direct effect on γ-secretase, as postulated for ibuprofen, as we and others have been unable to demonstrate an effect of pioglitazone or other PPARγ agonists on γ-secretase-dependent processing using *in vitro* assay systems (Sastre *et al.*, 2003). Importantly, the drug concentrations used to affect γ-secretase *in vitro* are far higher than those observed in human CSF samples after oral or intramuscular NSAID application (Bannwarth *et al.* 1989, 1995; Weggen *et al.*, 2001). In contrast, the observed CSF levels of NSAIDs are exactly in the range (low micromolar concentrations) where they start to act as effective PPARγ activators (Jaradat *et al.*, 2001; Kojo *et al.*, 2003).

In a previous study using APP transgenic mice, pioglitazone had failed to reduce amyloid levels significantly, even when administered for a longer period (Yan *et al.*, 2003). However, since only ~18% of orally administered pioglitazone crosses the intact blood–brain barrier in mammals (Maeshiba *et al.*, 1997), it seems likely that drug dosage, rather than treatment duration, is critical to observe drug effects in the brain. While Yan and colleagues observed a strong tendency of pioglitazone to reduce Aβ1–42 levels, we found a significant and strong reduction of soluble and deposited Aβ1–42 levels using twice the drug concentrations employed in the previous study.

The principal clinical usage of PPARγ agonists is for treatment of type II diabetes. The drugs act to enhance insulin sensitivity and normalize blood glucose levels (Patsouris *et al.*, 2004; Yki-Jarvinen, 2004). It is possible that the reported salutary effects of PPARγ might arise from improved

Downloaded from brain.oxfordjournals.org at Medical Center Library, Duke University on September 7, 2010

brain glucose utilization in addition to the anti-inflammatory actions of these drugs (Watson and Craft, 2003). Since insulin resistance increases amyloidosis in APP transgenic mice (Ho *et al.*, 2004), the amyloid-lowering effect of pioglitazone observed in this study may also be due to enhanced insulin sensitivity.

The data reported here support the use of PPARγ agonists in the treatment of Alzheimer's disease. Recent studies have documented the salutary effects of PPARγ agonists in animal models of multiple sclerosis (Niino *et al.*, 2001; Diab *et al.*, 2002; Feinstein *et al.*, 2002; Natarajan and Bright, 2002) and Parkinson's disease (Breidert *et al.*, 2002). The potent anti-inflammatory effects of PPARγ agonists suggest that they may have beneficial effects in treating other CNS diseases with an inflammatory component.

Acknowledgements

This study was supported by a grant from the Deutsche Forschungsgemeinschaft (SFB 4000, A8) to M.T.H. and T.K., and the NIH (AG 16740, AG008012), the Blanchett Hooker Rockefeller Foundation and the CART Fund of Rotary International to G.L.

References

Aisen PS. Evaluation of selective COX-2 inhibitors for the treatment of Alzheimer's disease. J Pain Symptom Manag 2002; 23: S35–40.

Aisen PS, Schafer KA, Grundman M, et al. Effects of rofecoxib or naproxen vs placebo on Alzheimer disease progression: a randomized controlled trial. J Am Med Assoc 2003; 289: 2819–26.

Akiyama H, Barger S, Barnum S, et al. Inflammation and Alzheimer's disease. Neurobiol Aging 2000; 21: 383–421.

Alafuzoff I, Overmyer M, Helisalmi S, Soininen H. Lower counts of astroglia and activated microglia in patients with Alzheimer's disease with regular use of non-steroidal anti-inflammatory drugs. J Alzheimers Dis 2000; 2: 37–46.

Bannwarth B, Lapicque F, Pehourcq F, et al. Stereoselective disposition of ibuprofen enantiomers in human cerebrospinal fluid. Br J Clin Pharmacol 1995; 40: 266–9.

Bannwarth B, Netter P, Pourel J, Royer RJ, Gaucher A. Clinical pharmacokinetics of nonsteroidal anti-inflammatory drugs in the cerebrospinal fluid. Biomed Pharmacother 1989; 43: 121–6.

Barelli H, Lebeau A, Vizzavona J, et al. Characterization of new polyclonal antibodies specific for 40 and 42 amino acid-long amyloid beta peptides: their use to examine the cell biology of presenilins and the immunohistochemistry of sporadic Alzheimer's disease and cerebral amyloid angiopathy cases. Mol Med 1997; 3: 695–707.

Benzing WC, Wujek JR, Ward EK, et al. Evidence for glial-mediated inflammation in aged APP(SW) transgenic mice. Neurobiol Aging 1999; 20: 581–9.

Blasko I, Apochal A, Boeck G, Hartmann T, Grubeck-Loebenstein B, Ransmayr G. Ibuprofen decreases cytokine-induced amyloid beta production in neuronal cells. Neurobiol Dis 2001; 8: 1094–101.

Bondolfi L, Calhoun M, Ermini F, et al. Amyloid-associated neuron loss and gliogenesis in the neocortex of amyloid precursor protein transgenic mice. J Neurosci 2002; 22: 515–22.

Bornemann KD, Wiederhold KH, Pauli C, et al. Abeta-induced inflammatory processes in microglia cells of APP23 transgenic mice. Am J Pathol 2001; 158: 63–73.

Breidert T, Callebert J, Heneka MT, Landreth G, Launay JM, Hirsch EC. Protective action of the peroxisome proliferator-activated receptor-gamma agonist pioglitazone in a mouse model of Parkinson's disease. J Neurochem 2002; 82: 615–24.

Chawla A, Barak Y, Nagy L, Liao D, Tontonoz P, Evans RM. PPAR-gamma dependent and independent effects on macrophage-gene expression in lipid metabolism and inflammation. Nat Med 2001; 7: 48–52.

Combs CK, Johnson DE, Karlo JC, Cannady SB, Landreth GE. Inflammatory mechanisms in Alzheimer's disease: inhibition of beta-amyloid-stimulated proinflammatory responses and neurotoxicity by PPARgamma agonists. J Neurosci 2000; 20: 558–67.

Daynes RA, Jones DC. Emerging roles of PPARs in inflammation and immunity. Nat Rev Immunol 2002; 2: 748–59.

Diab A, Deng C, Smith JD, et al. Peroxisome proliferator-activated receptor-gamma agonist 15-deoxy-Delta(12,14)-prostaglandin J(2) ameliorates experimental autoimmune encephalomyelitis. J Immunol 2002; 168: 2508–15.

Dingwall C. Spotlight on BACE: the secretases as targets for treatment in Alzheimer disease. J Clin Invest 2001; 108: 1243–6.

Eriksen JL, Sagi SA, Smith TE, et al. NSAIDs and enantiomers of flurbiprofen target gamma-secretase and lower Abeta 42 *in vivo*. J Clin Invest 2003; 112: 440–9.

Esler WP, Wolfe MS. A portrait of Alzheimer secretases—new features and familiar faces. Science 2001; 293: 1449–54.

Feinstein DL, Galea E, Gavrilyuk V, et al. Peroxisome proliferator-activated receptor-gamma agonists prevent experimental autoimmune encephalomyelitis. Ann Neurol 2002; 51: 694–702.

Frautschy SA, Yang F, Irrizarry M, et al. Microglial response to amyloid plaques in APPsw transgenic mice. Am J Pathol 1998; 152: 307–17.

Griffin WS, Sheng JG, Royston MC, et al. Glial–neuronal interactions in Alzheimer's disease: the potential role of a 'cytokine cycle' in disease progression. Brain Pathol 1998; 8: 65–72.

Hardy J, Allsop D. Amyloid deposition as the central event in the aetiology of Alzheimer's disease. Trends Pharmacol Sci 1991; 12: 383–8.

Heneka MT, Feinstein DL, Galea E, Gleichmann M, Wullner U, Klockgether T. Peroxisome proliferator-activated receptor gamma agonists protect cerebellar granule cells from cytokine-induced apoptotic cell death by inhibition of inducible nitric oxide synthase. J Neuroimmunol 1999; 100: 156–68.

Heneka MT, Klockgether T, Feinstein DL. Peroxisome proliferator-activated receptor-gamma ligands reduce neuronal inducible nitric oxide synthase expression and cell death *in vivo*. J Neurosci 2000; 20: 6862–7.

Heneka MT, Galea E, Gavriluyk V, et al. Noradrenergic depletion potentiates beta-amyloid-induced cortical inflammation: implications for Alzheimer's disease. J Neurosci 2002; 22: 2434–42.

Ho L, Qin W, Pompl PN, et al. Diet-induced insulin resistance promotes amyloidosis in a transgenic mouse model of Alzheimer's disease. FASEB J 2004; 18: 902–4.

Hsiao KK, Borchelt DR, Olson K, et al. Age-related CNS disorder and early death in transgenic FVB/N mice overexpressing Alzheimer amyloid precursor proteins. Neuron 1995; 15: 1203–18.

Hurley SD, Olschowka JA, O'Banion MK. Cyclooxygenase inhibition as a strategy to ameliorate brain injury. J Neurotrauma 2002; 19: 1–15.

Iadecola C, Niwa K, Nogawa S, et al. Reduced susceptibility to ischemic brain injury and N-methyl-D-aspartate-mediated neurotoxicity in cyclooxygenase-2-deficient mice. Proc Natl Acad Sci USA 2001; 98: 1294–9.

In t'Veld, Ruitenberg A, Hofman A, et al. Nonsteroidal antiinflammatory drugs and the risk of Alzheimer's disease. N Engl J Med 2001; 345: 1515–21.

Jantzen PT, Connor KE, DiCarlo G, et al. Microglial activation and beta-amyloid deposit reduction caused by a nitric oxide-releasing nonsteroidal anti-inflammatory drug in amyloid precursor protein plus presenilin-1 transgenic mice. J Neurosci 2002; 22: 2246–54.

Jaradat MS, Wongsud B, Phornchirasilp S, et al. Activation of peroxisome proliferator-activated receptor isoforms and inhibition of prostaglandin H(2) synthases by ibuprofen, naproxen, and indomethacin. Biochem Pharmacol 2001; 62: 1587–95.

Jiang C, Ting AT, Seed B. PPAR-gamma agonists inhibit production of monocyte inflammatory cytokines. Nature 1998; 391: 82–6.

Downloaded from brain.oxfordjournals.org at Medical Center Library, Duke University on September 7, 2010

Disposition of the New Antidiabetic Agent Pioglitazone in Rats, Dogs, and Monkeys

Yoshihiro Maeshiba, Yutaka Kiyota, Kenji Yamashita, Yoshinobu Yoshimura, Michio Motohashi, and Shigeharu Tanayama

Drug Analysis and Pharmacokinetics Research Laboratories, Pharmaceutical Development Division, Takeda Chemical Industries, Ltd., Osaka (Japan)

Summary

The disposition of pioglitazone (CAS 105355-27-9, AD-4833) was studied after oral administration to rats, dogs, and monkeys using ^{14}C-labeled drug. After oral dosing, pioglitazone was well absorbed from the gastrointestinal tract at an extent of 96, 95, and 90 % in rats, dogs, and monkeys, respectively. In rats, the concentration of pioglitazone in plasma reached a peak (C_{max} 0.71 μg/ml) at 4 h (t_{max}) after dosing and declined with a half-life ($t_{1/2}$) of 2.6 h. In dogs, t_{max}, C_{max} and $t_{1/2}$ were 0.5 h, 0.32 μg/ml and 2.1 h, and those for monkeys were 4.3 h, 0.48 μg/ml and 5.3 h, respectively. The drug was metabolized mainly to M-I to M-VI including the pharmacologically active metabolites (M-II, III, and IV). The pharmacologically active compounds (total of the unchanged compound and the above three active metabolites) accounted for 87, 71 and 73 % of the radioactivity in plasma of rats, dogs, and monkeys, respectively. The radioactivity was widely distributed in tissues after oral administration to rats, and decreased to the very low concentration within 24 to 72 h after dosing. Radioactivity dose was almost completely excreted in urine and feces.

Zusammenfassung

Verfügbarkeit des neuen Antidiabetikums Pioglitazon bei Ratte, Hund und Affe

Die Verfügbarkeit von Pioglitazon (CAS 105355-27-9, AD-4833) wurde nach oraler Verabreichung der ^{14}C-markierten Substanz an Ratten, Hunden und Affen untersucht. Pioglitazon wurde nach oraler Gabe im Magen-Darm-Trakt gut resorbiert; die Resorptionsrate betrug bei Ratten, Hunden und Affen 96, 95 bzw. 90 %. Bei Ratten erreichte die Pioglitazon-Konzentration im Plasma ihr Maximum (C_{max} 0.71 μg/ml) 4 h (t_{max}) nach Verabreichung und nahm danach mit einer Halbwertzeit ($t_{1/2}$) von 2,6 h wieder ab. Bei Hunden betrugen die Werte t_{max}, C_{max} und $t_{1/2}$ 0,5 h, 0,32 μg/ml bzw. 2,1 h und bei Affen 1,3 h, 0,48 μg/ml bzw. 5,3 h. Die Substanz wurde überwiegend zu M-I bis M-VI einschließlich der pharmakologisch aktiven Metaboliten (M-II, III und IV) metabolisiert. Die pharmakologisch aktiven Substanzen (Gesamtmenge der unveränderten Substanz und der drei oben genannten aktiven Metaboliten) erreichten einen Anteil an der Radioaktivität im Plasma von Ratten, Hunden und Affen von 87, 71 bzw. 73 %. Nach oraler Verabreichung an Ratten war die Radioaktivität in den Geweben weit verteilt und nahm 24 bis 72 h nach Gabe bis zur Minimalkonzentration ab. Die Radioaktivität wurde nahezu vollständig in Urin und Fäzes ausgeschieden.

Key words AD-4833, disposition · Antidiabetic agent · CAS 105355-27-9 · Pioglitazone

Arzneim.-Forsch./Drug Res. 47 (I), 29–35 (1997)

1. Introduction

Pioglitazone (HCl) ((±)-5-[p-[2-(5-ethyl-2-pyridyl) ethoxy] benzyl]-2,4-thiazolidinedione hydrochloride, CAS 105355-27-9, AD-4833[1] (HCl) (see Scheme 1) has potent hypoglycemic and hypolipidemic effects in animal models of non-insulin-dependent diabetes mellitus [1–12] and is now undergoing clinical trials in Japan and the USA. In a separate paper [13], we reported that pioglitazone was metabolized to M-I to M-VI after oral dosing in rats and dogs. Scheme 1 shows the postulated metabolic pathways of pioglitazone. Among these metabolites, M-II, M-III and M-IV exert pharmacological activity, although being somewhat less active than the parent drug [3]. In this paper, we describe the disposition of pioglitazone after oral or intravenous administration of ^{14}C-labeled drug ([^{14}C]pioglitazone HCl) to rats, dogs and monkeys.

[1] Manufacturer: Takeda Chemical Industries, Ltd., Osaka (Japan).

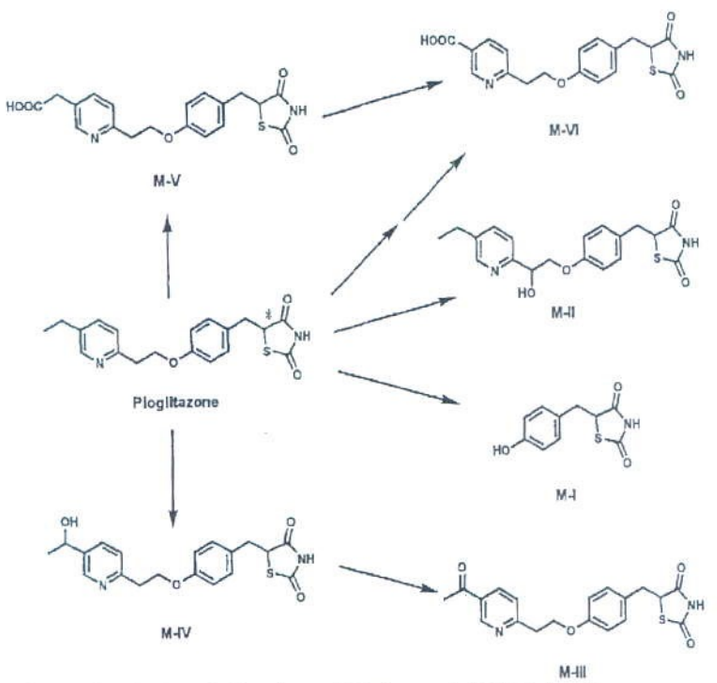
2. Materials and methods

2.1. Chemicals

Bulk pioglitazone (HCl) and its metabolites (M-I to M-VI) were prepared in house by Pharmaceutical Research Division, Takeda Chemical Industries, Ltd. (Osaka Japan) [3]. [^{14}C]Pioglitazone (HCl) with specific radioactivities of 4.8 to 5.5 MBq/mg were synthesized by Nemoto & Co., Ltd. (Tokyo, Japan) and T. N. Technos., Ltd. (Tokyo, Japan). The radiopurities verified by thin-layer chromatography (TLC) were > 98 %. All other chemicals and reagents were purchased from commercial sources.

2.2. Animals

Animals used in this study were male Jcl: Sprague Dawley rats (weight, 244 to 345 g; CLEA Japan Inc., Tokyo, Japan), male beagle dogs (weight, 8.0 to 12.0 kg; Oriental Yeast Co., Ltd., Tokyo, Japan) and male Cynomolgus monkeys (weight, 2.7 to 4.4 kg; Kasho Co., Ltd., Tokyo, Japan). They were fed laboratory chow (CE-2 for rats and CD-5 for dogs; CLEA Japan Inc., and Primate Chow # 5048 for monkeys; Purina Mills, Inc., Richmond, VA, USA), had free access to water, and were housed in temperature- and humidity-controlled rooms (20 to 26 °C



Scheme 1: Postulated metabolic pathways of pioglitazone. *: ^{14}C-labeled position.

and 40 to 75 %) with 12-h light-dark cycles for more than a week before use.

2.3. Dosing and sampling

[^{14}C]Pioglitazone (HCl) diluted appropriately with the unlabeled compound was dissolved in 0.5 mol/l citric acid for oral administration at a dose of 0.5 mg/10 ml/kg to rats, and 0.5 mg/2 ml/kg to dogs and monkeys. [^{14}C]Pioglitazone (HCl) was dissolved in dimethylsulfoxide for intravenous injection at a dose of 0.5 mg/ml/kg to rats, and 0.5 mg/0.2 ml/kg to dogs and monkeys. The compound was administered to fed animals. After dosing, serial samples of plasma, tissues, excreta, and respiratory air were collected according to the methods described previously [14, 15].

2.4. Absorption site

Absorption site in rats was studied according to the procedures reported previously [16]. [^{14}C]Pioglitazone (HCl) in 0.5 % methylcellulose suspension was injected into the following loop separately at a dose of 0.5 mg/2 ml/kg; stomach (whole), small intestine (upper, middle and lower) and large intestine (each 6 cm). At 0.25, 0.5, 1, 2 and 4 h after injection, the concentration of ^{14}C in plasma was measured.

2.5. In vitro metabolism

Slices (0.2 mm thick) of brain, heart, lung, liver, kidney, and duodeum of rats were prepared. [^{14}C]Pioglitazone (HCl) (2 μg) was incubated with the slices (0.2 g) or blood (0.2 ml) in Krebs-Ringer bicarbonate buffer (1 ml) for 2 h at 37 °C under O_2-CO_2 gas (95 : 5, v/v). After the incubation, the reaction mixture was homogenized and extracted with 6 ml of methanol for the determination of pioglitazone and its metabolites by TLC with solvent system A described below.

2.6. Analytical methods

The radioactivity in biological samples, organic solvent extracts, and silica gel from TLC plates was determined by a liquid scintillation spectrometry as reported previously [15, 16].

Pioglitazone and its metabolites in biological specimens were quantified by TLC as follows. The radioactive materials in plasma and aqueous homogenates of feces or tissues were extracted with acetone and methanol (both 5 vol.), respectively. A portion of acetone or methanol extracts, urine and bile were subjected to TLC using precoated silica gel 60 F_{254} plates (0.25 mm thick; E. Merck, Darmstadt, Germany). The solvent systems for determination of the unchanged compound and metabolites M-I to M-VI were as follows: system A, n-hexane-diethyl ether-ethanol-acetic acid (25 : 80 : 5 : 1, by vol.) and system B, chloroform-acetone-acetic acid (15 : 6 : 1, by vol.). System A was used for the quantitation of the unchanged compound and metabolites in plasma; Rf values for pioglitazone, M-I, M-II, M-III, M-IV, M-V and M-VI were 0.61, 0.73, 0.53, 0.46, 0.25, 0.14, and 0.29, respectively. The two dimensional TLC system using system A followed by B was adopted for the quantitation of the unchanged compound and metabolites in excreta and tissues; Rf values (x for system B, y for system A) of pioglitazone, M-I, M-II, M-III, M-IV, M-V and M-VI were (0.72, 0.61), (0.79, 0.73), (0.67, 0.53), (0.81, 0.46), (0.40, 0.25), (0.30, 0.14) and (0.52, 0.29), respectively. After development, the radioactive materials on the plate were located by radioluminography using bioimaging analyzer (BAS2000; Fuji Photo Film Co., Ltd., Tokyo, Japan) and imaging plates (Fuji Photo Film). The silica gel sections that corresponded to pioglitazone and its metabolites were scraped off the plate, and each radioactivity was counted. The remainder of the materials on the plate was also removed and counted, and was referred to as "other metabolites". To determine the conjugated metabolites, the samples were treated with β-glucuronidase containing phenol sulfatase (type H-1; Sigma, St. Louis, MO, USA).

2.7. Data processing

Data are expressed as the mean values ± standard deviations (S.D.) of the results for 3 to 5 animals. Peak time (t_{max}) and maximum concentration (C_{max}) were noted directly from the plasma concentration data. The apparent half-life ($t_{1/2}$) in plasma and area under the plasma concentration-time curve (AUC) were calculated by the linear regression analysis and the trapezoidal rule, respectively. Pharmacokinetic parameters for pioglitazone after intravenous administration were calculated with the following equations;

$$CL_{tot} = dose/AUC_{0\text{-}inf}$$

wherein CL_{tot} is total plasma clearance of the drug;

$$V_{dss} = CL_{tot} \cdot MRT$$

wherein V_{dss} is the estimated steady-state volume of distribution of the drug, and MRT is the mean residence time calculated by the moment analysis [17].

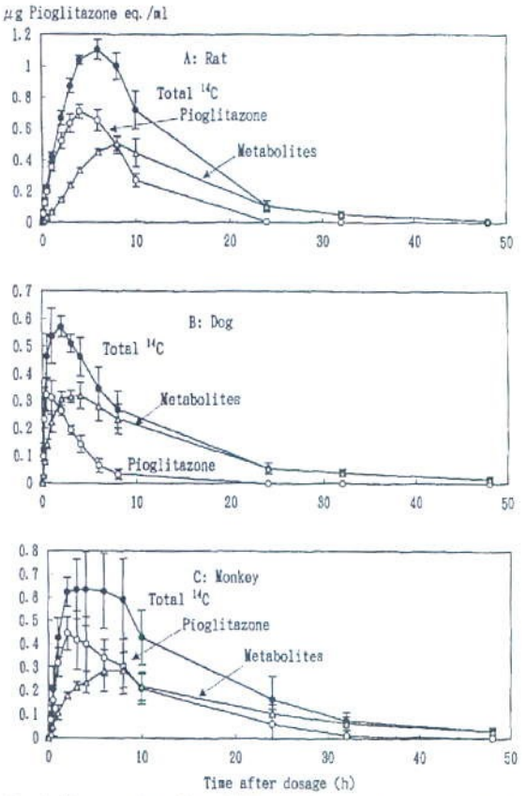


Fig. 1: Concentration of total ^{14}C and pioglitazone in plasma of rats, dogs, and monkeys after oral administration of [^{14}C]pioglitazone (HCl). Dose: 0.5 mg/kg. Data are the mean values ± S.D. (n = 3).

3. Results

3.1. Concentration in plasma

Fig. 1 shows the plasma concentrations of total radioactivity and the unchanged drug after oral administration of 0.5 mg/kg of [^{14}C]pioglitazone (HCl) to rats, dogs, and monkeys. Table 1 demonstrates the pharmacokinetic parameters of total ^{14}C and pioglitazone.

In rats, the concentration of pioglitazone in plasma reached a peak (C_{max} 0.71 µg/ml) at 4 h (t_{max}) after dosing and declined with $t_{1/2}$ of 2.6 h. In dogs, t_{max}, C_{max}, and $t_{1/2}$ were 0.5 h, 0.32 µg/ml, and 2.1 h, and those for monkeys were 4.3 h, 0.48 µg/ml, and 5.3 h, respectively.

Table 3: Absorption and bioavailability of [^{14}C]pioglitazone (HCl) after oral administration in rats, dogs, and monkeys.

Species	Route	Total ^{14}C		Pioglitazone	
		$AUC_{0-48\ h}$ [a] (µg · h/ml)	Absorption (%)	$AUC_{0-48\ h}$ [a] (µg · h/ml)	Bioavailability (%)
Rat	oral	15.35 ± 1.69	96	7.11 ± 0.54	85
	intravenous	15.98 ± 0.97		8.38 ± 1.01	
Dog	oral	6.80 ± 1.20	95	1.53 ± 0.18	94
	intravenous	7.18 ± 0.61		1.63 ± 0.25	
Monkey	oral	12.56 ± 3.99	90	5.55 ± 1.55	81
	intravenous	13.98 ± 3.66		6.82 ± 1.70	

Dose, 0.5 mg/kg. Data are the mean values and mean ± S.D. (n = 3). [a] Pioglitazone equivalents.

Table 4: Linearity of pharmacokinetics of [^{14}C]pioglitazone after oral administration in rats and dogs.

Species	Compound measured	Dose (mg/kg)	Pharmacokinetic parameters		
			t_{max} (h)	C_{max} [a] (µg/ml)	$AUC_{0-48\ h}$ [a] (µg · h/ml)
Rat	total ^{14}C	0.5	6.0 ± 0.0	1.05 ± 0.06	14.73 ± 0.33
		3	4.7 ± 1.2	6.44 ± 0.48	80.07 ± 10.24
		30	4.0 ± 0.0	51.76 ± 9.96	626.66 ± 51.45
	pioglitazone	0.5	4.0 ± 0.0	0.72 ± 0.08	7.61 ± 1.01
		3	4.0 ± 2.0	3.97 ± 0.56	37.05 ± 11.47
		30	2.7 ± 1.2	32.06 ± 6.60	290.39 ± 34.59
Dog	total ^{14}C	0.1	1.3 ± 0.6	0.09 ± 0.02	1.15 ± 0.17
		0.5	2.0 ± 0.0	0.46 ± 0.03	5.48 ± 0.60
		3	2.0 ± 0.0	2.53 ± 0.59	33.94 ± 2.46
	pioglitazone	0.1	0.8 ± 0.3	0.04 ± 0.01	0.21 ± 0.03
		0.5	1.2 ± 0.8	0.19 ± 0.01	0.89 ± 0.15
		3	1.0 ± 0.0	1.08 ± 0.22	5.38 ± 1.01

Data are the mean values ± S.D. (n = 3). [a] Pioglitazone equivalents.

Table 1: Pharmacokinetic parameters of radioactivity and pioglitazone in plasma after oral administration of [^{14}C]pioglitazone (HCl) to rats, dogs, and monkeys at a dose of 0.5 mg/kg.

Species	Compound	Pharmacokinetic parameter				
		t_{max} (h)	C_{max} [a] (µg/ml)	$t_{1/2}$ (h)		$AUC_{0-48\ h}$ [a] (µg · h/ml)
				α	β	
Rat	total ^{14}C	6.0 ± 0.0	1.11 ± 0.06		6.1 ± 0.7	15.4 ± 1.7
	pioglitazone	4.0 ± 0.0	0.71 ± 0.04		2.6 ± 0.1	7.11 ± 0.54
Dog	total ^{14}C	1.7 ± 0.6	0.59 ± 0.06	5.6 ± 1.6	14.2 ± 4.7	6.80 ± 1.20
	pioglitazone	0.5 ± 0.0	0.32 ± 0.06	2.1 ± 0.6		1.53 ± 0.18
Monkey	total ^{14}C	4.7 ± 3.1	0.73 ± 0.11		9.3 ± 1.3	12.6 ± 4.0
	pioglitazone	4.3 ± 3.2	0.48 ± 0.07		5.3 ± 0.8	5.55 ± 1.55

Data are the mean values ± S.D. (n = 3). [a] The concentration is expressed as µg pioglitazone eq./ml.

Table 2: Pharmacokinetic parameters of pioglitazone in plasma after intravenous administration of [^{14}C]pioglitazone (HCl) to rats, dogs, and monkeys at a dose of 0.5 mg/kg.

Species	Pharmacokinetic parameter					
	$t_{1/2}$ (h)		AUC_{0-inf} [a] (µg · h/ml)	MRT (h)	CL_{tot} (ml/h/kg)	V_{dss} (ml/kg)
	α	β				
Rat		2.4 ± 0.3	8.37 ± 1.02	3.74 ± 0.52	60.3 ± 7.2	223.2 ± 4.7
Dog		1.1 ± 0.1	1.54 ± 0.22	1.42 ± 0.10	328.7 ± 42.9	466.2 ± 52.1
Monkey	1.6 ± 0.1	5.3 ± 0.2	6.83 ± 1.72	4.09 ± 0.45	76.9 ± 22.4	309.7 ± 66.6

Data are the mean values ± S.D. (n = 3). [a] The concentration is epxressed as µg pioglitazone eq./ml.

Table 5: Composition of radioactive materials in the plasma of rats, dogs, and monkeys after oral administration of [^{14}C]pioglitazone (HCl) at a dose of 0.5 mg/kg.

Compound	$AUC_{0-48\,h}$ (μg · h/ml)		
	Rat	Dog	Monkey
Total ^{14}C	13.53 ± 1.29 (100)	5.48 ± 0.60 (100)	12.56 ± 3.99 (100)
Pioglitazone	7.22 ± 1.11 (53.3)	0.89 ± 0.15 (16.2)	5.55 ± 1.55 (44.2)
M- I	0.04 ± 0.02 (0.3)	0.12 ± 0.00 (2.2)	0.10 ± 0.04 (0.8)
M- II	1.30 ± 0.74 (9.6)	0.19 ± 0.00 (3.4)	0.36 ± 0.20 (2.9)
M-III	1.97 ± 0.20 (14.6)	0.43 ± 0.05 (7.8)	0.41 ± 0.19 (3.3)
M-IV	1.28 ± 0.07 (9.5)	2.41 ± 0.33 (44.0)	2.87 ± 0.56 (22.9)
M- V	0.60 ± 0.07 (4.4)	0.30 ± 0.03 (5.4)	0.93 ± 0.26 (7.4)
M-VI	0.12 ± 0.05 (0.9)	-[a]	-[a]
Others	1.00 ± 0.10 (7.4)	1.15 ± 0.13 (21.0)	2.35 ± 1.84 (18.7)

Data are the mean values ± S.D. (rat: n = 5, dog and monkey: n = 3). Figures in parentheses denote ratio of AUC of each compound to that of total ^{14}C. [a] Not detected.

Table 6: Plasma concentration of radioactivity after injection of [^{14}C]pioglitazone (HCl) into the gastrointestinal loops in rats.

Injection site	$AUC_{0-4\,h}$[a] (μg · h/ml)
Stomach	0.54 ± 0.14
Small intestine – upper	1.00 ± 0.18
Small intestine – middle	0.95 ± 0.14
Small intestine – lower	0.98 ± 0.14
Large intestine	0.47 ± 0.07

Data are the mean values ± S.D. (n = 3). [a] Pioglitazone equivalents.

The total plasma clearance (CL_{tot}) and the volume of distribution (V_{dss}) for pioglitazone were calculated to be 60.3 ml/h/kg and 223.2 ml/kg in rats, 328.7 ml/h/kg and 466.2 ml/kg in dogs, and 76.9 ml/h/kg and 309.7 ml/kg in monkeys, respectively (Table 2).

As calculated by the AUC ratio for the radioactivity after oral and intravenous administration of [^{14}C] pioglitazone (HCl), 96, 95, and 90 % of the radioactivity dosed were absorbed in rats, dogs, and monkeys, respectively (Table 3). The bioavailability of pioglitazone was 85, 94, and 81 % in rats, dogs, and monkeys, respectively (Table 3).

Both C_{max}s and AUCs for the unchanged compound and total ^{14}C were almost proportionately increased to the dose in the ranges of 0.5 to 30 mg/kg for rats and 0.1 to 3 mg/kg for dogs, respectively (Table 4).

Table 5 shows the metabolite composition in plasma after oral administration of [^{14}C]pioglitazone (HCl) to these three species. As calculated by the AUCs, 53, 16 and 44 % of the radioactivity in plasma were accounted for by the unchanged compound in rats, dogs and monkeys, respectively. The major metabolites were M-III, M-II and M-IV in rats, M-IV, M-III and M-V in dogs, and M-IV and M-V in monkeys, respectively.

Table 6 shows the concentration of radioactivity in plasma after intragastric, intra-small-intestinal (upper, middle and lower part) and intra-large-intestinal administrations of [^{14}C]pioglitazone (HCl) to rats. The concentrations of radioactivity in plasma after injection in three parts of small intestine were almost the same and higher than those in stomach and large intestine.

3.2. Distribution in tissues

Table 7 shows the concentration of radioactivity in tissues at 0.5, 2, 6, 10, 24 and 72 h after oral administration of [^{14}C]pioglitazone (HCl) to rats. The radioactivity was distributed widely in tissues and peaked at 6 h after dosing in most tissues except in the stomach. The concentrations of radioactivity at that time in all tissues tested except liver were lower than that in plasma. At 6 h after dosing, the concentration of radioactivity was highest in the liver, followed in decreased order by plasma, kidney, Harder's gland, adrenal gland and heart; it was lowest in the brain and eye ball. The radioactivity in tissues decreased to the very low concentrations within 24 to 72 h.

The metabolite composition in tissues of rats was determined in plasma, brain, heart, lung, liver, kidney, fat and skeletal muscle at 2, 6 and 10 h after oral administration of [^{14}C]pioglitazone (HCl) (Table 8). The unchanged compound was mainly detected in all tissues.

3.3. In vitro metabolism

[^{14}C]Pioglitazone (HCl) was incubated with blood, and slices of the brain, heart, lung, kidney and duodenum of rat in Krebs-Ringer bicarbonate buffer at 37 °C for 2 h. The

Table 7: Concentrations of radioactive materials in tissues after oral administration of [^{14}C]pioglitazone (HCl) in rats.

Tissues	Concentration of ^{14}C (μg pioglitazone equivalents/ml or g)					
	30 min	2 h	6 h	10 h	24 h	72 h
Plasma	0.28 ± 0.03	0.87 ± 0.04	0.97 ± 0.03	0.52 ± 0.16	0.06 ± 0.01	< 0.01
Brain	0.03 ± 0.00	0.08 ± 0.00	0.08 ± 0.01	0.03 ± 0.01	< 0.01	< 0.01
Spinal cord	0.03 ± 0.00	0.09 ± 0.01	0.09 ± 0.01	0.04 ± 0.01	< 0.01	< 0.01
Pituitary	0.09 ± 0.01	0.29 ± 0.03	0.34 ± 0.01	0.19 ± 0.05	0.02 ± 0.01	< 0.01
Eye ball	0.02 ± 0.00	0.05 ± 0.01	0.07 ± 0.01	0.04 ± 0.01	0.01 ± 0.00	< 0.01
Harder's gland	0.17 ± 0.02	0.60 ± 0.06	0.64 ± 0.07	0.32 ± 0.08	0.06 ± 0.00	0.01 ± 0.00
Submaxillary gland	0.09 ± 0.01	0.26 ± 0.02	0.27 ± 0.01	0.14 ± 0.04	0.02 ± 0.00	< 0.01
Thyroid	0.07 ± 0.01	0.24 ± 0.01	0.26 ± 0.01	0.14 ± 0.04	0.03 ± 0.00	0.01 ± 0.00
Thymus	0.04 ± 0.00	0.12 ± 0.00	0.14 ± 0.00	0.08 ± 0.02	0.01 ± 0.00	< 0.01
Heart	0.11 ± 0.01	0.30 ± 0.02	0.34 ± 0.02	0.17 ± 0.05	0.02 ± 0.00	< 0.01
Lung	0.10 ± 0.02	0.25 ± 0.03	0.30 ± 0.03	0.16 ± 0.03	0.02 ± 0.00	< 0.01
Liver	0.47 ± 0.05	1.28 ± 0.05	1.60 ± 0.15	1.10 ± 0.27	0.13 ± 0.02	0.02 ± 0.00
Spleen	0.05 ± 0.01	0.15 ± 0.00	0.17 ± 0.01	0.09 ± 0.03	0.01 ± 0.00	< 0.01
Pancreas	0.07 ± 0.01	0.20 ± 0.02	0.22 ± 0.02	0.11 ± 0.03	0.01 ± 0.00	< 0.01
Adrenal gland	0.14 ± 0.02	0.39 ± 0.02	0.42 ± 0.02	0.22 ± 0.07	0.04 ± 0.00	0.01 ± 0.00
Kidney	0.17 ± 0.02	0.49 ± 0.03	0.79 ± 0.03	0.48 ± 0.16	0.08 ± 0.01	0.01 ± 0.00
Testis	0.03 ± 0.00	0.16 ± 0.01	0.19 ± 0.02	0.11 ± 0.03	0.01 ± 0.00	< 0.01
Skeletal muscle	0.03 ± 0.00	0.08 ± 0.00	0.10 ± 0.01	0.05 ± 0.02	0.01 ± 0.00	< 0.01
Skin	0.05 ± 0.00	0.18 ± 0.01	0.21 ± 0.03	0.12 ± 0.03	0.02 ± 0.00	< 0.01
Epididymal fat	0.04 ± 0.00	0.13 ± 0.00	0.13 ± 0.01	0.08 ± 0.03	0.01 ± 0.01	0.01 ± 0.00
Brown fat	0.09 ± 0.01	0.32 ± 0.07	0.33 ± 0.01	0.20 ± 0.05	0.09 ± 0.02	0.03 ± 0.01
Bone marrow	0.05 ± 0.01	0.16 ± 0.01	0.19 ± 0.01	0.10 ± 0.03	0.02 ± 0.00	< 0.01
Stomach	0.90 ± 0.16	0.54 ± 0.04	0.40 ± 0.07	0.16 ± 0.06	0.02 ± 0.01	< 0.01
Intestine	0.12 ± 0.04	0.25 ± 0.01	0.35 ± 0.03	0.30 ± 0.10	0.04 ± 0.01	< 0.01

Dose, 0.5 mg/kg. Data are the mean values ± S.D. (n = 3).

Table 8: Composition of radioactive materials in tissues after oral administration of [^{14}C]pioglitazone (HCl) in rats.

Tissues	Time (h)	Concentration of ^{14}C (μg Pioglitazone equivalents/ml or g)								
		Total ^{14}C	Pioglitazone	M-I	M-II	M-III	M-IV	M-V	M-VI	Others
Plasma	2	0.87 ± 0.04	0.68 ± 0.06	< 0.01	0.02 ± 0.02	0.04 ± 0.00	0.04 ± 0.00	0.02 ± 0.01	< 0.01	0.07 ± 0.01
	6	0.97 ± 0.03	0.57 ± 0.07	< 0.01	0.06 ± 0.03	0.09 ± 0.01	0.08 ± 0.01	0.04 ± 0.01	< 0.01	0.13 ± 0.02
	10	0.52 ± 0.16	0.23 ± 0.06	< 0.01	0.04 ± 0.04	0.08 ± 0.02	0.06 ± 0.02	0.02 ± 0.01	< 0.01	0.09 ± 0.03
Brain	2	0.08 ± 0.00	0.07 ± 0.00	< 0.01	< 0.01	< 0.01	< 0.01	< 0.01	< 0.01	< 0.01
	6	0.08 ± 0.01	0.06 ± 0.01	< 0.01	< 0.01	< 0.01	0.01 ± 0.00	< 0.01	< 0.01	0.01 ± 0.00
	10	0.03 ± 0.01	0.02 ± 0.00	< 0.01	< 0.01	< 0.01	0.01 ± 0.00	< 0.01	< 0.01	0.01 ± 0.00
Heart	2	0.30 ± 0.02	0.20 ± 0.03	< 0.01	0.01 ± 0.00	0.01 ± 0.00	0.02 ± 0.00	0.01 ± 0.00	< 0.01	0.05 ± 0.01
	6	0.34 ± 0.02	0.18 ± 0.05	< 0.01	0.02 ± 0.01	0.02 ± 0.00	0.05 ± 0.01	0.01 ± 0.00	< 0.01	0.07 ± 0.03
	10	0.17 ± 0.05	0.06 ± 0.01	< 0.01	0.01 ± 0.01	0.01 ± 0.00	0.04 ± 0.00	0.01 ± 0.00	< 0.01	0.04 ± 0.02
Lung	2	0.25 ± 0.03	0.19 ± 0.03	< 0.01	< 0.01	< 0.01	0.02 ± 0.00	0.01 ± 0.00	< 0.01	0.03 ± 0.00
	6	0.30 ± 0.03	0.17 ± 0.03	< 0.01	0.01 ± 0.00	< 0.01	0.05 ± 0.00	0.01 ± 0.00	< 0.01	0.05 ± 0.01
	10	0.16 ± 0.03	0.07 ± 0.01	< 0.01	0.01 ± 0.01	< 0.01	0.04 ± 0.01	0.01 ± 0.00	< 0.01	0.03 ± 0.01
Liver	2	1.28 ± 0.05	0.82 ± 0.05	< 0.01	0.02 ± 0.01	0.02 ± 0.02	0.12 ± 0.01	0.11 ± 0.01	< 0.01	0.19 ± 0.01
	6	1.60 ± 0.15	0.71 ± 0.15	< 0.01	0.05 ± 0.02	0.01 ± 0.00	0.29 ± 0.01	0.14 ± 0.01	0.02 ± 0.01	0.39 ± 0.02
	10	1.10 ± 0.27	0.34 ± 0.10	< 0.01	0.04 ± 0.03	0.02 ± 0.01	0.29 ± 0.09	0.08 ± 0.03	0.02 ± 0.00	0.31 ± 0.04
Kidney	2	0.49 ± 0.03	0.24 ± 0.02	0.01 ± 0.00	0.01 ± 0.01	< 0.01	0.06 ± 0.00	0.09 ± 0.02	< 0.01	0.09 ± 0.00
	6	0.79 ± 0.03	0.22 ± 0.03	< 0.01	0.02 ± 0.01	0.01 ± 0.00	0.14 ± 0.00	0.15 ± 0.02	0.01 ± 0.00	0.23 ± 0.03
	10	0.48 ± 0.16	0.09 ± 0.03	< 0.01	0.02 ± 0.02	0.01 ± 0.00	0.12 ± 0.03	0.09 ± 0.05	0.01 ± 0.00	0.14 ± 0.04
Skeletal muscle	2	0.08 ± 0.00	0.06 ± 0.00	< 0.01	< 0.01	< 0.01	0.01 ± 0.00	< 0.01	< 0.01	0.01 ± 0.00
	6	0.10 ± 0.01	0.05 ± 0.01	< 0.01	< 0.01	0.01 ± 0.00	0.01 ± 0.00	0.01 ± 0.00	< 0.01	0.02 ± 0.00
	10	0.05 ± 0.02	0.02 ± 0.01	< 0.01	< 0.01	< 0.01	0.01 ± 0.00	< 0.01	< 0.01	0.01 ± 0.00
Epididymal fat	2	0.13 ± 0.00	0.05 ± 0.01	< 0.01	< 0.01	< 0.01	< 0.01	< 0.01	< 0.01	0.07 ± 0.01
	6	0.13 ± 0.01	0.04 ± 0.01	< 0.01	< 0.01	< 0.01	< 0.01	< 0.01	< 0.01	0.09 ± 0.01
	10	0.08 ± 0.03	0.02 ± 0.01	< 0.01	< 0.01	< 0.01	< 0.01	< 0.01	< 0.01	0.05 ± 0.02
Brown fat	2	0.32 ± 0.07	0.14 ± 0.04	< 0.01	< 0.01	< 0.01	0.01 ± 0.01	0.01 ± 0.00	< 0.01	0.15 ± 0.02
	6	0.33 ± 0.01	0.12 ± 0.01	< 0.01	0.01 ± 0.00	< 0.01	0.02 ± 0.01	0.01 ± 0.00	< 0.01	0.16 ± 0.01
	10	0.20 ± 0.05	0.05 ± 0.01	< 0.01	0.01 ± 0.00	< 0.01	0.02 ± 0.01	0.01 ± 0.00	< 0.01	0.11 ± 0.03

Dose, 0.5 mg/kg. Data are the mean values ± S.D. (n = 3).

Table 9: In vitro metabolism of [^{14}C]pioglitazone (HCl) incubated with rat tissue slices.

Tissues	Metabolic activity (μg/2 h/0.2 g tissue)	Formation rate (μg/2 h/0.2 g tissue)				
		M-II	M-III	M-IV	M-V	M-VI
Blood	< 0.01	< 0.01	< 0.01	< 0.01	< 0.01	< 0.01
Brain	0.03 ± 0.03	< 0.01	< 0.01	0.01 ± 0.01	< 0.01	< 0.01
Heart	< 0.01	< 0.01	< 0.01	0.01 ± 0.01	< 0.01	< 0.01
Lung	0.02 ± 0.02	0.01 ± 0.01	< 0.01	0.02 ± 0.01	0.01 ± 0.00	< 0.01
Liver	0.98 ± 0.13	0.04 ± 0.01	0.10 ± 0.02	0.11 ± 0.01	0.16 ± 0.03	0.02 ± 0.01
Kidney	0.70 ± 0.10	0.02 ± 0.03	0.06 ± 0.02	0.13 ± 0.03	0.45 ± 0.05	0.01 ± 0.01
Duodenum	0.29 ± 0.07	0.02 ± 0.01	0.01 ± 0.00	0.08 ± 0.01	0.04 ± 0.01	< 0.01

Blood (0.2 ml) and tissue slices (0.2 g) were incubated with [^{14}C]pioglitazone (2 μg/ml) for 2 h at 37 °C. Data are the mean values ± S.D. (n = 3).

unchanged compound and the metabolites were determined. Table 9 shows the decrease of pioglitazone content and the formation rate of metabolites in each tissue. The metabolic activity was highest in the liver, followed in decreased order by kidney and duodenum. Almost no metabolism was observed in blood, brain, heart and lung. In liver, M-V, M-IV, M-III and M-II, in kidney, M-V, and in duodenum, M-IV were mainly formed, respectively.

3.4. Excretion

3.4.1. Excretion into urine, feces and expired air

Table 10 shows the excretion of radioactivity in urine and feces after oral administration of [^{14}C]pioglitazone (HCl) to rats, dogs and monkeys. Most of the radioactivity dosed was excreted within 72 h in rats, 96 h in dogs and 168 h in monkeys. The radioactivity was largely excreted in feces of rats and dogs, whereas in monkeys it was excreted predominantly in urine. Only 1.2 % of the dose was excreted into the expired air of rats within 72 h.

Table 11 shows the metabolite composition in urine and feces after oral administration of [^{14}C]pioglitazone (HCl) to rats, dogs, and monkeys. In urine of rats and monkeys, M-V was predominantly excreted and in urine of dogs, M-I and M-V were mainly detected. In feces of rats, M-V and M-IV were largely excreted, and in feces of dogs and monkeys, M-V was mainly detected.

3.4.2. Biliary excretion and reabsorption

Table 10 and 11 also show the excretion of radioactivity and metabolite composition in bile after intraduodenal administration of [^{14}C]pioglitazone (HCl) to biliary-cannulated rats. Within 24 h, 60 % of the radioactivity dosed was excreted into bile, and the main components were M-IV and M-V.

To examine the enterohepatic circulation, the radioactive bile (10 ml/kg) was administered intraduodenally to other biliary-cannulated rats. Within 24 h, 38 and 13 % of the radioactivity dosed were excreted into bile and urine, respectively. Thus, the drug-related materials excreted into bile are partly reabsorbed via enterohepatic circulation.

4. Discussion

We studied the disposition of pioglitazone after oral administration of [^{14}C]pioglitazone (HCl) to rats, dogs, and monkeys. The study concerning the absorption site in rats showed that pioglitazone was well absorbed from

Table 10: Excretion of radioactive materials in urine, feces, and bile after oral administration of [^{14}C]pioglitazone (HCl) in rats, dogs, and monkeys.

Species	Time (h)	Cumulative excretion (% of dose)			
		Urine	Feces	Bile	Total
Rat	4	2.1 ± 2.3	ND	ND	ND
	8	11.0 ± 3.8	ND	ND	ND
	24	32.4 ± 1.2	40.2 ± 11.7	ND	72.6 ± 12.8
	48	35.5 ± 0.5	61.7 ± 1.9	ND	97.2 ± 1.6
	72	35.9 ± 0.6	63.2 ± 1.3	ND	99.1 ± 0.8
	96	36.0 ± 0.6	63.4 ± 1.3	ND	99.4 ± 0.8
Rat[a)]	4	0.5 ± 0.1	ND	12.8 ± 2.6	ND
	8	2.4 ± 1.1	ND	31.9 ± 5.2	ND
	24	13.7 ± 3.9	15.9 ± 2.1[b)]	60.3 ± 3.4	89.9 ± 2.9
Dog	4	0.8 ± 1.4	ND	ND	ND
	8	1.4 ± 1.3	ND	ND	ND
	24	11.7 ± 0.3	25.4 ± 25.6	ND	37.0 ± 25.3
	48	15.1 ± 1.0	60.4 ± 26.5	ND	75.5 ± 25.6
	72	16.0 ± 1.5	79.9 ± 1.7	ND	95.9 ± 1.6
	96	16.3 ± 1.5	80.8 ± 1.5	ND	97.1 ± 1.4
	120	16.4 ± 1.5	81.1 ± 1.4	ND	97.5 ± 1.4
Monkey	4	8.4 ± 2.9	ND	ND	ND
	8	24.6 ± 3.5	ND	ND	ND
	24	59.8 ± 2.6	1.3 ± 2.1	ND	61.2 ± 2.6
	48	69.7 ± 1.4	5.2 ± 3.3	ND	74.8 ± 2.7
	72	73.9 ± 1.5	10.7 ± 5.3	ND	84.6 ± 3.9
	96	75.9 ± 2.1	13.7 ± 6.1	ND	89.6 ± 4.0
	120	76.8 ± 2.4	16.1 ± 5.2	ND	92.9 ± 2.8
	144	77.2 ± 2.4	17.1 ± 4.7	ND	94.3 ± 2.4
	168	77.4 ± 2.5	17.6 ± 4.4	ND	95.0 ± 2.3

Dose, 0.5 mg/kg. Data are the mean values ± S.D. (n = 3). ND, not determined. [a)] Biliary-cannulated rats (intraduodenal administration). [b)] Include gut contents.

the wide range of small intestine. The absorption extent after oral administration was high for all of these three species; 96, 95 and 90 % in rats, dogs and monkeys, respectively. Pioglitazone after oral administration also showed the high bioavailability, 85, 94, and 81 % in rats, dogs, and monkeys, respectively. These findings show only a little part of the drug undergo first-pass effect during absorption, although in vitro study showed that pioglitazone was partly metabolized in rat duodenum. The unchanged compound in plasma of rats, dogs, and monkeys was 53, 16, and 44 % of the total radioactivity, respectively. The total concentrations of pioglitazone, M-II, M-III and M-IV, which have the pharmacological activity [3], accounted for 87, 71 and 73 % of the total radioactivity in plasma in these species, respectively. These results suggest that these metabolites contribute, at least in part, to the pharmacological action after oral dosing of pioglitazone.

In vitro study using liver and kidney slices showed that all identified metabolites except M-I were detected. In the kidney, M-V was predominantly formed, which agreed well with that the main compound excreted in urine of rats was M-V. In the liver, M-V was formed in higher rate than M-IV, M-III and M-II. However, concentrations of M-III, M-II, and M-IV in plasma were higher than that of M-V. On the other hand, M-V was largely excreted in urine and bile. These findings would show that among the metabolites formed in the liver, M-V is more easily excreted than the unchanged compound, M-II, M-III, and M-IV due probably to the more hydrophilicity of M-V than the latter compounds.

The radioactivity was widely distributed in tissues of rats after oral administration, and the highest concentration was found in the liver at 6 h after dosing. The radioactivity in tissues decreased to the very low concentrations within 24 to 72 h in all tissues investigated.

In most tissues, the concentrations of radioactivity were lower than that in plasma. This coincides with the very small distribution volume of pioglitazone after intravenous administration to rats (V_{dss} = 223 ml/kg). The binding of pioglitazone and its metabolites to rat plasma proteins was very high (more than 99 %), which may be partly the cause of this relatively low concentrations of radioactivity in rat tissues.

The absorption extent was very high and pioglitazone administered intraduodenally to the biliary-cannulated rats was largely excreted into bile. Further the metabolite composition in bile and feces were similar and little amount of the unchanged compound was detected in feces. These findings suggest that the radioactivity in feces is excreted mostly via hepato-biliary route after absorption and not due to the unabsorbed compound.

In conclusion, after oral administration to rats, dogs and monkeys, pioglitazone was well absorbed from wide range of small intestine, metabolized mainly to M-I to M-VI and quantitatively excreted in urine and feces via

Table 11: Composition of radioactive materials in excreta after oral administration of [^{14}C]pioglitazone (HCl) in rats, dogs, and monkeys.

Species	Sample	Total ^{14}C (% of dose)		Composition of metabolites (% of dose)							
				Pioglitazone	M-I	M-II	M-III	M-IV	M-V	M-VI	Others
Rat	48-h urine	35.5 ± 0.5	U	< 0.1	0.1	< 0.1	< 0.1	0.1	9.5	2.8	
			C	< 0.1	1.7	< 0.1	< 0.1	1.9	1.4[a)]	0.1	
			T	< 0.1	1.8	< 0.1	< 0.1	2.0	10.9	2.9	17.9
	48-h feces	61.7 ± 1.9	U	1.7	< 0.1	2.7	0.2	1.8	13.7	4.0	
			C	< 0.1	0.2	< 0.1	< 0.1	8.9	2.4[a)]	0.3	
			T	1.7	0.2	2.7	0.2	10.7	16.1	4.3	25.8
	24-h bile	60.3 ± 3.4	U	0.1	< 0.1	0.1	0.1	0.2	10.9	2.8	
			C	0.1	0.6	4.0	< 0.1	10.9	9.6[a)]	0.2	
			T	0.2	0.6	4.1	0.1	11.1	20.5	3.0	20.7
Dog	72-h urine	16.0 ± 1.5	U	0.2	0.5	0.2	0.1	0.3	1.4	0.3	
			C	< 0.1	2.0	0.2	0.1	0.3	0.4[a)]	0.1	
			T	0.2	2.5	0.3	0.2	0.6	1.9	0.4	9.9
	72-h feces	79.9 ± 1.7	U	0.6	1.4	0.6	0.4	4.9	32.9	4.6	
			C	0.3	0.2	< 0.1	0.2	3.3	15.5[a)]	< 0.1	
			T	0.9	1.6	0.6	0.5	8.1	48.4	4.6	15.0
Monkey	72-h urine	73.9 ± 1.5	U	< 0.1	0.6	< 0.1	< 0.1	0.3	35.9	4.4	
			C	0.1	6.3	1.3	< 0.1	1.3	1.9[a)]	0.3	
			T	0.1	7.0	1.3	0.1	1.6	37.8	4.7	21.4
	72-h feces	10.7 ± 5.3	U	< 0.1	< 0.1	< 0.1	< 0.1	0.1	5.2	2.0	
			C	0.2	0.1	< 0.1	< 0.1	0.6	0.2[a)]	< 0.1	
			T	0.2	0.1	< 0.1	< 0.1	0.7	5.4	2.0	2.3

Dose, 0.5 mg/kg. Total radioactivity: the mean values ± S.D. (n = 3). Metabolites: the mean values (n = 3). U: unconjugates, C: conjugates (glucuronide and/or sulfate), T = U + C. [a)] Include taurine conjugate.

hepato-biliary route. The pharmacologically active compounds (total of pioglitazone, M-II, M-III and M-IV) accounted for 87, 71, and 73 % of the radioactivity in plasma of rats, dogs, and monkeys, respectively. The radioactivity was distributed widely in tissues after oral administration to rats, and decreased to the very low concentration within 24 to 72 h after dosing.

5. References

[1] Sohda, T., Mizuno, K., Momose, Y. et al., J. Med. Chem. **35**, 2617 (1992) – [2] Sohda, T., Momose, Y., Meguro, K. et al., Arzneim.-Forsch./Drug Res. **40 (I)**, 37 (1990) – [3] Sohda, T., Ikeda, H., Meguro, K., Chem. Pharm. Bull. **43**, 2168 (1995) – [4] Ikeda, H., Taketomi, S., Sugiyama, Y. et al., Arzneim.-Forsch./Drug Res. **40 (I)**, 156 (1990) – [5] Sugiyama, Y., Taketomi, S., Shimura, Y. et al., Arzneim.-Forsch./Drug Res. **40 (I)**, 263 (1990) – [6] Sugiyama, Y., Shimura, Y., Ikeda, H., Arzneim.-Forsch./Drug Res. **40 (I)**, 436 (1990) – [7] Castle, C. K., Colca, J. R., Melchior, G. W., Aterioscler. Thromb. **13**, 302 (1993) – [8] Kobayashi, M., Iwanishi, M., Egawa, K. et al., Diabetes **41** 476 (1992) – [9] Hofmann, C., Lorenz, K., Colca, J. R., Endocrinology **129**, 1915 (1991) – [10] Hofmann, C., Edwards III, C. W., Hillman, R. M. et al., Endocrinology **130**, 735 (1992) – [11] Kletzien, R. F., Clarke, S. D., Ulrich, R. G., Mol. Pharmacol. **41**, 393 (1992) – [12] Kletzien, R. F., Foellmi, L. A., Harris, P. K. W. et al., Mol. Pharmacol. **42**, 558 (1992) – [13] Kiyota, Y., Kondo, T., Maeshiba, Y. et al., Arzneim.-Forsch./Drug Res. **47 (I)**, 22 (1997) – [14] Tanayama, S., Shirakawa, Y., Kanai, Y. et al., Xenobiotica **4**, 33 (1974) – [15] Tanayama, S., Kobayashi, T., Kanai, Y., Xenobiotica **8**, 365 (1978) – [16] Kondo, T., Kurata, Y., Yoshida, K. et al., Biol. Pharm. Bull. **18**, 330 (1995) – [17] Yamaoka, K., Nakagawa, T., Uno, T., J. Pharmacokinet. Biopharm. **6**, 547 (1978)

Correspondence: Yoshihiro Maeshiba, Drug Analysis and Pharmacokinetics Research Laboratories, Pharmaceutical Development Division, Takeda Chemical Industries, Ltd., 2-17-85, Juso-Honmachi, Yodogawa-ku, Osaka, 532 (Japan)

ArzneimForsch DrugRes

Lipidsenker

Lipid Reducers

Synthesis and Antihyperlipaemic Activity of Some Novel N-Cyanovinylformamidines

Chamanlal J. Shishoo[a], Mahesh T. Chhabria[a], Thakorebhai P. Gandhi[b], and Ramkrishna A. Bangaru[b]

Department of Pharmaceutical Chemistry, L. M. College of Pharmacy[a], and Department of Pharmacology, Cadila Pharmaceuticals Ltd.[b], Ahmedabad (India)

Summary

Potent antihyperlipaemic activity has been observed in a series of novel N-cyanovinylformamidines when tested in hyperlipaemic rats. Two of the compounds (**11** and **15**) were found more potent than gemfibrozil at 50 mg/kg/d dose level in reducing serum cholesterol and triglyceride levels and also in elevating serum HDL level. A good three-dimensional structural similarity has been observed between these two compounds and clofibrate and gemfibrozil, respectively. Acute toxicity studies carried out in mice indicated compound **11** to be safe even at a dose level of 4.5 g/kg. The title compounds were synthesized by the reaction of α-cyanoketene S,N-acetals with formamidineacetate under controlled reaction conditions.

Disposition of the New Antidiabetic Agent Pioglitazone in Rats, Dogs, and Monkeys

Yoshihiro Maeshiba, Yutaka Kiyota, Kenji Yamashita, Yoshinobu Yoshimura, Michio Motohashi, and Shigeharu Tanayama

Drug Analysis and Pharmacokinetics Research Laboratories, Pharmaceutical Development Division, Takeda Chemical Industries, Ltd., Osaka (Japan)

Summary

The disposition of pioglitazone (CAS 105355-27-9, AD-4833) was studied after oral administration to rats, dogs, and monkeys using ^{14}C-labeled drug. After oral dosing, pioglitazone was well absorbed from the gastrointestinal tract at an extent of 96, 95, and 90 % in rats, dogs, and monkeys, respectively. In rats, the concentration of pioglitazone in plasma reached a peak (C_{max} 0.71 μg/ml) at 4 h (t_{max}) after dosing and declined with a half-life ($t_{1/2}$) of 2.6 h. In dogs, t_{max}, C_{max} and $t_{1/2}$ were 0.5 h, 0.32 μg/ml and 2.1 h, and those for monkeys were 4.3 h, 0.48 μg/ml and 5.3 h, respectively. The drug was metabolized mainly to M-I to M-VI including the pharmacologically active metabolites (M-II, III, and IV). The pharmacologically active compounds (total of the unchanged compound and the above three active metabolites) accounted for 87, 71 and 73 % of the radioactivity in plasma of rats, dogs, and monkeys, respectively. The radioactivity was widely distributed in tissues after oral administration to rats, and decreased to the very low concentration within 24 to 72 h after dosing. Radioactivity dose was almost completely excreted in urine and feces.

Zusammenfassung

Verfügbarkeit des neuen Antidiabetikums Pioglitazon bei Ratte, Hund und Affe

Die Verfügbarkeit von Pioglitazon (CAS 105355-27-9, AD-4833) wurde nach oraler Verabreichung der ^{14}C-markierten Substanz an Ratten, Hunden und Affen untersucht. Pioglitazon wurde nach oraler Gabe im Magen-Darm-Trakt gut resorbiert; die Resorptionsrate betrug bei Ratten, Hunden und Affen 96, 95 bzw. 90 %. Bei Ratten erreichte die Pioglitazon-Konzentration im Plasma ihr Maximum (C_{max} 0.71 μg/ml) 4 h (t_{max}) nach Verabreichung und nahm danach mit einer Halbwertzeit ($t_{1/2}$) von 2,6 h wieder ab. Bei Hunden betrugen die Werte t_{max}, C_{max} und $t_{1/2}$ 0,5 h, 0,32 μg/ml bzw. 2,1 h und bei Affen 4,3 h, 0,48 μg/ml bzw. 5,3 h. Die Substanz wurde überwiegend zu M-I bis M-VI einschließlich der pharmakologisch aktiven Metaboliten (M-II, III und IV) metabolisiert. Die pharmakologisch aktiven Substanzen (Gesamtmenge der unveränderten Substanz und der drei oben genannten aktiven Metaboliten) erreichten einen Anteil an der Radioaktivität im Plasma von Ratten, Hunden und Affen von 87, 71 bzw. 73 %. Nach oraler Verabreichung an Ratten war die Radioaktivität in den Geweben weit verteilt und nahm 24 bis 72 h nach Gabe bis zur Minimalkonzentration ab. Die Radioaktivität wurde nahezu vollständig in Urin und Fäzes ausgeschieden.

Key words AD-4833, disposition · Antidiabetic agent · CAS 105355-27-9 · Pioglitazone

Arzneim.-Forsch./Drug Res. 47 (I), 29–35 (1997)

1. Introduction

Pioglitazone (HCl) ((±)-5-[p-[2-(5-ethyl-2-pyridyl) ethoxy] benzyl]- 2,4- thiazolidinedione hydrochloride, CAS 105355-27-9, AD-4833[1]) (HCl) (see Scheme 1) has potent hypoglycemic and hypolipidemic effects in animal models of non-insulin-dependent diabetes mellitus [1–12] and is now undergoing clinical trials in Japan and the USA. In a separate paper [13], we reported that pioglitazone was metabolized to M-I to M-VI after oral dosing in rats and dogs. Scheme 1 shows the postulated metabolic pathways of pioglitazone. Among these metabolites, M-II, M-III and M-IV exert pharmacological activity, although being somewhat less active than the parent drug [3]. In this paper, we describe the disposition of pioglitazone after oral or intravenous administration of ^{14}C-labeled drug ([^{14}C]pioglitazone HCl) to rats, dogs and monkeys.

[1] Manufacturer: Takeda Chemical Industries, Ltd., Osaka (Japan).

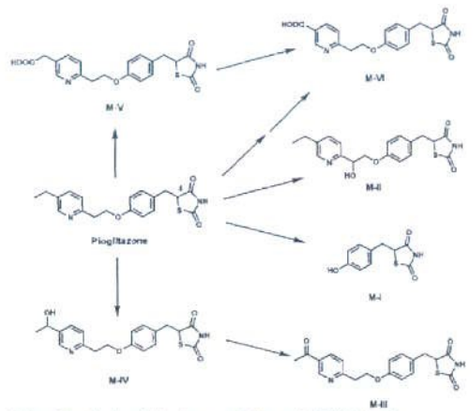
2. Materials and methods

2.1. Chemicals

Bulk pioglitazone (HCl) and its metabolites (M-I to M-VI) were prepared in house by Pharmaceutical Research Division, Takeda Chemical Industries, Ltd. (Osaka Japan) [3]. [^{14}C]Pioglitazone (HCl) with specific radioactivities of 4.8 to 5.5 MBq/mg were synthesized by Nemoto & Co., Ltd. (Tokyo, Japan) and T. N. Technos, Ltd. (Tokyo, Japan). The radiopurities verified by thin-layer chromatography (TLC) were > 98 %. All other chemicals and reagents were purchased from commercial sources.

2.2. Animals

Animals used in this study were male Jcl: Sprague Dawley rats (weight, 244 to 345 g; CLEA Japan Inc., Tokyo, Japan), male beagle dogs (weight, 8.0 to 12.0 kg; Oriental Yeast Co., Ltd., Tokyo, Japan) and male Cynomolgus monkeys (weight, 2.7 to 4.4 kg; Kaibo Co., Ltd., Tokyo, Japan). They were fed laboratory chow (CE-2 for rats and CD-5 for dogs; CLEA Japan Inc., and Primate Chow # 5048 for monkeys; Purina Mills, Inc., Richmond, VA, USA), had free access to water, and were housed in temperature- and humidity-controlled rooms (20 to 26 °C and 40 to 75 %) with 12-h light-dark cycles for more than a week before use.



Scheme 1: Postulated metabolic pathways of pioglitazone. *: ^{14}C-labeled position.

2.3. Dosing and sampling

[^{14}C]Pioglitazone (HCl) diluted appropriately with the unlabeled compound was dissolved in 0.5 mol/l citric acid for oral administration at a dose of 0.5 mg/10 ml/kg to rats, and 0.5 mg/2 ml/kg to dogs and monkeys. [^{14}C]Pioglitazone (HCl) was dissolved in dimethylsulfoxide for intravenous injection at a dose of 0.5 mg/ml/kg to rats, and 0.5 mg/0.2 ml/kg to dogs and monkeys. The compound was administered to fed animals. After dosing, serial samples of plasma, tissues, excreta, and respiratory air were collected according to the methods described previously [14, 15].

2.4. Absorption site

Absorption site in rats was studied according to the procedures reported previously [16]. [^{14}C]Pioglitazone (HCl) in 0.5 % methylcellulose suspension was injected into the following loop separately at a dose of 0.5 mg/2 ml/kg: stomach (whole), small intestine (upper, middle and lower) and large intestine (each 6 cm). At 0.25, 0.5, 1, 2 and 4 h after injection, the concentration of ^{14}C in plasma was measured.

2.5. In vitro metabolism

Slices (0.2 mm thick) of brain, heart, lung, liver, kidney, and duodenum of rats were prepared. [^{14}C]Pioglitazone (HCl) (2 μg) was incubated with the slices (0.2 g) or blood (0.2 ml) in Krebs-Ringer bicarbonate buffer (1 ml) for 2 h at 37 °C under O_2-CO_2 gas (95 : 5, v/v). After the incubation, the reaction mixture was homogenized and extracted with 6 ml of methanol for the determination of pioglitazone and its metabolites by TLC with solvent system A described below.

2.6. Analytical methods

The radioactivity in biological samples, organic solvent extracts, and silica gel from TLC plates was determined by a liquid scintillation spectrometry as reported previously [15, 16].

Pioglitazone and its metabolites in biological specimens were quantified by TLC as follows. The radioactive materials in plasma and aqueous homogenates of feces or tissues were extracted with acetone and methanol (both 5 vol.), respectively. A portion of acetone or methanol extracts, urine and bile were subjected to TLC using precoated silica gel 60 F_{254} plates (0.25 mm thick; E. Merck, Darmstadt, Germany). The solvent systems for determination of the unchanged compound and metabolites M-I to M-VI were as follows: system A, n-hexane-diethyl ether-ethanol-acetic acid (25 : 80 : 5 : 1, by vol.) and system B, chloroform-acetone-acetic acid (15 : 6 : 1, by vol.). System A was used for the quantitation of the unchanged compound and metabolites in plasma; Rf values for pioglitazone, M-I, M-II, M-III, M-IV, M-V and M-VI were 0.61, 0.73, 0.53, 0.46, 0.25, 0.14, and 0.29, respectively. The two dimensional TLC system using system A followed by B was adopted for the quantitation of the unchanged compound and metabolites in excreta and tissues; Rf values (x for system B, y for system A) of pioglitazone, M-I, M-II, M-III, M-IV, M-V and M-VI were (0.72, 0.61), (0.79, 0.73), (0.67, 0.53), (0.81, 0.46), (0.40, 0.25), (0.30, 0.14) and (0.52, 0.29), respectively. After development, the radioactive materials on the plate were located by radioluminography using bioimaging analyzer (BAS2000; Fuji Photo Film Co., Ltd., Tokyo, Japan) and imaging plates (Fuji Photo Film). The silica gel sections that corresponded to pioglitazone and its metabolites were scraped off the plate, and each radioactivity was counted. The remainder of the materials on the plate was also removed and counted, and was referred to as "other metabolites". To determine the conjugated metabolites, the samples were treated with β-glucuronidase containing phenol sulfatase (type H-1; Sigma, St. Louis, MO, USA).

2.7. Data processing

Data are expressed as the mean values ± standard deviations (S.D.) of the results for 3 to 5 animals. Peak time (t_{max}) and maximum concentration (C_{max}) were noted directly from the plasma concentration data. The apparent half-life ($t_{1/2}$) in plasma and area under the plasma concentration-time curve (AUC) were calculated by the linear regression analysis and the trapezoidal rule, respectively. Pharmacokinetic parameters for pioglitazone after intravenous administration were calculated with the following equations;

$$CL_{tot} = dose/AUC_{0\text{-}\infty}$$

wherein CL_{tot} is total plasma clearance of the drug;

$$V_{dss} = CL_{tot} \cdot MRT$$

wherein V_{dss} is the estimated steady-state volume of distribution of the drug, and MRT is the mean residence time calculated by the moment analysis [17].

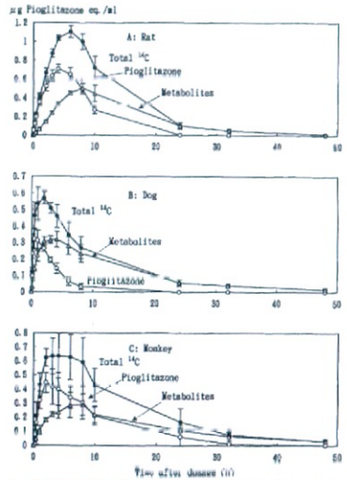


Fig. 1: Concentration of total ^{14}C and pioglitazone in plasma of rats, dogs, and monkeys after oral administration of [^{14}C]pioglitazone (HCl). Dose: 0.5 mg/kg. Data are the mean values ± S.D. (n = 3).

3. Results

3.1. Concentration in plasma

Fig. 1 shows the plasma concentrations of total radioactivity and the unchanged drug after oral administration of 0.5 mg/kg of [^{14}C]pioglitazone (HCl) to rats, dogs, and monkeys. Table 1 demonstrates the pharmacokinetic parameters of total ^{14}C and pioglitazone.

In rats, the concentration of pioglitazone in plasma reached a peak (C_{max} 0.71 μg/ml) at 4 h (t_{max}) after dosing and declined with $t_{1/2}$ of 2.6 h. In dogs, t_{max}, C_{max}, and $t_{1/2}$ were 0.5 h, 0.32 μg/ml, and 2.1 h, and those for monkeys were 4.3 h, 0.48 μg/ml, and 5.3 h, respectively.

Table 1: Pharmacokinetic parameters of radioactivity and pioglitazone in plasma after oral administration of [^{14}C]pioglitazone (HCl) to rats, dogs, and monkeys at a dose of 0.5 mg/kg.

Species	Compound	Pharmacokinetic parameter				
		t_{max} (h)	C_{max} [a] (μg/ml)	$t_{1/2}$ (h) α	$t_{1/2}$ (h) β	$AUC_{0-48\,h}$ [a] (μg · h/ml)
Rat	total ^{14}C	6.0 ± 0.0	1.11 ± 0.06		6.1 ± 0.7	15.4 ± 1.7
	pioglitazone	4.0 ± 0.0	0.71 ± 0.04		2.6 ± 0.1	7.11 ± 0.54
Dog	total ^{14}C	1.7 ± 0.6	0.59 ± 0.06	5.6 ± 1.6	14.2 ± 4.7	6.80 ± 1.20
	pioglitazone	0.5 ± 0.0	0.32 ± 0.06	2.1 ± 0.6		1.53 ± 0.18
Monkey	total ^{14}C	4.7 ± 3.1	0.72 ± 0.11		9.3 ± 1.3	14.6 ± 4.0
	pioglitazone	4.3 ± 3.2	0.48 ± 0.07		5.3 ± 0.8	5.55 ± 1.55

Data are the mean values ± S.D. (n = 3). [a] The concentration is expressed as μg pioglitazone eq./ml.

Table 2: Pharmacokinetic parameters of pioglitazone in plasma after intravenous administration of [^{14}C]pioglitazone (HCl) to rats, dogs, and monkeys at a dose of 0.5 mg/kg.

Species	Pharmacokinetic parameter					
	$t_{1/2}$ (h) α	$t_{1/2}$ (h) β	AUC_{0-inf} [a] (μg · h/ml)	MRT (h)	CL_{tot} (ml/h/kg)	V_{dss} (ml/kg)
Rat		2.4 ± 0.3	8.37 ± 1.02	3.74 ± 0.52	60.3 ± 7.2	223.2 ± 4.7
Dog		1.1 ± 0.1	1.54 ± 0.22	1.42 ± 0.10	328.7 ± 42.9	466.2 ± 52.1
Monkey	1.6 ± 0.1	5.3 ± 0.2	6.83 ± 1.72	4.09 ± 0.45	76.9 ± 22.4	309.7 ± 66.6

Data are the mean values ± S.D. (n = 3). [a] The concentration is expressed as μg pioglitazone eq./ml.

Table 3: Absorption and bioavailability of [^{14}C]pioglitazone (HCl) after oral administration in rats, dogs, and monkeys.

Species	Route	Total ^{14}C		Pioglitazone	
		$AUC_{0-48\,h}$ [a] (μg · h/ml)	Absorption (%)	$AUC_{0-48\,h}$ [a] (μg · h/ml)	Bioavailability (%)
Rat	oral	15.35 ± 1.69	96	7.11 ± 0.54	85
	intravenous	15.98 ± 0.97		8.38 ± 1.01	
Dog	oral	6.80 ± 1.20	95	1.53 ± 0.18	94
	intravenous	7.18 ± 0.61		1.63 ± 0.23	
Monkey	oral	12.56 ± 3.99	90	5.55 ± 1.55	81
	intravenous	13.98 ± 3.66		6.82 ± 1.70	

Dose, 0.5 mg/kg. Data are the mean values and mean ± S.D. (n = 3). [a] Pioglitazone equivalents.

Table 4: Linearity of pharmacokinetics of [^{14}C]pioglitazone after oral administration in rats and dogs.

Species	Compound measured	Dose (mg/kg)	Pharmacokinetic parameters		
			t_{max} (h)	C_{max} [a] (μg/ml)	$AUC_{0-48\,h}$ [a] (μg · h/ml)
Rat	total ^{14}C	0.5	6.0 ± 0.0	1.05 ± 0.06	14.73 ± 0.33
		3	4.7 ± 1.2	6.44 ± 0.48	80.07 ± 10.24
		30	4.0 ± 0.0	51.76 ± 9.96	626.66 ± 51.45
	pioglitazone	0.5	4.0 ± 0.0	0.72 ± 0.08	7.61 ± 1.01
		3	4.0 ± 2.0	3.97 ± 0.56	37.05 ± 11.47
		30	2.7 ± 1.2	32.06 ± 6.60	290.39 ± 34.59
Dog	total ^{14}C	0.1	1.3 ± 0.6	0.09 ± 0.02	1.15 ± 0.17
		0.5	2.0 ± 0.0	0.46 ± 0.03	5.48 ± 0.60
		3	2.0 ± 0.0	2.53 ± 0.59	33.94 ± 2.46
	pioglitazone	0.1	0.8 ± 0.3	0.04 ± 0.01	0.21 ± 0.03
		0.5	1.2 ± 0.8	0.19 ± 0.01	0.89 ± 0.15
		3	1.0 ± 0.0	1.06 ± 0.22	8.58 ± 1.01

Data are the mean values ± S.D. (n = 3). [a] Pioglitazone equivalents.

Table 5: Composition of radioactive materials in the plasma of rats, dogs, and monkeys after oral administration of [^{14}C]pioglitazone (HCl) at a dose of 0.5 mg/kg.

Compound	$AUC_{0-48\,h}$ (μg · h/ml)		
	Rat	Dog	Monkey
Total ^{14}C	13.53 ± 1.29 (100)	5.48 ± 0.60 (100)	12.56 ± 3.99 (100)
Pioglitazone	7.22 ± 1.11 (53.3)	0.89 ± 0.15 (16.2)	5.55 ± 1.55 (44.2)
M– I	0.04 ± 0.02 (0.3)	0.12 ± 0.00 (2.2)	0.10 ± 0.04 (0.8)
M– II	1.30 ± 0.74 (9.6)	0.19 ± 0.00 (3.4)	0.36 ± 0.20 (2.9)
M–III	1.97 ± 0.20 (14.6)	0.43 ± 0.05 (7.8)	0.41 ± 0.19 (3.3)
M–IV	1.28 ± 0.07 (9.5)	2.41 ± 0.33 (44.0)	2.87 ± 0.56 (22.9)
M– V	0.60 ± 0.07 (4.4)	0.30 ± 0.03 (5.4)	0.93 ± 0.26 (7.4)
M–VI	0.12 ± 0.05 (0.9)	–[a]	–[a]
Others	1.00 ± 0.10 (7.4)	1.15 ± 0.13 (21.0)	2.35 ± 1.84 (18.7)

Data are the mean values ± S.D. (rat: n = 5, dog and monkey: n = 3). Figures in parentheses denote ratio of AUC of each compound to that of total ^{14}C. [a] Not detected.

Table 6: Plasma concentration of radioactivity after injection of [^{14}C]pioglitazone (HCl) into the gastrointestinal loops in rats.

Injection site	$AUC_{0-6\,h}$ [a] (μg · h/ml)
Stomach	0.54 ± 0.14
Small intestine – upper	1.00 ± 0.18
Small intestine – middle	0.95 ± 0.14
Small intestine – lower	0.98 ± 0.14
Large intestine	0.47 ± 0.07

Data are the mean values ± S.D. (n = 3). [a] Pioglitazone equivalents.

The total plasma clearance (CL_{tot}) and the volume of distribution (V_{dss}) for pioglitazone were calculated to be 60.3 ml/h/kg and 223.2 ml/kg in rats, 328.7 ml/h/kg and 466.2 ml/kg in dogs, and 76.9 ml/h/kg and 309.7 ml/kg in monkeys, respectively (Table 2).

As calculated by the AUC ratio for the radioactivity after oral and intravenous administration of [^{14}C] pioglitazone (HCl), 96, 95, and 90 % of the radioactivity dosed were absorbed in rats, dogs, and monkeys, respectively (Table 3). The bioavailability of pioglitazone was 85, 94, and 81 % in rats, dogs, and monkeys, respectively (Table 3).

Both C_{max}s and AUCs for the unchanged compound and total ^{14}C were almost proportionately increased to the dose in the ranges of 0.5 to 30 mg/kg for rats and 0.1 to 3 mg/kg for dogs, respectively (Table 4).

Table 5 shows the metabolite composition in plasma after oral administration of [^{14}C]pioglitazone (HCl) to these three species. As calculated by the AUCs, 53, 16 and 44 % of the radioactivity in plasma were accounted for by the unchanged compound in rats, dogs and monkeys, respectively. The major metabolites were M-III, M-II and M-IV in rats, M-IV, M-III and M-V in dogs, and M-IV and M-V in monkeys, respectively.

Table 6 shows the concentration of radioactivity in plasma after intragastric, intra-small-intestinal (upper, middle and lower part) and intra-large-intestinal administrations of [^{14}C]pioglitazone (HCl) to rats. The concentrations of radioactivity in plasma after injection in three parts of small intestine were almost the same and higher than those in stomach and large intestine.

3.2. Distribution in tissues

Table 7 shows the concentration of radioactivity in tissues at 0.5, 2, 6, 10, 24 and 72 h after oral administration of [^{14}C]pioglitazone (HCl) to rats. The radioactivity was distributed widely in tissues and peaked at 6 h after dosing in most tissues except in the stomach. The concentrations of radioactivity at that time in all tissues tested except liver were lower than that in plasma. At 6 h after dosing, the concentration of radioactivity was highest in the liver, followed in decreased order by plasma, kidney, Harder's gland, adrenal gland and heart; it was lowest in the brain and eye ball. The radioactivity in tissues decreased to the very low concentrations within 24 to 72 h.

The metabolite composition in tissues of rats was determined in plasma, brain, heart, lung, liver, kidney, fat and skeletal muscle at 2, 6 and 10 h after oral administration of [^{14}C]pioglitazone (HCl) (Table 8). The unchanged compound was mainly detected in all tissues.

3.3. In vitro metabolism

[^{14}C]Pioglitazone (HCl) was incubated with blood, and slices of the brain, heart, lung, kidney and duodenum of rat in Krebs-Ringer bicarbonate buffer at 37 °C for 2 h. The

Table 7: Concentrations of radioactive materials in tissues after oral administration of [^{14}C]pioglitazone (HCl) in rats.

Tissues	Concentration of ^{14}C (μg pioglitazone equivalents/ml or g)					
	30 min	2 h	6 h	10 h	24 h	72 h
Plasma	0.28 ± 0.03	0.87 ± 0.04	0.97 ± 0.03	0.52 ± 0.16	0.06 ± 0.01	< 0.01
Brain	0.03 ± 0.00	0.08 ± 0.00	0.08 ± 0.01	0.03 ± 0.01	< 0.01	< 0.01
Spinal cord	0.03 ± 0.00	0.09 ± 0.01	0.09 ± 0.01	0.04 ± 0.01	< 0.01	< 0.01
Pituitary	0.09 ± 0.01	0.29 ± 0.03	0.34 ± 0.01	0.19 ± 0.05	0.02 ± 0.01	< 0.01
Eye ball	0.02 ± 0.00	0.05 ± 0.01	0.07 ± 0.01	0.04 ± 0.01	0.01 ± 0.00	< 0.01
Harder's gland	0.17 ± 0.02	0.60 ± 0.06	0.64 ± 0.07	0.32 ± 0.08	0.06 ± 0.00	0.01 ± 0.00
Submaxillary gland	0.09 ± 0.01	0.26 ± 0.02	0.27 ± 0.01	0.14 ± 0.04	0.02 ± 0.00	< 0.01
Thyroid	0.07 ± 0.01	0.24 ± 0.01	0.26 ± 0.01	0.14 ± 0.04	0.03 ± 0.00	0.01 ± 0.00
Thymus	0.04 ± 0.00	0.12 ± 0.00	0.14 ± 0.00	0.08 ± 0.02	0.01 ± 0.00	< 0.01
Heart	0.11 ± 0.01	0.30 ± 0.02	0.34 ± 0.02	0.17 ± 0.05	0.02 ± 0.00	< 0.01
Lung	0.10 ± 0.02	0.25 ± 0.03	0.30 ± 0.03	0.16 ± 0.02	0.03 ± 0.00	< 0.01
Liver	0.47 ± 0.03	1.28 ± 0.05	1.60 ± 0.15	1.10 ± 0.27	0.13 ± 0.02	0.02 ± 0.00
Spleen	0.05 ± 0.01	0.15 ± 0.00	0.17 ± 0.01	0.09 ± 0.03	0.01 ± 0.00	< 0.01
Pancreas	0.07 ± 0.01	0.20 ± 0.02	0.22 ± 0.02	0.11 ± 0.03	0.01 ± 0.00	< 0.01
Adrenal gland	0.14 ± 0.02	0.39 ± 0.02	0.42 ± 0.02	0.22 ± 0.07	0.04 ± 0.00	0.01 ± 0.00
Kidney	0.17 ± 0.02	0.49 ± 0.03	0.79 ± 0.03	0.48 ± 0.16	0.08 ± 0.01	0.01 ± 0.00
Testis	0.03 ± 0.00	0.16 ± 0.01	0.19 ± 0.02	0.11 ± 0.03	0.01 ± 0.00	< 0.01
Skeletal muscle	0.03 ± 0.00	0.08 ± 0.00	0.10 ± 0.01	0.05 ± 0.02	0.01 ± 0.00	< 0.01
Skin	0.05 ± 0.00	0.18 ± 0.01	0.21 ± 0.03	0.12 ± 0.03	0.02 ± 0.00	< 0.01
Epididymal fat	0.04 ± 0.00	0.13 ± 0.00	0.13 ± 0.01	0.08 ± 0.03	0.01 ± 0.01	0.01 ± 0.00
Brown fat	0.09 ± 0.01	0.32 ± 0.07	0.33 ± 0.01	0.20 ± 0.05	0.09 ± 0.02	0.03 ± 0.01
Bone marrow	0.05 ± 0.01	0.16 ± 0.01	0.19 ± 0.01	0.10 ± 0.03	0.02 ± 0.00	< 0.01
Stomach	0.90 ± 0.16	0.54 ± 0.04	0.40 ± 0.07	0.16 ± 0.06	0.02 ± 0.01	< 0.01
Intestine	0.12 ± 0.04	0.25 ± 0.01	0.35 ± 0.03	0.30 ± 0.10	0.04 ± 0.01	< 0.01

Dose, 0.5 mg/kg. Data are the mean values ± S.D. (n = 3).

Table 8. Composition of radioactive materials in tissues after oral administration of [^{14}C]pioglitazone (HCl) in rats.

Tissues	Time (h)	Concentration of ^{14}C (µg Pioglitazone equivalents/ml or g)								
		Total ^{14}C	Pioglitazone	M-I	M-II	M-III	M-IV	M-V	M-VI	Others
Plasma	2	0.87 ± 0.04	0.68 ± 0.06	< 0.01	0.02 ± 0.02	0.04 ± 0.00	0.04 ± 0.00	0.02 ± 0.01	< 0.01	0.07 ± 0.01
	6	0.97 ± 0.03	0.57 ± 0.07	< 0.01	0.06 ± 0.03	0.09 ± 0.01	0.08 ± 0.01	0.04 ± 0.01	< 0.01	0.13 ± 0.02
	10	0.52 ± 0.16	0.23 ± 0.06	< 0.01	0.04 ± 0.04	0.08 ± 0.02	0.06 ± 0.02	0.02 ± 0.01	< 0.01	0.09 ± 0.03
Brain	2	0.08 ± 0.00	0.07 ± 0.00	< 0.01	< 0.01	< 0.01	< 0.01	< 0.01	< 0.01	< 0.01
	6	0.08 ± 0.01	0.06 ± 0.01	< 0.01	< 0.01	< 0.01	0.01 ± 0.00	< 0.01	< 0.01	0.01 ± 0.00
	10	0.03 ± 0.01	0.02 ± 0.00	< 0.01	< 0.01	< 0.01	0.01 ± 0.00	< 0.01	< 0.01	0.01 ± 0.00
Heart	2	0.30 ± 0.02	0.20 ± 0.03	< 0.01	0.01 ± 0.00	0.01 ± 0.00	0.02 ± 0.00	0.01 ± 0.00	< 0.01	0.05 ± 0.01
	6	0.34 ± 0.02	0.18 ± 0.05	< 0.01	0.02 ± 0.01	0.02 ± 0.00	0.05 ± 0.01	0.01 ± 0.00	< 0.01	0.07 ± 0.03
	10	0.17 ± 0.03	0.06 ± 0.01	< 0.01	0.01 ± 0.01	0.01 ± 0.00	0.04 ± 0.00	0.01 ± 0.00	< 0.01	0.04 ± 0.02
Lung	2	0.25 ± 0.03	0.19 ± 0.03	< 0.01	< 0.01	< 0.01	0.01 ± 0.00	0.01 ± 0.00	< 0.01	0.03 ± 0.00
	6	0.30 ± 0.03	0.17 ± 0.03	< 0.01	0.01 ± 0.00	< 0.01	0.05 ± 0.00	0.01 ± 0.00	< 0.01	0.05 ± 0.01
	10	0.16 ± 0.03	0.07 ± 0.01	< 0.01	0.01 ± 0.01	< 0.01	0.04 ± 0.01	0.01 ± 0.00	< 0.01	0.03 ± 0.01
Liver	2	1.28 ± 0.05	0.82 ± 0.05	< 0.01	0.02 ± 0.01	0.02 ± 0.02	0.12 ± 0.01	0.11 ± 0.01	< 0.01	0.19 ± 0.01
	6	1.60 ± 0.15	0.71 ± 0.15	< 0.01	0.05 ± 0.02	0.01 ± 0.00	0.29 ± 0.01	0.14 ± 0.01	0.02 ± 0.01	0.36 ± 0.02
	10	1.10 ± 0.27	0.34 ± 0.10	< 0.01	0.04 ± 0.03	0.02 ± 0.01	0.29 ± 0.09	0.08 ± 0.01	0.02 ± 0.00	0.31 ± 0.04
Kidney	2	0.49 ± 0.03	0.24 ± 0.02	0.01 ± 0.00	0.01 ± 0.01	< 0.01	0.06 ± 0.00	0.09 ± 0.02	< 0.01	0.09 ± 0.00
	6	0.79 ± 0.03	0.22 ± 0.03	< 0.01	0.02 ± 0.01	0.01 ± 0.00	0.14 ± 0.00	0.15 ± 0.02	0.01 ± 0.00	0.23 ± 0.03
	10	0.48 ± 0.16	0.09 ± 0.03	< 0.01	0.02 ± 0.02	0.01 ± 0.00	0.12 ± 0.03	0.09 ± 0.03	0.01 ± 0.00	0.14 ± 0.04
Skeletal muscle	2	0.08 ± 0.00	0.06 ± 0.00	< 0.01	< 0.01	< 0.01	0.01 ± 0.00	< 0.01	< 0.01	0.01 ± 0.00
	6	0.10 ± 0.01	0.05 ± 0.01	< 0.01	< 0.01	0.01 ± 0.00	0.01 ± 0.00	0.01 ± 0.00	< 0.01	0.02 ± 0.00
	10	0.05 ± 0.02	0.02 ± 0.01	< 0.01	< 0.01	< 0.01	0.01 ± 0.00	< 0.01	< 0.01	0.01 ± 0.00
Epididymal fat	2	0.13 ± 0.00	0.05 ± 0.01	< 0.01	< 0.01	< 0.01	< 0.01	< 0.01	< 0.01	0.07 ± 0.01
	6	0.13 ± 0.01	0.04 ± 0.01	< 0.01	< 0.01	< 0.01	< 0.01	< 0.01	< 0.01	0.09 ± 0.01
	10	0.08 ± 0.03	0.02 ± 0.01	< 0.01	< 0.01	< 0.01	< 0.01	< 0.01	< 0.01	0.05 ± 0.02
Brown fat	2	0.32 ± 0.07	0.14 ± 0.04	< 0.01	< 0.01	< 0.01	0.01 ± 0.01	0.01 ± 0.00	< 0.01	0.15 ± 0.02
	6	0.23 ± 0.01	0.12 ± 0.01	< 0.01	0.01 ± 0.00	< 0.01	0.02 ± 0.01	0.01 ± 0.00	< 0.01	0.16 ± 0.01
	10	0.20 ± 0.05	0.05 ± 0.01	< 0.01	0.01 ± 0.00	< 0.01	0.02 ± 0.01	0.01 ± 0.00	< 0.01	0.11 ± 0.03

Dose, 0.5 mg/kg. Data are the mean values ± S.D. (n = 3).

Table 9. In vitro metabolism of [^{14}C]pioglitazone (HCl) incubated with rat tissue slices.

Tissues	Metabolic activity (µg/2 h/0.2 g tissue)	Formation rate (µg/2 h/0.2 g tissue)				
		M-II	M-III	M-IV	M-V	M-VI
Blood	< 0.01	< 0.01	< 0.01	< 0.01	< 0.01	< 0.01
Brain	0.03 ± 0.03	< 0.01	< 0.01	0.01 ± 0.01	< 0.01	< 0.01
Heart	< 0.01	< 0.01	< 0.01	0.01 ± 0.01	< 0.01	< 0.01
Lung	0.02 ± 0.02	0.01 ± 0.01	< 0.01	0.02 ± 0.01	0.01 ± 0.00	< 0.01
Liver	0.98 ± 0.13	0.04 ± 0.01	0.10 ± 0.02	0.11 ± 0.01	0.16 ± 0.03	0.02 ± 0.01
Kidney	0.70 ± 0.10	0.02 ± 0.03	0.06 ± 0.02	0.13 ± 0.03	0.45 ± 0.05	0.01 ± 0.01
Duodenum	0.29 ± 0.07	0.02 ± 0.01	0.01 ± 0.00	0.08 ± 0.01	0.04 ± 0.01	< 0.01

Blood (0.2 ml) and tissue slices (0.2 g) were incubated with [^{14}C]pioglitazone (2 µg/ml) for 2 h at 37 °C. Data are the mean values ± S.D. (n = 3).

unchanged compound and the metabolites were determined. Table 9 shows the decrease of pioglitazone content and the formation rate of metabolites in each tissue. The metabolic activity was highest in the liver, followed in decreased order by kidney and duodenum. Almost no metabolism was observed in blood, brain, heart and lung. In liver, M-V, M-IV, M-III and M-II, in kidney, M-V, and in duodenum, M-IV were mainly formed, respectively.

3.4. Excretion

3.4.1. Excretion into urine, feces and expired air

Table 10 shows the excretion of radioactivity in urine and feces after oral administration of [^{14}C]pioglitazone (HCl) to rats, dogs and monkeys. Most of the radioactivity dosed was excreted within 72 h in rats, 96 h in dogs and 168 h in monkeys. The radioactivity was largely excreted in feces of rats and dogs, whereas in monkeys it was excreted predominantly in urine. Only 1.2 % of the dose was excreted into the expired air of rats within 72 h.

Table 11 shows the metabolite composition in urine and feces after oral administration of [^{14}C]pioglitazone (HCl) to rats, dogs and monkeys. In urine of rats and monkeys, M-V was predominantly excreted and in urine of dogs, M-I and M-V were mainly detected. In feces of rats, M-V and M-IV were largely excreted, and in feces of dogs and monkeys, M-V was mainly detected.

3.4.2. Biliary excretion and reabsorption

Table 10 and 11 also show the excretion of radioactivity and metabolite composition in bile after intraduodenal administration of [^{14}C]pioglitazone (HCl) to biliary-cannulated rats. Within 24 h, 60 % of the radioactivity dosed was excreted into bile, and the main components were M-IV and M-V.

To examine the enterohepatic circulation, the radioactive bile (10 ml/kg) was administered intraduodenally to other biliary-cannulated rats. Within 24 h, 38 and 13 % of the radioactivity dosed were excreted into bile and urine, respectively. Thus, the drug-related materials excreted into bile are partly reabsorbed via enterohepatic circulation.

4. Discussion

We studied the disposition of pioglitazone after oral administration of [^{14}C]pioglitazone (HCl) to rats, dogs, and monkeys. The study concerning the absorption site in rats showed that pioglitazone was well absorbed from

Table 10. Excretion of radioactive materials in urine, feces, and bile after oral administration of [^{14}C]pioglitazone (HCl) in rats, dogs, and monkeys.

Species	Time (h)	Cumulative excretion (% of dose)			
		Urine	Feces	Bile	Total
Rat	4	2.1 ± 2.3	ND	ND	ND
	8	11.0 ± 3.8	ND	ND	ND
	24	32.4 ± 1.2	40.2 ± 11.7	ND	72.6 ± 12.8
	48	35.5 ± 0.5	61.7 ± 1.9	ND	97.2 ± 1.6
	72	35.9 ± 0.6	63.2 ± 1.3	ND	99.1 ± 0.8
	96	36.0 ± 0.6	63.4 ± 1.3	ND	99.4 ± 0.8
Rat[a)]	4	0.5 ± 0.1	ND	12.8 ± 2.6	ND
	8	2.4 ± 1.1	ND	21.9 ± 5.2	ND
	24	13.7 ± 3.9	15.9 ± 2.1[b)]	60.3 ± 3.4	89.9 ± 2.9
Dog	4	0.8 ± 1.4	ND	ND	ND
	8	1.4 ± 1.3	ND	ND	ND
	24	11.7 ± 0.3	25.4 ± 25.6	ND	37.0 ± 25.3
	48	15.1 ± 1.0	60.4 ± 26.5	ND	75.5 ± 25.6
	72	16.0 ± 1.5	79.9 ± 1.7	ND	95.9 ± 1.6
	96	16.3 ± 1.5	80.8 ± 1.5	ND	97.1 ± 1.4
	120	16.4 ± 1.5	81.1 ± 1.4	ND	97.5 ± 1.4
Monkey	4	8.4 ± 2.9	ND	ND	ND
	8	24.6 ± 3.5	ND	ND	ND
	24	39.8 ± 2.6	1.3 ± 2.1	ND	61.2 ± 2.6
	48	69.7 ± 1.4	5.2 ± 3.3	ND	74.8 ± 2.7
	72	73.9 ± 1.5	10.7 ± 5.3	ND	84.6 ± 3.9
	96	75.9 ± 2.1	13.7 ± 6.1	ND	89.6 ± 4.0
	120	75.8 ± 2.4	16.1 ± 5.2	ND	92.9 ± 2.8
	144	77.2 ± 2.4	17.1 ± 4.7	ND	94.3 ± 2.4
	168	77.4 ± 2.5	17.6 ± 4.4	ND	95.0 ± 2.3

Dose, 0.5 mg/kg. Data are the mean values ± S.D. (n = 3). ND, not determined. [a)] Biliary-cannulated rats (intraduodenal administration). [b)] Include gut contents.

the wide range of small intestine. The absorption extent after oral administration was high for all of these three species; 96, 95 and 90 % in rats, dogs and monkeys, respectively. Pioglitazone after oral administration also showed the high bioavailability, 85, 94, and 81 % in rats, dogs, and monkeys, respectively. These findings show only a little part of the drug undergo first-pass effect during absorption, although in vitro study showed that pioglitazone was partly metabolized in rat duodenum. The unchanged compound in plasma of rats, dogs, and monkeys was 53, 16, and 44 % of the total radioactivity, respectively. The total concentrations of pioglitazone, M-II, M-III and M-IV, which have the pharmacological activity [3], accounted for 87, 71 and 73 % of the total radioactivity in plasma in these species, respectively. These results suggest that these metabolites contribute, at least in part, to the pharmacological action after oral dosing of pioglitazone.

In vitro study using liver and kidney slices showed that all identified metabolites except M-I were detected. In the kidney, M-V was predominantly formed, which agreed well with that the main compound excreted in urine of rats was M-V. In the liver, M-V was formed in higher rate than M-IV, M-III and M-II. However, concentrations of M-III, M-II, and M-IV in plasma were higher than that of M-V. On the other hand, M-V was largely excreted in urine and bile. These findings would show that among the metabolites formed in the liver, M-V is more easily excreted than the unchanged compound, M-II, M-III, and M-IV due probably to the more hydrophilicity of M-V than the latter compounds.

The radioactivity was widely distributed in tissues of rats after oral administration, and the highest concentration was found in the liver at 6 h after dosing. The radioactivity in tissues decreased to the very low concentrations within 24 to 72 h in all tissues investigated.

In most tissues, the concentrations of radioactivity were lower than that in plasma. This coincides with the very small distribution volume of pioglitazone after intravenous administration to rats (V_{dss} = 223 ml/kg). The binding of pioglitazone and its metabolites to rat plasma proteins was very high (more than 99 %), which may be partly the cause of this relatively low concentrations of radioactivity in rat tissues.

The absorption extent was very high and pioglitazone administered intraduodenally to the biliary-cannulated rats was largely excreted into bile. Further the metabolite composition in bile and feces were similar and little amount of the unchanged compound was detected in feces. These findings suggest that the radioactivity in feces is excreted mostly via hepato-biliary route after absorption and not due to the unabsorbed compound.

In conclusion, after oral administration to rats, dogs and monkeys, pioglitazone was well absorbed from wide range of small intestine, metabolized mainly to M-I to M-VI and quantitatively excreted in urine and feces via

Table 11. Composition of radioactive materials in excreta after oral administration of [^{14}C]pioglitazone (HCl) in rats, dogs, and monkeys.

Species	Sample	Total ^{14}C (% of dose)		Composition of metabolites (% of dose)							
				Pioglitazone	M-I	M-II	M-III	M-IV	M-V	M-VI	Others
Rat	48-h urine	35.5 ± 0.5	U	< 0.1	0.1	< 0.1	< 0.1	0.1	9.5	2.8	
			C	< 0.1	1.7	< 0.1	< 0.1	1.9	1.4[a)]	0.1	
			T	< 0.1	1.8	< 0.1	< 0.1	2.0	10.9	2.9	17.9
	48-h feces	61.7 ± 1.9	U	1.7	< 0.1	2.7	0.2	1.8	13.7	4.0	
			C	< 0.1	0.2	< 0.1	< 0.1	8.9	2.4[a)]	0.3	
			T	1.7	0.2	2.7	0.2	10.7	16.1	4.3	25.8
	24-h bile	60.3 ± 3.4	U	0.1	< 0.1	0.1	0.1	0.2	10.9	2.8	
			C	0.1	0.6	4.0	< 0.1	10.9	9.6[a)]	0.2	
			T	0.2	0.6	4.1	0.1	11.1	20.5	3.0	20.7
Dog	72-h urine	16.0 ± 1.5	U	0.2	0.5	0.2	0.1	0.3	1.4	0.3	
			C	< 0.1	2.0	0.2	0.1	0.3	0.4[a)]	0.1	
			T	0.2	2.5	0.3	0.2	0.6	1.9	0.4	9.9
	72-h feces	79.9 ± 1.7	U	0.6	1.4	0.6	0.4	4.9	32.9	4.6	
			C	0.3	0.2	< 0.1	0.2	3.3	15.5[a)]	< 0.1	
			T	0.9	1.6	0.6	0.5	8.1	48.4	4.6	13.0
Monkey	72-h urine	73.9 ± 1.5	U	< 0.1	0.6	< 0.1	< 0.1	0.3	35.9	4.4	
			C	0.1	6.3	1.3	< 0.1	1.3	1.9[a)]	0.3	
			T	0.1	7.0	1.3	0.1	1.6	37.8	4.7	21.4
	72-h feces	10.7 ± 5.3	U	< 0.1	< 0.1	< 0.1	< 0.1	0.1	5.2	2.0	
			C	0.2	0.1	< 0.1	< 0.1	0.6	0.3[a)]	< 0.1	
			T	0.2	0.1	< 0.1	< 0.1	0.7	5.4	2.0	2.3

Dose, 0.5 mg/kg. Total radioactivity: the mean values ± S.D. (n = 3). Metabolites: the mean values (n = 3). U: unconjugates, C: conjugates (glucuronide and/or sulfate), T = U + C. [a)] Include taurine conjugate.

hepato-biliary route. The pharmacologically active compounds (total of pioglitazone, M-II, M-III and M-IV) accounted for 87, 71, and 73 % of the radioactivity in plasma of rats, dogs, and monkeys, respectively. The radioactivity was distributed widely in tissues after oral administration to rats, and decreased to the very low concentration within 24 to 72 h after dosing.

5. References

[1] Sohda, T., Mizuno, K., Momose, Y. et al., J. Med. Chem. **35**, 2617 (1992) – [2] Sohda, T., Momose, Y., Meguro, K. et al., Arzneim.-Forsch./Drug Res. **40 (I)**, 37 (1990) – [3] Sohda, T., Ikeda, H., Meguro, K., Chem. Pharm. Bull. **43**, 2168 (1995) – [4] Ikeda, H., Taketomi, S., Sugiyama, Y. et al., Arzneim.-Forsch./Drug Res. **40 (I)**, 156 (1990) – [5] Sugiyama, Y., Taketomi, S., Shimura, Y. et al., Arzneim.-Forsch./Drug Res. **40 (I)**, 263 (1990) – [6] Sugiyama, Y., Shimura, Y., Ikeda, H., Arzneim.-Forsch./Drug Res. **40 (I)**, 436 (1990) – [7] Castle, C. K., Colca, J. R., Melchior, G. W., Aterioscler. Thromb. **13**, 302 (1993) – [8] Kobayashi, M., Iwanishi, M., Egawa, K. et al., Diabetes **41** 476 (1992) – [9] Hofmann, C., Lorenz, K., Colca, J. R., Endocrinology **129**, 1915 (1991) – [10] Hofmann, C., Edwards III, C. W., Hillman, R. M. et al., Endocrinology **130**, 735 (1992) – [11] Klatman, R. F., Clarke, S. D., Ulrich, R. G., Mol. Pharmacol. **41**, 393 (1992) – [12] Kletzien, R. F., Foellmi, L. A., Harris, P. K. W. et al., Mol. Pharmacol. **42**, 558 (1992) – [13] Kiyota, Y., Kondo, T., Maeshiba, Y. et al., Arzneim.-Forsch./Drug Res. **47 (I)**, 22 (1997) – [14] Tanayama, S., Shirakawa, Y., Kanai, Y. et al., Xenobiotics **4**, 33 (1974) – [15] Tanayama, S., Kobayashi, T., Kanai, Y., Xenobiotics **8**, 365 (1978) – [16] Kondo, T., Kurata, Y., Yoshida, K. et al., Biol. Pharm. Bull. **18**, 330 (1995) – [17] Yamaoka, K., Nakagawa, T., Uno, T., J. Pharmacokinet. Biopharm. **6**, 547 (1978)

Correspondence: Yoshihiro Maeshiba, Drug Analysis and Pharmacokinetics Research Laboratories, Pharmaceutical Development Division, Takeda Chemical Industries, Ltd., 2-17-85, Juso-Honmachi, Yodogawa-ku, Osaka, 532 (Japan)

Synthesis and Antihyperlipaemic Activity of Some Novel N-Cyanovinylformamidines

Chamanlal J. Shishoo[a], Mahesh T. Chhabria[a], Thakorebhai P. Gandhi[b], and Ramkrishna A. Bangaru[b]

Department of Pharmaceutical Chemistry, L. M. College of Pharmacy[a], and Department of Pharmacology, Cadila Pharmaceuticals Ltd.[b], Ahmedabad (India)

Summary

Potent antihyperlipaemic activity has been observed in a series of novel N-cyanovinylformamidines when tested in hyperlipaemic rats. Two of the compounds (**11** and **15**) were found more potent than gemfibrozil at 50 mg/kg/d dose level in reducing serum cholesterol and triglyceride levels and also in elevating serum HDL level. A good three-dimensional structural similarity has been observed between these two compounds and clofibrate and gemfibrozil, respectively. Acute toxicity studies carried out in mice indicated compound **11** to be safe even at a dose level of 4.5 g/kg. The title compounds were synthesized by the reaction of α-cyanoketene S,N-acetals with formamidineacetate under controlled reaction conditions.

Neurotherapeutics: The Journal of the American Society for Experimental NeuroTherapeutics

PPARγ Agonists as Therapeutics for the Treatment of Alzheimer's Disease

Gary Landreth,* Qingguang Jiang,* Shweta Mandrekar,* and Michael Heneka†

*Alzheimer Research Laboratory, Department of Neurosciences, Case Western Reserve University School of Medicine, Cleveland, Ohio 44106; †Department of Neurology, Molecular Neurobiology Unit, University of Munster, Munster, 48149, Germany

Summary: Alzheimer's disease (AD) is characterized by the deposition of β-amyloid within the brain parenchyma and is accompanied by the impairment of neuronal metabolism and function, leading to extensive neuronal loss. The disease involves the perturbation of synaptic function, energy, and lipid metabolism. The development of amyloid plaques results in the induction of a microglial-mediated inflammatory response. The nuclear receptor peroxisome proliferator-activated receptor gamma (PPARγ) is a ligand-activated transcription factor whose biological actions are to regulate glucose and lipid metabolism and suppress inflammatory gene expression. Thus, agonists of this receptor represent an attractive therapeutic target for AD. There is now an extensive body of evidence that has demonstrated the efficacy of PPARγ agonists in ameliorating disease-related pathology and improved learning and memory in animal models of AD. Recent clinical trials of the PPARγ agonist rosiglitazone have shown significant improvement in memory and cognition in AD patients. Thus, PPARγ represents an important new therapeutic target in treating AD.
Key Words: Peroxisome proliferator-activated receptor gamma, thiazolidinedione, Alzheimer's disease, amyloid beta, inflammation, apolipoprotein E.

INTRODUCTION

The nuclear receptor peroxisome proliferator-activated receptor gamma (PPARγ) is a newly recognized therapeutic target for the treatment of Alzheimer's disease (AD). This review provides an overview of the biological actions of this ligand-activated transcription factor, and it addresses some of the central issues that have arisen with the use of its agonists as a treatment of AD. Despite the fact that the thiazolidinedione (TZD) class of PPARγ agonists is widely prescribed for the treatment of type II diabetes mellitus, comparatively little is known about PPARγ actions in the brain. Recently, agonists of PPARγ have been shown to be efficacious in a number of CNS disease models[1], and this has stimulated investigations examining the underlying biological actions of these receptors in the brain. The suggestion that PPARγ might be of utility in treatment for AD arose from consideration of its effects on insulin action, energy metabolism, lipid metabolism, and inflammation. This discussion is particularly timely as the outcomes of the first clinical trials of these drugs are being reported.[2] The mechanisms subserving their actions in AD are presently unclear. Thus, an active debate of these issues is needed as these agents are being advanced into phase III clinical trials for the treatment of AD. Several potential mechanisms have been proposed as rationales for the therapeutic use of PPARγ agonists in AD. There is presently no consensus on what is the dominant mode of PPARγ action, and it is probable that PPARγ agonists act through multiple parallel pathways to affect disease pathophysiology in both humans and animal models of the disease.

The PPARs are a family of three (α/γ/δ) related nuclear receptors that act as whole body lipid sensors, and each member functions to regulate a unique subset of genes responsible for lipid and energy metabolism.[3] The receptors act by mediating the body's response to dietary intake. PPARγ is of particular importance as this nuclear receptor acts to regulate both lipid and carbohydrate metabolism and participates in the regulation of serum glucose levels, as well as regulating insulin sensitivity.[4] The natural ligands of PPARγ include long-chain fatty acids, eicosanoids, oxidized lipoproteins, and lipids, cor-

Address Correspondence to: Gary Landreth, M.D., Department of Neurosciences, Alzheimer Research Laboratory, School of Medicine, Case Western Reserve University, 10900 Euclid Avenue, Cleveland, OH 44106. E-mail: gel2@case.edu.

responding well to its function in regulating the metabolic response to dietary lipid intake.[5] Thus, PPARγ has been targeted for drug development for the treatment of type II diabetes mellitus. Two thiazolidinedione (TZD) agonists of PPARγ, Actos (pioglitazone) (Takeda Pharmaceuticals North America, Inc., Deerfield, IL), and Avandia (rosiglitazone) (GlaxoSmithKline, Research Triangle Park, NC) are Food and Drug Administration-approved and widely prescribed for this disease. However, the use of these drugs for CNS treatments is under close scrutiny due to their poor blood-brain-barrier (BBB) permeability. Pioglitazone does pass the BBB, but it does so poorly.[6] The BBB permeability of rosiglitazone has been controversial. Rosiglitazone was initially characterized as BBB impermeant;[7] however, Strum et al.[8] have recently reported that the drug can be found in the brain after oral administration. A 7-day oral treatment regimen resulted in brain levels of rosiglitazone in the submicromolar range (0.26–0.45 μM).[8] It remains to be determined how rosiglitazone made its way into the brain, and whether this is also observed in humans.

PPARγ regulation of gene expression

Transactivation. PPARγ is a ligand-activated transcription factor that binds to sequence-specific promoter elements of its target genes and directly regulates their expression.[9] The PPAR subfamily of nuclear receptors acts as dominant regulators of lipid metabolism.[3] These receptors rapidly transcriptionally transactivate gene expression in response to ligands that are directly obtained from the diet or generated through normal metabolic processes. PPARγ regulates a specific subset of genes, most prominently those responsible for lipid metabolism and storage.

PPARγ forms an obligate heterodimer with the retinoid X receptor. This receptor complex binds to PPAR responsive elements within the promoters of its target genes.[10,11] In the absence of ligand, the transcriptional activity of PPARγ is suppressed through its constitutive association with a nuclear corepressor complex, comprised of NCoR/SMRT and histone deacetylases. The corepressor complex maintains chromatin in a condensed state and prevents recruitment of coactivator complexes and transcriptional initiation. With binding of the ligand to the receptor, the corepressor complex is dismissed and the transcriptional coactivators are recruited to the promoter, initiating the formation of active transcription complex that is coupled to the basal transcriptional apparatus.[12]

Anti-inflammatory actions of PPARγ

PPARγ agonists robustly inhibit pro-inflammatory gene expression and this effect underlies many of the beneficial actions of these drugs.[13] The major anti-inflammatory effect of PPARγ is to functionally inactivate NFκB-dependent promoters. Several mechanisms have been proposed to account for repression of gene expression.[14,15] However, Pascual et al.[16] have recently provided compelling evidence that PPARγ blocks NFκB-dependent gene expression through corepressor interference. Inflammatory genes are normally repressed through the association of the co-repressors—NCoR with the κBRE elements, present in the promoters of these genes. With ligand binding, a fraction of PPARγ in the nucleus becomes sumoylated, and these modified receptors then bind to the κBRE promoter element, preventing the dissociation of the repressor functionally inactivating the promoter and blocking gene expression. Agonists of PPARγ are attractive therapeutic agents owing to their ability to act broadly to inhibit inflammatory gene expression.

Effects of PPARγ agonists in animal models of AD

Several studies using murine models of AD have been carried out to determine the therapeutic utility of PPARγ agonists in disease progression. Yan et al.[17] investigated the effects of a PPARγ agonist in Tg2576 mice. Aged Tg2576 mice (12-months old) with established plaque pathology were treated orally with pioglitazone (120 ppm, 20 mg/kg/day) for 4 months. Pioglitazone was used in these studies due to its ability to pass the BBB, albeit poorly.[6] The nonsteroidal anti-inflammatory drug, ibuprofen, served as a positive control in these experiments since Lim et al.[18] had previously shown plaque reduction in this animal model after oral ibuprofen therapy. Ibuprofen treatment resulted in approximately 60% reduction in plaque number. However, pioglitazone-treated animals did not exhibit a statistically significant change in plaque pathology. Both ibuprofen and pioglitazone treatment resulted in a small, but significant, reduction in the levels of soluble Aβ peptides. Ibuprofen-treated animals exhibited a dramatic reduction in soluble $A\beta_{42}$ levels. Although soluble $A\beta_{42}$ levels in pioglitazone-treated animals were lower, they did not reach statistical significance. In addition, pioglitazone had no effect on the number of activated microglia. This experiment demonstrated that pioglitazone exhibited effects on soluble Aβ levels in the brain; however, it did not significantly affect AD-related pathology or microglial-mediated inflammation. These findings were interpreted as evidence that the poor penetration of pioglitazone into the brain, due to its poor BBB permeability, limited its efficacy.

Heneka et al.[19] conducted a study using a dose of pioglitazone that was twofold higher (240 ppm; 40/mg/kg/day) in younger animals. They used a different mouse model that overexpresses human amyloid precursor protein (APP) with London mutation (V717I). These animals were treated at 10 months of age (just as they are beginning to exhibit plaque pathology) for only 7 days. Ibuprofen-treated animals comprised the controls for this study. The higher dosage of pioglitazone resulted in an

approximate 20 to 25% reduction in Aβ plaque burden and in $A\beta_{42}$ levels in the brain.[19] In addition, there was a significant reduction in microglial activation. This study provided the first conclusive evidence that PPARγ agonists could suppress AD-related pathology.

In another study, Pedersen and Flynn[20] examined the effect of the PPARγ agonist rosiglitazone in Tg2576 mice. An unappreciated phenotype that these mice display is metabolic abnormality, including increased fasting serum glucocorticoid levels and insulin resistance. A 6- week treatment of rosiglitazone restored insulin responsiveness in these mice[20] and lowered glucocorticoid levels. Importantly, rosiglitazone treatment rescued behavioral deficits displayed by these mice.[7] The authors have argued that the improved behavior may result from suppression of glucocorticoid levels, as glucocorticoids have been well described to have negative effects on learning and memory and act to impair insulin receptor function.[21–23] This study suggests that rosiglitazone could elicit its effects by acting on peripheral systems. Rosiglitazone treatment did not result in any changes in Aβ plaque pathology, but selectively reduced brain $A\beta_{42}$ levels. This study noted that AD patients also exhibit elevated levels of plasma cortisol. The hypothesis that rosiglitazone reactions in the Tg2576 mice arise from its effects on peripheral glucocorticoid levels is compelling. Interestingly, although PPARγ agonists have not been previously reported to have analogous effects on glucocorticoids in humans, recent studies have suggested that rosiglitazone may be a short-term treatment option for hypercortisolemia in Cushing's patients.[24–26] However, the results of these studies are not conclusive[27] and the relevance of this mechanism to AD therapy warrants further investigation.

Clinical trials

Two Food and Drug Administration-approved PPARγ agonists have been tested for their efficacy in AD patient populations. Watson et al.[28] have reported the results of a small clinical study examining the effects of rosiglitazone in patients with mild AD. They found that 6 months of drug treatment resulted in enhanced memory and cognitive function compared with placebo-treated control patients.[28] Geldmacher et al.[29] have studied of the actions of pioglitazone in mild to moderate AD cases. This study, designed primarily as a safety trial, demonstrated a small but statistically insignificant improvement in memory. PPARγ agonists have a generally favorable side effect profile, and are well tolerated and safe in the elderly.[30] Recently, however, rosiglitazone usage was found to be associated with an increased risk for cardiovascular side effects.[31] In contrast, pioglitazone has been found to be cardioprotective.[32]

The results of a phase II clinical trial, enrolling over 500 patients with mild to moderate AD, was recently reported by Risner et al.[2] These patients were treated with rosiglitazone (or placebo) for 6 months. Patients receiving rosiglitazone were found to have enhanced attention and memory, compared with those receiving the placebo. Importantly, patients possessing an *apolipoprotein E4* (*APOE4*) allele did not respond to the therapy. This latter observation is consistent with previous studies by Craft et al.[33–35] demonstrating a functional interaction of apolipoprotein E (ApoE) isoforms with efficacy of insulin action on cognition. A large phase III trial of rosiglitazone in AD patients is currently underway.

Mechanisms of PPARγ agonist action

AD is a complex neurodegenerative disorder. The etiology of the disease has proven to be divergent with contributions from genetics, the environment as well as the normal aging process. There is ample evidence that multiple physiological functions are altered in AD. PPARγ exhibits pleiotropic physiological functions in multiple systems. Therefore, PPARγ agonists could exert their salutary effects in treating AD by regulating multiple aspects involved in AD, including Aβ homeostasis, insulin sensitivity, energy metabolism, lipid metabolism, and inflammation (FIG. 1).

Aβ homeostasis. PPARγ involvement in ameliorating AD-related pathology has been the focus of a number of recent studies that have been directed at dissecting the mechanisms through which PPARγ regulates Aβ metabolism. These studies have led to contradictory results. One mechanism through which PPARγ is able to accomplish this is by regulating Aβ production. When neuroblastoma cells (stably transfected with human APP) were stimulated with inflammatory cytokines, they activated the APP processing enzyme beta-secretase (BACE1), resulting in an increase in Aβ secretion. This was inhibited after PPARγ activation through its ability to suppress BACE1 transcription.[36] Indeed, there is a PPARγ response element in the promoter region of the BACE1 gene, and binding of PPARγ to this response element suppresses BACE1 expression and inhibits Aβ production.[37]

A subsequent study by d'Abramo et al.[38] reported that PPARγ activation resulted in inhibition of APP expression. Moreover, overexpression of PPARγ in cultured cells decreased Aβ secretion by promoting the increased ubiquitination of APP and subsequent degradation.

Camacho et al.[39] have reported an alternative mechanism by which PPARγ may affect Aβ homeostasis. They have shown that activation of endogenous PPARγ or overexpression of the receptor lead to the dramatically enhanced clearance of Aβ from the media of both neuronal and non-neuronal cells. The mechanism subserving this effect is unknown.

Energy metabolism. There is ample documentation that glucose utilization is impaired in brain regions in-

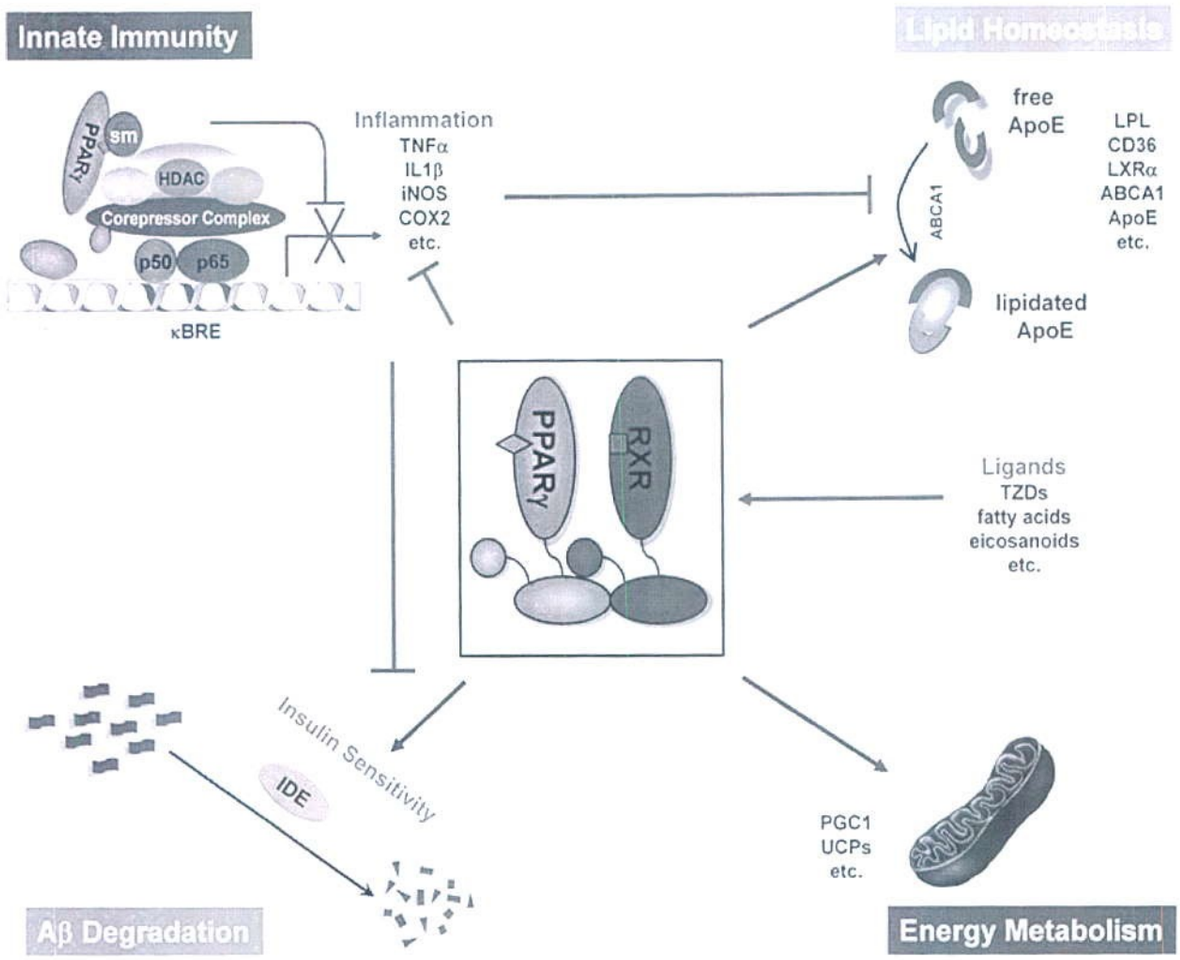


FIG. 1. Potential mechanisms of PPARγ in the treatment of Alzheimer's disease. ABCA1 = ATP-binding cassette A1; ApoE = apolipoprotein E; κBRE = kappa B response element; COX2 = cyclooxygenase 2; HDAC = histone deacetylase; IDE = insulin degrading enzyme; IL1β = interleukin 1 beta; iNOS = inducible nitric oxide synthase; LPL = lipoprotein lipase; LXRα = liver X receptor alpha; PGC1 = peroxisome proliferator-activated receptor gamma coactivator 1; RXR = retinoid X receptor; sm = small ubiquitin-related modifier; TNFα = tumor necrosis factor alpha; TZDs = thiazolidinediones; UCPs = uncoupling proteins.

volved in memory and cognition in AD patients. Significantly, AD patients exhibit impaired cerebral glucose metabolism before the symptomatic onset of the disease and in the absence of detectable structural changes in the brain.[40] Interestingly, several studies have also shown an *APOE4* dose-dependent impairment in glucose utilization in brain regions affected by the disease.[41–46]

PPARγ plays critical roles in energy metabolism due to its direct effects on mitochondrial function and ultimately ATP production. Mitochondria may be key players in the cerebral hypometabolism observed in AD, as this organelle plays critical roles in both energy metabolism as well as neuronal apoptosis. In the diseased brain, the numbers of neuronal mitochondria are greatly reduced and those remaining have very distinct morphological changes in their size and in the number of cristae they contain.[47] Roses et al.[48] have postulated that the PPARγ agonists act to improve mitochondrial function and this may be the basis of their beneficial effects on memory and cognition in AD patients.

PPARγ activation by pioglitazone resulted in a significant increase in mitochondrial DNA copy number as well as the expression of genes involved in mitochondrial biogenesis in fat tissue.[49] A recent study has found analogous changes within the brain in response to oral rosiglitazone treatment.[8] Strum et al.[8] have reported that PPARγ activation stimulated brain mitochondrial biogenesis and this stimulation was dependent on the ApoE isoforms. PPARγ may elicit these changes through the peroxisome proliferator-activated receptor gamma coactivator 1 (PGC1) family of proteins. These coactivators positively regulate mitochondrial function and metabolism.[50] PPARγ has been reported to stimulate the expression of PGC-1α,[51] which in turn, induces expression of the uncoupling proteins that stimulate mitochondrial biogenesis and respiration in muscle cells.[52–54] Proliferator-

activated receptor gamma coactivator 1 also stimulates the expression of a variety of genes that are vital for the mitochondrial oxidative phosphorylation pathway, as well as duplication of mitochondrial DNA content.[55,56] It should be noted that TZD agonists of PPARγ also have effects on mitochondrial metabolism that are receptor-independent.[57] The relationship between PPARγ, ApoE, and energy metabolism is not clear and warrants further investigation.

Insulin sensitivity. A number of studies have suggested that perturbation of insulin metabolism is associated with AD,[34,58–61] and individuals with type II diabetes mellitus are twice as likely to develop AD when compared with gender-matched healthy subjects.[62–67] Insulin resistance and hyperinsulinemia, two characteristics of type II diabetes mellitus, have been shown to have a high correlation with memory impairment and risk for AD. PPARγ agonists are widely prescribed for the treatment of type II diabetes mellitus. An extensive body of evidence demonstrates a critical role for PPARγ in the regulation of insulin sensitivity. The ability to activate PPARγ is closely correlated with the antidiabetic actions of TZDs, suggesting that receptor-dependent activation of PPARγ target genes may underlie the insulin sensitizing effect of this class of drugs.[68,69]

There is substantial evidence establishing a role of insulin in cognition. Insulin can pass across the BBB and enter the CNS via a receptor-mediated transport process. An acute increase in peripheral insulin concentrations results in the rapid elevation of CSF and brain insulin levels.[70] Insulin receptors in the mammalian brain have a very specific pattern of expression and are localized to the hippocampus and medial temporal cortex, both of which are areas associated with memory. In addition, brain insulin receptor signaling has been reported to be significantly reduced in AD, an indication of insulin resistance.[71,72] Craft et al.[73] have found that insulin administration improves memory. In addition, raising plasma insulin levels to those characteristic in insulin resistance is accompanied by parallel increases in plasma and brain levels of Aβ peptides and inflammatory markers.[74] Diet-induced insulin resistance is also associated with enhanced Aβ peptide levels and plaque formation, which was argued to arise from increased γ-secretase activity and lower IDE activity.[75]

It has been postulated that hyperinsulinemia in the brain may contribute to amyloid build-up due to inhibition of Aβ degradation by IDE, which degrades both insulin and Aβ peptides.[76,77] IDE levels have been shown to be reduced in the brains of AD patients and are further reduced by 50% in brains of AD patients homozygous for the *APOE4* allele.[78] Genetic ablation or partial loss of *Ide* leads to hyperinsulinemia and elevated Aβ levels.[79–81] It has been postulated that inhibition of IDE proteolytic activity may impair Aβ clearance, thereby initiating or accelerating the disease process. Recently, rosiglitazone has been shown to increase brain IDE levels in an animal model of AD.[82] Thus, *Ide* could potentially be responsible for the association between hyperinsulinemia and AD. However, it remains controversial whether this relationship is physiologically relevant, owing to the low levels of insulin in the brain.

Dyslipidemia. Genetic studies and epidemiological observations strongly suggest a relationship between dyslipidemia and AD. Elevated serum cholesterol levels have been reported to correlate with an increased incidence of AD.[83,84] Consistent with this linkage, individuals on statin therapy exhibit a greatly reduced risk (~70%) for AD.[85] Several genes regulating cholesterol homeostasis have been reported to be associated with AD, including *APOE*, *LRP1*, *ABCA1*, *NR1H2* + (*LXRβ*), *CYP46*, *ACAT*, and *CETP*,[86,87] and even PPARγ itself.[88,89] Little is known about the role of PPARγ in regulating CNS lipid metabolism.

The *APOE* gene is the best known bona fide risk factor for sporadic AD.[86] ApoE plays an important role in lipid transport throughout the body. It participates in lipoprotein metabolism, cholesterol homeostasis, and local lipid transport processes. In the brain, it is primarily synthesized and secreted within high-density lipoprotein (HDL) particles by astrocytes, and mediates the efficient transport and recycling of cholesterol within the CNS.[90–92] In humans, three naturally occurring variants of *APOE*, E2, E3, and E4 have been demonstrated to modify the risk or age of onset of late-onset AD (LOAD). The mechanism by which *APOE4* modifies the risk remains unknown, but has been postulated to play a role in Aβ clearance and deposition.

The lipidation of ApoE is carried out primarily by the ATP-binding cassette A1, which is a lipid transporter that mediates the loading of ApoE with phospholipids and cholesterol. ApoE acts as a structural scaffold for the formation of HDL particles. ABCA1 acts to regulate ApoE function in the CNS.[90,91] Recently, three independent groups, in four different animal models of AD, reported that inactivation of the *Abca1* gene facilitates Aβ fibrillogenesis and deposition within the brain.[93–95] Conversely, overexpression of human *Abca1* in mice resulted in reduced Aβ levels and plaque burden.[96] Importantly, the expression of the *Abca1* gene is transcriptionally regulated by the nuclear receptors, liver X receptors (LXRs), PPARγ, and RXR. The *NR1H2* gene has recently been reported to be genetically associated with AD.[97] Genetic ablation of either LXR genes results in increased number and size of plaques in an animal model of AD.[98] Thus, regulation of the lipidation status of ApoE is an important determinant of Aβ clearance and deposition.

A significant subset of the actions of PPARγ activation arises from its ability to induce the expression of a

related nuclear receptor, LXRα. LXRα regulates genes that are involved in lipid metabolism and reverse cholesterol transport, including *Apoe* and *Abca1*, among others. It has been demonstrated that there is a reciprocal positive regulation of both receptors that comprises a feed-forward mechanism to orchestrate the expression of both classes of receptors. PPARγ activation stimulates LXRα expression and vice versa. Recent evidence suggests that this results in synergistic induction of both PPARγ and LXR target gene expression.[99] PPARγ agonists have been shown to increase both ABCA1 and ApoE mRNA and protein levels and this effect is believed to be secondary to its induction of LXRα expression.[100–102] Significantly, it has recently been reported that rosiglitazone treatment of mice expressing the human *APOE4* allele induces a two-fold increase in brain ApoE4 mRNA.[8]

ApoE has been demonstrated to play essential roles in axonal growth[103] and synaptogenesis.[104] These effects of ApoE are isoform-dependent with ApoE3 promoting and ApoE4 inhibiting neurite outgrowth.[105–109] Interestingly, Brodbeck et al.[110] have recently reported that ApoE4 exposure is associated with decreased dendritic spine density of cortical neurons and this effect could be ameliorated by treatment of cultured cortical neurons with rosiglitazone.[110]

Inflammation. The AD brain is characterized by a significant microglial-mediated inflammatory response. Aβ plaque deposition results in the accumulation of microglia that become physically associated with deposited amyloid.[111] Microglia are the tissue macrophages of the brain and are derived from a myeloid lineage. The formation of Aβ fibrils and their deposition in the parenchyma of the brain elicits the phenotypic activation of microglia.[112] The persistent activation of abundant plaque-associated microglia typifies the human disease and its murine models. The activation of Aβ-stimulated signaling pathways mediates the acquisition of a reactive, pro-inflammatory phenotype accompanied by the elaboration of a wide range of pro-inflammatory cytokines, chemokines, acute phase proteins, as well as reactive nitrogen and oxygen species. A number of inflammatory cytokines, chemokines, and activated glial markers have also been found at elevated levels in the AD brain.[113–117] The chronic activation of microglia and their production of pro-inflammatory molecules is postulated to accelerate the disease progress, culminating in neuronal death. Inflammation has been proposed to exacerbate amyloid deposition and disease progression, whereas anti-inflammatory therapies inhibit Aβ generation and slow disease progress.

The role of PPARγ in regulating the microglial inflammatory responses has attracted substantial attention.[118] The anti-inflammatory actions of PPARγ agonists have been proposed to account for their positive effects in a number of animal models of CNS disease including AD.[1] There is extensive and compelling evidence that PPARγ agonists robustly suppress pro-inflammatory gene expression. PPARγ agonists have been reported to inhibit the expression of inflammatory cytokines, chemokines, matrix metallopeptidases (MMPs), cyclooxygenase 2 (COX-2) and inducible nitric oxide synthase (iNOS), each of which is reliant upon NFκB-dependent transcriptional effects.[13] There are now over nearly 30 studies showing microglial activation in response to inflammatory stimuli, including fibrillar Aβ.[119] Heneka et al.[120] have shown that pioglitazone acts to suppress iNOS and COX2 expression in the brain of the murine model of AD. A recent study in aged mice has provided compelling evidence that rosiglitazone treatment is associated with elevated levels of the anti-inflammatory cytokine interleukin-4 in the brain, which the authors suggest may underlie the anti-inflammatory actions of PPARγ agonists.[121]

Acknowledgments: This work was supported by grants from the National Institutes of Health (Grant nos. AG16704 and AG030482), the American Health Assistance Foundation and the Blanchette Hooker Rockefeller Foundation. MH was supported by grants from the Deutsche Forschungsgemeinschaft (DFG [German Research Foundation]).

REFERENCES

1. Sundararajan S, Jiang Q, Heneka M, et al. PPARgamma as a therapeutic target in central nervous system diseases. Neurochem Int 2006;49:136–144.
2. Risner ME, Saunders AM, Altman JF, et al. Efficacy of rosiglitazone in a genetically defined population with mild-to-moderate Alzheimer's disease. Pharmacogenomics J 2006;6:246.
3. Kersten S, Desvergne B, Wahli W. Roles of PPARs in health and disease. Nature 2000;405:421–424.
4. Bookout AL, Jeong Y, Downes M, et al. Anatomical profiling of nuclear receptor expression reveals a hierarchical transcriptional network. Cell 2006;126:789–799.
5. Lehrke M, Lazar M. The many faces of PPARgamma. Cell (Cambridge) 2005;123:993–999.
6. Maeshiba Y, Kiyota Y, Yamashita K, et al. Disposition of the new antidiabetic agent pioglitazone in rats, dogs, and monkeys. Arzneimittelforschung 1997;47:29–35.
7. Pedersen W, McMillan P, Kulstad J, et al. Rosiglitazone attenuates learning and memory deficits in Tg2576 Alzheimer mice. Exp Neurol 2006;199:265-273.
8. Strum JC, Shehee R, Virley D, et al. Rosiglitazone induces mitochondrial biogenesis in mouse brain. J Alzheimers Dis 2007; 11:45–51.
9. Glass CK. Going nuclear in metabolic and cardiovascular disease. Eur J Clin Invest 2006;116:556–560.
10. Berger J, Moller DE. The mechanisms of action of PPARs. Annu Rev Med 2002;53:409–435.
11. Aranda A, Pascual A. Nuclear hormone receptors and gene expression. Physiol Rev 2001;81:1269–1304.
12. Glass CK, Rosenfeld MG. The coregulator exchange in transcriptional functions of nuclear receptors. Genes Dev 2000;14:121–141.
13. Daynes RA, Jones DC. Emerging roles of PPARs in inflammation and immunity. Nat Rev Immunol 2002;2:748–759.
14. Subbaramaiah K, Lin DT, Hart JC, et al. Peroxisome Proliferator-activated receptor gamma ligands suppress the transcriptional activation of cyclooxygenase-2: evidence for involvement of ac-

tivator protein-1 and CREB-binding protein/p300. J Biol Chem 2001;276:12440–12448.
15. Li M, Pascual G, Glass CK. Peroxisome proliferator-activated receptor gamma-dependent repression of the inducible nitric oxide synthase gene. Mol Cell Biol 2000;20:4699–4707.
16. Pascual G, Fong AL, Ogawa S, et al. A SUMOylation-dependent pathway mediates transrepression of inflammatory response genes by PPAR-gamma. Nature 2005;437:759–763.
17. Yan Q, Zhang J, Liu H, et al. Anti-inflammatory drug therapy alters beta-amyloid processing and deposition in an animal model of Alzheimer's disease. J Neurosci 2003;23:7504–7509.
18. Lim GP, Yang F, Chu T, et al. Ibuprofen suppresses plaque pathology and inflammation in a mouse model for Alzheimer's disease. J Neurosci 2000;20:5709–5714.
19. Heneka M, Sastre M, Dumitrescu-Ozimek L, et al. Acute treatment with the PPARg agonist pioglitazone and ibuprofen reduces glial inflammation and Abeta1-42 levels in APPV717I transgenic mice. Brain 2005;128:1442-1453.
20. Pedersen WA, Flynn ER, Insulin resistance contributes to aberrant stress responses in the Tg2576 mouse model of Alzheimer's disease. Neurobiol Dis 2004;17:500–506.
21. Andrews R, Walker B. Glucocorticoids and insulin resistance: old hormones, new targets. Clinical science (London, England: 1979) 1999;96:513–523.
22. Andrews RC, Herlihy O, Livingstone DE, et al. Abnormal cortisol metabolism and tissue sensitivity to cortisol in patients with glucose intolerance. J Clin Endocrinol Metab 2002;87:5587–5593.
23. Pomara N, Greenberg WM, Branford MD, et al. Therapeutic implications of HPA axis abnormalities in Alzheimer's disease: review and update. Psychopharmacol Bull 2003;37:120–134.
24. Morcos M, Fohr B, Tafel J, et al. Long-term treatment of central Cushing's syndrome with rosiglitazone. Exp Clin Endocrinol Diabetes 2007;115:292–297.
25. Ambrosi B, Dall'Asta C, Cannavo S, et al. Effects of chronic administration of PPAR-gamma ligand rosiglitazone in Cushing's disease. Eur J Endocrinol 2004;151:173–178.
26. Heaney AP, Fernando M, Yong WH, et al. Functional PPAR-gamma receptor is a novel therapeutic target for ACTH-secreting pituitary adenomas. Nat Med 2002;8:1281–1287.
27. Catrina SB, Virtanen K, Hallsten K, et al. Effect of rosiglitazone on early-morning plasma cortisol levels. Neuro Endocrinol Lett 2005;26:763–764; author reply 765.
28. Watson GS, Cholerton BA, Reger MA, et al. Preserved cognition in patients with early Alzheimer disease and amnestic mild cognitive impairment during treatment with rosiglitazone: a preliminary study. Am J Geriatr Psychiatry 2005;13:950–958.
29. Geldmacher D, Fritsch T, McClendon M, et al. A pilot study of pioglitazone in Alzheimer Disease. Int Conf Alz Dis Rel. Dementias; Madrid, July, 2006.
30. Waugh J, Keating GM, Plosker GL, et al. Pioglitazone: a review of its use in type 2 diabetes mellitus. Drugs 2006;66:85–109.
31. Nissen SE, Wolski K. Effect of rosiglitazone on the risk of myocardial infarction and death from cardiovascular causes. N Engl J Med 2007;356:2457–2471.
32. Lincoff AM, Wolski K, Nicholls SJ, et al. Pioglitazone and risk of cardiovascular events in patients with type 2 diabetes mellitus: a meta-analysis of randomized trials. JAMA 2007;298:1180–1188.
33. Kuusisto J, Koivisto K, Mykkanen L, et al. Association between features of the insulin resistance syndrome and Alzheimer's disease independently of apolipoprotein E4 phenotype: cross sectional population based study. BMJ 1997;315:1045–1049.
34. Craft S, Asthana S, Schellenberg G, et al. Insulin metabolism in Alzheimer's disease differs according to apolipoprotein E genotype and gender. Neuroendocrinology 1999;70:146–152.
35. Craft S, Asthana S, Schellenberg G, et al. Insulin effects on glucose metabolism, memory, and plasma amyloid precursor protein in Alzheimer's disease differ according to apolipoprotein-E genotype. Ann N Y Acad Sci 2000;903:222–228.
36. Sastre M, Dewachter I, Landreth GE, et al. Nonsteroidal anti-inflammatory drugs and peroxisome proliferator-activated receptor-gamma agonists modulate immunostimulated processing of amyloid precursor protein through regulation of beta-secretase. J Neurosci 2003;23:9796–9804.
37. Sastre M, Dewachter I, Rossner S, et al. Nonsteroidal anti-inflammatory drugs repress beta-secretase gene promoter activity by the activation of PPARgamma. Proc Natl Acad Sci U S A 2006;103:443–448.
38. d'Abramo C, Massone S, Zingg JM, et al. Role of peroxisome proliferator-activated receptor gamma in amyloid precursor protein processing and amyloid beta-mediated cell death. Biochem J 2005;391:693–698.
39. Camacho IE, Serneels L, Spittaels K, et al. Peroxisome proliferator-activated receptor gamma induces a clearance mechanism for the amyloid-beta peptide. J Neurosci 2004;24:10908–10917.
40. Mosconi L, Tsui WH, De Santi S, et al. Reduced hippocampal metabolism in MCI and AD: automated FDG-PET image analysis. Neurology 2005;64:1860–1867.
41. Reiman EM, Chen K, Alexander GE, et al. Functional brain abnormalities in young adults at genetic risk for late-onset Alzheimer's dementia. Proc Natl Acad Sci U S A 2004;101:284–289.
42. Reiman EM, Caselli RJ, Chen K, et al. Declining brain activity in cognitively normal apolipoprotein E epsilon 4 heterozygotes: a foundation for using positron emission tomography to efficiently test treatments to prevent Alzheimer's disease. Proc Natl Acad Sci U S A 2001;98:3334–3339.
43. Small GW, Ercoli LM, Silverman DH, et al. Cerebral metabolic and cognitive decline in persons at genetic risk for Alzheimer's disease. Proc Natl Acad Sci U S A 2000;97:6037–6042.
44. Small GW, Mazziotta JC, Collins MT, et al. Apolipoprotein E type 4 allele and cerebral glucose metabolism in relatives at risk for familial Alzheimer disease. JAMA 1995;273:942–947.
45. Reiman EM, Chen K, Alexander GE, et al. Correlations between apolipoprotein E epsilon4 gene dose and brain-imaging measurements of regional hypometabolism. Proc Natl Acad Sci U S A 2005;102:8299–8302.
46. Bookheimer SY, Strojwas MH, Cohen MS, et al. Patterns of brain activation in people at risk for Alzheimer's disease. N Engl J Med 2000;343:450–456.
47. Castellani R, Hirai K, Aliev G, et al. Role of mitochondrial dysfunction in Alzheimer's disease. J Neurosci Res 2002;70:357–360.
48. Roses AD, Saunders AM, Huang Y, et al. Complex disease-associated pharmacogenetics: drug efficacy, drug safety, and confirmation of a pathogenetic hypothesis (Alzheimer's disease). Pharmacogenomics J 2007;7:10–28.
49. Bogacka I, Xie H, Bray GA, et al. Pioglitazone induces mitochondrial biogenesis in human subcutaneous adipose tissue in vivo. Diabetes 2005;54:1392–1399.
50. Handschin C, Spiegelman BM. Peroxisome proliferator-activated receptor gamma coactivator 1 coactivators, energy homeostasis, and metabolism. Endocr Rev 2006;27:728–735.
51. Hondares E, Mora O, Yubero P, et al. Thiazolidinediones and rexinoids induce peroxisome proliferator-activated receptor-coactivator (PGC)-1alpha gene transcription: an autoregulatory loop controls PGC-1alpha expression in adipocytes via peroxisome proliferator-activated receptor-gamma coactivation. Endocrinology 2006;147:2829–2838.
52. Wu Z, Puigserver P, Andersson U, et al. Mechanisms controlling mitochondrial biogenesis and respiration through the thermogenic coactivator PGC-1. Cell 1999;98:115–124.
53. Kelly LJ, Vicario PP, Thompson GM, et al. Peroxisome proliferator-activated receptors gamma and alpha mediate in vivo regulation of uncoupling protein (UCP-1, UCP-2, UCP-3) gene expression. Endocrinology 1998;139:4920–4927.
54. Puigserver P, Wu Z, Park CW, et al. A cold-inducible coactivator of nuclear receptors linked to adaptive thermogenesis. Cell 1998;92:829–839.
55. Houten SM, Auwerx J. PGC-1alpha: turbocharging mitochondria. Cell 2004;119:5–7.
56. Mootha VK, Lindgren CM, Eriksson KF, et al. PGC-1alpha-responsive genes involved in oxidative phosphorylation are coordinately downregulated in human diabetes. Nat Genet 2003;34:267–273.

57. Feinstein DL, Spagnolo A, Akar C, et al. Receptor-independent actions of PPAR thiazolidinedione agonists: is mitochondrial function the key? Biochem Pharmacol 2005;70:177–188.
58. Biessels GJ, Staekenborg S, Brunner E, et al. Risk of dementia in diabetes mellitus: a systematic review. Lancet Neurol 2006;5: 64–74.
59. Razay G, Vreugdenhil A, Wilcock G. The metabolic syndrome and Alzheimer disease. Archives of Neurology 2007;64:93–96.
60. Razay G, Wilcock GK. Hyperinsulinaemia and Alzheimer's disease. Age Ageing 1994;23:396–399.
61. Craft S, Peskind E, Schwartz MW, et al. Cerebrospinal fluid and plasma insulin levels in Alzheimer's disease: relationship to severity of dementia and apolipoprotein E genotype. Neurology 1998;50:164–168.
62. Leibson CL, Rocca WA, Hanson VA, et al. The risk of dementia among persons with diabetes mellitus: a population-based cohort study. Ann N Y Acad Sci 1997;826:422–427.
63. Ott A, Stolk RP, van Harskamp F, et al. Diabetes mellitus and the risk of dementia: The Rotterdam Study. Neurology 1999;53: 1937–1942.
64. Xu WL, Qiu CX, Wahlin A, et al. Diabetes mellitus and risk of dementia in the Kungsholmen project: a 6-year follow-up study. Neurology 2004;63:1181–1186.
65. Arvanitakis Z, Wilson RS, Bienias JL, et al. Diabetes mellitus and risk of Alzheimer disease and decline in cognitive function. Arch Neurol 2004;61:661–666.
66. Peila R, Rodriguez BL, Launer LJ. Type 2 diabetes, APOE gene, and the risk for dementia and related pathologies: The Honolulu-Asia Aging Study. Diabetes 2002;51:1256–1262.
67. Haan MN, Mungas DM, Gonzalez HM, et al. Prevalence of dementia in older Latinos: the influence of type 2 diabetes mellitus, stroke and genetic factors. J Am Geriatr Soc 2003;51:169–177.
68. Willson TM, Lambert MH, Kliewer SA. Peroxisome proliferator-activated receptor gamma and metabolic disease. Annu Rev Biochem 2001;70:341–367.
69. Picard F, Auwerx J. PPAR(gamma) and glucose homeostasis. Annu Rev Nutr 2002;22:167–197.
70. Wallum BJ, Taborsky GJ, Jr., Porte D, Jr., et al. Cerebrospinal fluid insulin levels increase during intravenous insulin infusions in man. J Clin Endocrinol Metab 1987;64:190–194.
71. Frolich L, Blum-Degen D, Riederer P, et al. A disturbance in the neuronal insulin receptor signal transduction in sporadic Alzheimer's disease. Ann N Y Acad Sci 1999;893:290–293.
72. Messier C, Teutenberg K. The role of insulin, insulin growth factor, and insulin-degrading enzyme in brain aging and Alzheimer's disease. Neural Plast 2005;12:311–328.
73. Craft S, Asthana S, Cook DG, et al. Insulin dose-response effects on memory and plasma amyloid precursor protein in Alzheimer's disease: interactions with apolipoprotein E genotype. Psychoneuroendocrinology 2003;28:809–822.
74. Craft S. Insulin resistance syndrome and Alzheimer disease: pathophysiologic mechanisms and therapeutic implications. Alzheimer Dis Assoc Disord 2006;20:298–301.
75. Ho L, Qin W, Pompl PN, et al. Diet-induced insulin resistance promotes amyloidosis in a transgenic mouse model of Alzheimer's disease. Faseb J 2004;18:902–904.
76. Eckman EA, Eckman CB. Abeta-degrading enzymes: modulators of Alzheimer's disease pathogenesis and targets for therapeutic intervention. Biochem Soc Trans 2005;33:1101–1105.
77. Leissring MA. Proteolytic degradation of the amyloid beta-protein: the forgotten side of Alzheimer's disease. Curr Alzheimer Res 2006;3:431–435.
78. Cook DG, Leverenz JB, McMillan PJ, et al. Reduced hippocampal insulin-degrading enzyme in late-onset Alzheimer's disease is associated with the apolipoprotein E-epsilon4 allele. Am J Pathol 2003;162:313–319.
79. Farris W, Leissring MA, Hemming ML, et al. Alternative splicing of human insulin-degrading enzyme yields a novel isoform with a decreased ability to degrade insulin and amyloid beta-protein. Biochemistry (Washington) 2005;44:6513–6525.
80. Farris W, Mansourian S, Leissring MA, et al. Partial loss-of-function mutations in insulin-degrading enzyme that induce diabetes also impair degradation of amyloid beta-protein. Am J Pathol 2004;164:1425–1434.
81. Farris W, Mansourian S, Chang Y, et al. Insulin-degrading enzyme regulates the levels of insulin, amyloid beta-protein, and the beta-amyloid precursor protein intracellular domain in vivo. Proc Natl Acad Sci U S A 2003;100:4162–4167.
82. Pedersen WA, McMillan PJ, Kulstad JJ, et al. Rosiglitazone attenuates learning and memory deficits in Tg2576 Alzheimer mice. Exp Neurol 2006;199:265–273.
83. Panza F, Capurso C, D'Introno A, et al. Serum total cholesterol as a biomarker for Alzheimer's disease: mid-life or late-life determinations? Exp Gerontol 2006;41:805–806.
84. Notkola IL, Sulkava R, Pekkanen J, et al. Serum total cholesterol, apolipoprotein E epsilon 4 allele, and Alzheimer's disease. Neuroepidemiology 1998;17:14–20.
85. Wolozin B, Kellman W, Ruosseau P, et al. Decreased prevalence of Alzheimer disease associated with 3-hydroxy-3-methyglutaryl coenzyme A reductase inhibitors. Archives of Neurology 2000; 57:1439–1443.
86. Puglielli L, Tanzi RE, Kovacs DM. Alzheimer's disease: the cholesterol connection. Nature Neuroscience 2003;6:345–351.
87. Wollmer MA, Streffer JR, Lutjohann D, et al. ABCA1 modulates CSF cholesterol levels and influences the age at onset of Alzheimer's disease. Neurobiol Aging 2003;24:421–426.
88. Hamilton G, Proitsi P, Jehu L, et al. Candidate gene association study of insulin signaling genes and Alzheimer's disease: evidence for SOS2, PCK1, and PPARgamma as susceptibility loci. Am J Med Genet B Neuropsychiatr Genet 2007;144:508–516.
89. Scacchi R, Pinto A, Gambina G, et al. The peroxisome proliferator-activated receptor gamma (PPAR-gamma2) Pro12Ala polymorphism is associated with higher risk for Alzheimer's disease in octogenarians. Brain Res 2007;1139:1–5.
90. Wahrle SE, Jiang H, Parsadanian M, et al. ABCA1 is required for normal central nervous system ApoE levels and for lipidation of astrocyte-secreted apoE. J Biol Chem 2004;279:40987–40993.
91. Hirsch-Reinshagen V, Zhou S, Burgess BL, et al. Deficiency of ABCA1 impairs apolipoprotein E metabolism in brain. J Biol Chem 2004;279:41197–41207.
92. Xu Q, Bernardo A, Walker D, et al. Profile and regulation of apolipoprotein E (ApoE) expression in the CNS in mice with targeting of green fluorescent protein gene to the ApoE locus. J Neurosci 2006;26:4985–4994.
93. Koldamova R, Staufenbiel M, Lefterov I. Lack of ABCA1 considerably decreases brain ApoE level and increases amyloid deposition in APP23 mice. J Biol Chem 2005;280: 43224–43235.
94. Hirsch-Reinshagen V, Maia LF, Burgess BL, et al. The absence of ABCA1 decreases soluble ApoE levels but does not diminish amyloid deposition in two murine models of Alzheimer disease. J Biol Chem 2005;280:43243–43256.
95. Wahrle SE, Jiang H, Parsadanian M, et al. Deletion of Abca1 increases Abeta deposition in the PDAPP transgenic mouse model of Alzheimer disease. J Biol Chem 2005;280:43236–43242.
96. Wahrle SE, Jiang H, Parsadanian M, et al. Overexpression of ABCA1 reduces amyloid deposition in the PDAPP mouse model of Alzheimer disease. J Clin Invest 2008;Epub ahead of print.
97. Adighibe O, Arepalli S, Duckworth J, et al. Genetic variability at the LXR gene (NR1H2) may contribute to the risk of Alzheimer's disease. Neurobiol Aging 2006;27:1431–1434.
98. Zelcer N, Khanlou N, Clare R, et al. Attenuation of neuroinflammation and Alzheimer's disease pathology by liver x receptors. Proc Natl Acad Sci U S A 2007;104:10601–10606.
99. Piraino G, Cook JA, O'Connor M, et al. Synergistic effect of peroxisome proliferator activated receptor-gamma and liver X receptor-alpha in the regulation of inflammation in macrophages. Shock 2006;26:146–153.
100. Calkin AC, Forbes JM, Smith CM, et al. Rosiglitazone attenuates atherosclerosis in a model of insulin insufficiency independent of its metabolic effects. Arterioscler Thromb Vasc Biol 2005;25: 1903–1909.
101. Llaverias G, Rebollo A, Pou J, et al. Effects of rosiglitazone and atorvastatin on the expression of genes that control cholesterol

homeostasis in differentiating monocytes. Biochem Pharmacol 2006;71:605–614.
102. Yue L, Rasouli N, Ranganathan G, et al. Divergent effects of peroxisome proliferator-activated receptor gamma agonists and tumor necrosis factor alpha on adipocyte ApoE expression. J Biol Chem 2004;279:47626–47632.
103. Arakawa R, Hayashi M, Remaley AT, et al. Phosphorylation and stabilization of ATP binding cassette transporter A1 by synthetic amphiphilic helical peptides. J Biol Chem 2004;279:6217–6220.
104. Mauch DH, Nagler K, Schumacher S, et al. CNS synaptogenesis promoted by glia-derived cholesterol. Science 2001;294:1354–1357.
105. Nathan BP, Jiang Y, Wong GK, et al. Apolipoprotein E4 inhibits, and apolipoprotein E3 promotes neurite outgrowth in cultured adult mouse cortical neurons through the low-density lipoprotein receptor-related protein. Brain Res 2002;928:96–105.
106. DeMattos RB, Curtiss LK, Williams DL. A minimally lipidated form of cell-derived apolipoprotein E exhibits isoform-specific stimulation of neurite outgrowth in the absence of exogenous lipids or lipoproteins. J Biol Chem 1998;273:4206–4212.
107. Fagan AM, Bu G, Sun Y, et al. Apolipoprotein E-containing high density lipoprotein promotes neurite outgrowth and is a ligand for the low density lipoprotein receptor-related protein. J Biol Chem 1996;271:30121–30125.
108. Holtzman DM, Pitas RE, Kilbridge J, et al. Low density lipoprotein receptor-related protein mediates apolipoprotein E-dependent neurite outgrowth in a central nervous system-derived neuronal cell line. Proc Natl Acad Sci U S A 1995;92:9480–9484.
109. Nathan BP, Bellosta S, Sanan DA, et al. Differential effects of apolipoproteins E3 and E4 on neuronal growth in vitro. Science 1994;264:850–852.
110. Brodbeck J, Balestra ME, Saunders AM, et al. Rosiglitazone increases dendritic spine density and rescues spine loss caused by apolipoprotein E4 in primary cortical neurons. Proc Natl Acad Sci U S A 2008;105:1343–1346.
111. Akiyama H, Barger S, Barnum S, et al. Inflammation and Alzheimer's disease. Neurobiol Aging 2000;21:383–421.
112. Cooper NR, Bradt BM, O'Barr S, et al. Focal inflammation in the brain: role in Alzheimer's disease. Immunol Res 2000;21:159–165.
113. Rogers J, Webster S, Lue LF, et al. Inflammation and Alzheimer's disease pathogenesis. Neurobiol Aging 1996;17:681–686.
114. Rogers J, Shen Y. A perspective on inflammation in Alzheimer's disease. Ann N Y Acad Sci 2000;924:132–135.
115. Colangelo V, Schurr J, Ball MJ, et al. Gene expression profiling of 12633 genes in Alzheimer hippocampal CA1: transcription and neurotrophic factor down-regulation and up-regulation of apoptotic and pro-inflammatory signaling. J Neurosci Res 2002;70:462–473.
116. Wyss-Coray T. Inflammation in Alzheimer disease: driving force, bystander or beneficial response? Nat Med 2006;12:1005–1015.
117. Wyss-Coray T, Mucke L. Inflammation in neurodegenerative disease–a double-edged sword. Neuron 2002;35:419–432.
118. Bernardo A, Minghetti L. PPAR-gamma agonists as regulators of microglial activation and brain inflammation. Curr Pharm Des 2006;12:93–109.
119. Heneka MT, Landreth GE. PPARs in the brain. Biochim Biophys Acta 2007;1771:1031–1045.
120. Heneka MT, Klockgether T, Feinstein DL. Peroxisome proliferator-activated receptor-gamma ligands reduce neuronal inducible nitric oxide synthase expression and cell death in vivo. J Neurosci 2000;20:6862–6867.
121. Loane DJ, Deighan BF, Clarke RM, et al. Interleukin-4 mediates the neuroprotective effects of rosiglitazone in the aged brain. Neurobiol Aging 2007.

Having described our invention, we claim:

1. The use of from 0.5 to 9 milligrams of pioglitazone in the manufacture of a pharmaceutical formulation for treating cognitive impairment of the Alzheimer's type in a subject.

2. The use of claim 1, wherein said treating comprises delaying the onset of cognitive impairment of the Alzheimer's type.

3. The use of claim 1, wherein said treating comprises delaying the onset of cognitive impairment of the Alzheimer's type in a human subject at increased risk of developing cognitive impairment of the Alzheimer's type within the next 5-7 years, said risk based upon the subject's age and rs10524523 genotype.

4. The use of claim 1, claim 2 or claim 3, wherein said pioglitazone is formulated in unit dosage form.

5. The use of claim 4, wherein said unit dosage form comprises from 0.5 to 6 milligrams of pioglitazone.

6. The use of claim 4 or claim 5, wherein said unit dosage form comprises from 0.5 to 1.5 milligrams of pioglitazone.

7. The use of any one of claims 1 to 6, wherein said pharmaceutical formulation is a tablet.

8. The use of any one of claims 1 to 6, wherein said pharmaceutical formulation is a capsule.

9. The use of any one of claims 1 to 6, wherein said pharmaceutical formulation is a caplet.

10. The use of any one of claims 1 to 6, wherein said pharmaceutical formulation is a liquid.

11. The use of any one of claims 1 to 6, wherein said pharmaceutical formulation is a semi-solid.

12. The use of any one of claims 1 to 6, wherein said pharmaceutical formulation is a solid.

13. The use of any one of claims 1 to 4, wherein said pioglitazone is formulated to provide an AUC of from about 0.15 μg•h/mL to about 3.6 μg•h/mL.

14. The use of from 0.5 to 9 milligrams of pioglitazone in the manufacture of a pharmaceutical formulation for treating cognitive decline in a subject in need thereof.

15. The use according to any one of claims 1 to 14, wherein said subject is at increased risk of developing cognitive impairment of the Alzheimer's type within the next 5-7 years, said risk based upon the subject's age.

16. The use of any one of claims 1 to 15, wherein said subject is at least 50 years old.

17. The use of any one of claims 1 to 15, wherein said subject is at least 55 years old.

18. The use of any one of claims 1 to 15, wherein said subject is at least 60 years old.

19. The use of any one of claims 1 to 15, wherein said subject is at least 62 years old.

20. The use of any one of claims 1 to 15, wherein said subject is at least 68 years old.

21. The use of any one of claims 1 to 15, wherein said subject is at least 70 years old.

22. The use of any one of claims 1 to 21, wherein said subject is a Caucasian subject.

23. The use of any one of claims 1 to 21, wherein said subject is a non-Caucasian subject.

24. The use of any one of claims 1 to 23, wherein one or two APOE2 alleles are absent in a subject.

25. The use of any one of claims 1 to 24, wherein the pharmaceutical formulation is formulated for administration once daily.

26. The use of any one of claims 2 to 25, wherein said delaying comprises delaying the onset of impairment in episodic memory.

27. A method of determining increased risk of developing cognitive impairment of the Alzheimer's type that can be treated with from 0.5 to 9 mg pioglitazone in a human subject at a predetermined age or age range, comprising:
detecting from a biological sample of said subject the rs10524523 genotype of said subject, wherein each allele of the rs10524523 genotype is assigned as:
(a) short (S, less than 19 T residues);
(b) long (L, 19-29 residues); or
(c) very long (VL, 30 or more residues); and
determining from said rs10524523 genotype whether said subject is at increased risk in developing cognitive impairment of the Alzheimer's type at said predetermined age or age range, wherein:
(1) age greater than about 62 and L,L or L,VL indicates increased risk;
(2) age greater than about 62 and VL,VL does not indicate increased risk;
(3) age greater than about 74 and S,L indicates increased risk;
(4) age greater than about 77 and S,S indicates increased risk; and
(5) age greater than about 76 and S,VL indicates increased risk.

28. The method of claim 27, wherein said determining further comprises detecting from a biological sample of said subject the APOE genotype of said subject, wherein the presence of an APOE2 allele in said genotype indicates the subject is not at increased risk.

29. A method of determining whether to administer from 0.5 to 9 milligrams of pioglitazone to a human subject for treatment of cognitive impairment of the Alzheimer's type, comprising:

detecting from a biological sample of said subject the rs10524523 genotype of the subject, wherein each allele is assigned as:

(a) short (S, less than 19 T residues);

(b) long (L, 19-29 residues); or

(c) very long (VL, 30 or more residues); and

determining from said rs10524523 genotype and from the age of said human subject whether to administer low dose pioglitazone to said subject for treatment of cognitive impairment of the Alzheimer's type, wherein:

(1) age greater than about 62 and L,L or L,VL indicates treatment;

(2) age greater than about 62 and VL,VL does not indicate treatment;

(3) age greater than about 74 and S,L indicates treatment;

(4) age greater than about 77 and S,S indicates treatment; and

(5) age greater than about 76 and S,VL indicates treatment.

30. The method of claim 29, wherein said determining further comprises detecting from a biological sample of said subject the APOE genotype of said subject, wherein the presence of an APOE2 allele in said genotype does not indicate treatment.

31. The method of claim 29 or claim 30, wherein said subject has normal cognition.

32. The use of from 0.5 to 9 milligrams of pioglitazone in the manufacture of a pharmaceutical formulation for delaying the onset of Alzheimer's disease in a subject at

risk of developing Alzheimer's disease, wherein said risk is determined based on the presence of at least one genetic variant of the TOMM40 gene, wherein said genetic variant is an rs10524523 allele, and wherein the presence of said at least one genetic variant indicates a risk of developing Alzheimer's disease.

33. The use of from 0.5 to 9 milligrams of pioglitazone in the manufacture of a pharmaceutical formulation for delaying the onset of mild cognitive impairment in a subject at risk for developing mild cognitive impairment, wherein said risk is determined based on the presence of at least one genetic variant of the TOMM40 gene, wherein said genetic variant is an rs10524523 allele, and wherein the presence of said at least one genetic variant indicates a risk of developing mild cognitive impairment.

34. The use of from 0.5 to 9 milligrams of pioglitazone in the manufacture of a pharmaceutical formulation for delaying the onset of amnestic mild cognitive impairment in a subject at risk of developing Alzheimer's disease, wherein said risk is determined based on the presence of at least one genetic variant of the TOMM40 gene, wherein said genetic variant is an rs10524523 allele, and wherein the presence of said at least one genetic variant indicates a risk of developing Alzheimer's disease.

35. The use of from 0.5 to 9 milligrams of pioglitazone in the manufacture of a pharmaceutical formulation for of delaying the onset of preclinical Alzheimer's disease in a subject at risk of developing Alzheimer's disease, wherein said risk is determined based on the presence of at least one genetic variant of the TOMM40 gene, wherein said genetic variant is an rs10524523 allele, and wherein the presence of said at least one genetic variant indicates a risk of developing Alzheimer's disease.

36. The use of from 0.5 to 9 milligrams of pioglitazone in the manufacture of a pharmaceutical formulation for delaying the onset of prodromal Alzheimer's disease in a subject at risk of developing Alzheimer's disease, wherein said risk is determined based on the presence of at least one genetic variant of the TOMM40 gene, wherein said genetic

variant is an rs10524523 allele, and wherein the presence of said at least one genetic variant indicates a risk of developing Alzheimer's disease.

37. The use of from 0.5 to 9 milligrams of pioglitazone in the manufacture of a pharmaceutical formulation for delaying the onset of physiological changes associated with Alzheimer's disease in a subject at risk of developing Alzheimer's disease, wherein said risk is determined based on the presence of at least one genetic variant of the TOMM40 gene, wherein said genetic variant is an rs10524523 allele, and wherein the presence of said at least one genetic variant indicates a risk of developing Alzheimer's disease.

38. The use of any one of claims 32 to 37, wherein the pharmaceutical formulation is formulated at a dosage of pioglitazone of 0.5 mg to 6 mg per day.

39. The use of any one of claims 32 to 37, wherein the pharmaceutical formulation provides an AUC of from about 0.15 μg•h/mL to about 3.6 μg•h/mL.

40. The use according to any one of claims 32 to 37, wherein the pharmaceutical formulation is formulated as part of a daily treatment regimen.

41. The use according to any one of claims 32 to 40, wherein said pharmaceutical formulation is a tablet.

42. The use according to any one of claims 32 to 40, wherein said pharmaceutical formulation is a capsule.

43. The use according to any one of claims 32 to 40, wherein said pharmaceutical formulation is a caplet.

44. The use according to any one of claims 32 to 40, wherein said pharmaceutical formulation is a liquid.

45. The use according to any one of claims 34 to 42, wherein said pharmaceutical formulation is a semi-solid.

46. The use according to any one of claims 32 to 40, wherein said pharmaceutical formulation is a solid.

47. The use of claim 41, wherein said tablet is an orally disintegrating tablet.

48. The use of claim 45, wherein said semi-solid pharmaceutical formulation is selected from a group of semi-solid pharmaceutical formulations consisting of a gel, cream, lotion, ointment, salve and balm.

49. The use of claim 44, wherein the liquid is formulated for oral administration.

50. The use of claim 44, wherein the liquid is formulated for injection.

51. The use of claim 44, wherein the liquid is formulated for intra-nasal administration.

52. The use of claim 45, wherein the semi-solid pharmaceutical formulation is formulated for intra-nasal administration.

53. The use of claim 45, wherein the semi-solid pharmaceutical formulation is formulated for topical administration.

54. The use of claim 46, wherein said pharmaceutical formulation is a powder.

55. The use of claim 46, wherein the solid pharmaceutical formulation is formulated for topical administration.

56. The use according to any one of claims 32 to 55, wherein said subject has normal cognition.

57. The use of any one of claims 32 to 56, wherein the subject is younger than 60.

58. The use of any one of claims 32 to 56, wherein the subject is between the ages of 60 and 70.

59. The use of any one of claims 32 to 58, wherein the subject has one copy of the long TOMM40 rs10524523 allele.

60. The use of any one of claims 32 to 58, wherein the subject has two copies of the long TOMM40 rs10524523 allele.

61. The use of any one of claims 32 to 60, wherein the subject has an increased risk of developing Alzheimer's disease as compared to a control subject.

62. The use of claim 61, wherein the control subject carries at least one copy of the TOMM40 rs10524523 allele comprising a poly-T repeat that is less than 19 nucleotides in length.

63. The use of claim 61, wherein the control subject does not have a copy of the TOMM40 rs10524523 allele comprising a poly-T repeat that is greater than 19 nucleotides in length.

64. The use of any one of claims 32 to 63, wherein the pharmaceutical formulation is a bioequivalent formulation.

65. The use of any one of claims 32 to 63, wherein the pharmaceutical formulation is a pharmaceutically equivalent formulation.

66. The use of claims 32 to 63, wherein the pharmaceutical formulation is a therapeutically equivalent formulation.

67. The use according to any one of claims 32 to 66, wherein the pioglitazone is formulated in a unit dose.

68. The use of claim 67, wherein the unit dosage comprises from 0.5 to 6 mg of pioglitazone.

69. The use of claims 67 or 68, wherein the unit dosage comprises from 0.5 to 1.5 mg of pioglitazone.

70. The use of claim 3, wherein the determination of said risk based upon the subject's age and rs10524523 genotype comprises:
detecting from a biological sample of said subject the rs10524523 genotype of said subject, wherein each allele of the rs10524523 genotype is assigned as:
(a) short (S, less than 19 T residues);
(b) long (L, 19-29 residues); or
(c) very long (VL, 30 or more residues); and
determining from said rs10524523 genotype whether said subject is at increased risk in developing cognitive impairment of the Alzheimer's type at said predetermined age or age range, wherein:
(1) age greater than about 62 and L,L or L,VL indicates increased risk;
(2) age greater than about 62 and VL,VL does not indicate increased risk;
(3) age greater than about 74 and S,L indicates increased risk;
(4) age greater than about 77 and S,S indicates increased risk; and
(5) age greater than about 76 and S,VL indicates increased risk.

71. The use of claim 70, wherein said determining further comprises detecting from a biological sample of said subject the APOE genotype of said subject, wherein the presence of an APOE2 allele in said genotype indicates the subject is not at increased risk.

72. The use according to any one of claims 1, 14, and 32 to 37, substantially as herein described with reference to any one of the examples and/or figures.

73. A method according to any one of claims 27 or 29, substantially as herein described with reference to any one of the examples and/or figures.

SUPERINTENDENCIA DE INDUSTRIA Y COMERCIO
NIT : 800.176.089-2
- / -

Industria y Comercio
SUPERINTENDENCIA

RECIBO DE CAJA

No. 15 - 102061

Bogotá D.C., Septiembre 17 de 2015 - 08:33:51

RECIBIDO DE : CAVELIER ABOGADOS NI 860.041.367 RE

*** Soporte del Pago ***

TIPO PAGO	BANCO	CUENTA	No. PAGO	FECHA PAGO	VR PAGO
RECIBO DE CA	SIC ** RECIBO **	999999999	101435	16/09/2015	530.000.00
RECIBO DE CA	SIC ** RECIBO **	999999999	101436	16/09/2015	530.000.00
RECIBO DE CA	SIC ** RECIBO **	999999999	101437	16/09/2015	536.000.00
RECIBO DE CA	SIC ** RECIBO **	999999999	101438	16/09/2015	536.000.00
RECIBO DE CA	SIC ** RECIBO **	999999999	101439	16/09/2015	536.000.00

*** Conceptos Pagados ***

CANT.	RENTISTICO	CONCEPTO	Vr.UNDITARIO	Vr.CONCEPTO
1	50005-01-03	CAMBIO DE MODALIDAD Y MODIFICACION EN N CREACION CORRECCION A SOLICITUD EN TRAMITE / MODOFICA	132.000.00	132.000.00
				$132.000.00

SON: **CIENTO TREINTA Y DOS MIL PESOS MONEDA CORRIENTE***

Responsable: _____

Recibo de Caja Aplicado al Expediente No. _____

SUPERINTENDENCIA DE INDUSTRIA Y COMERCIO
No. 13-187439- -00015-0000
Fecha: 2015-09-18 17:35:26 Dep: 2020 DIR NUEVASCR
Tra: 11 PATENTEIY!! Eve: 378 FASENACIONAL!
Act: 412 REPOSPRESRECU Folios: 79

Colo-20376-841-001-1